ARL 63-16

THE DESIGN AND INITIAL OPERATION OF A MAGNETIC MODEL SUSPENSION AND FORCE MEASUREMENT SYSTEM

EDWARD LEE TILTON, III
WILLIAM J. PARKIN
EUGENE E. COVERT
JAMES B. COFFIN
JOHN E. CHRISINGER

MASSACHUSETTS INSTITUTE OF TECHNOLOGY
CAMBRIDGE, MASSACHUSETTS

JANUARY 1963

AERONAUTICAL RESEARCH LABORATORIES
OFFICE OF AEROSPACE RESEARCH
UNITED STATES AIR FORCE

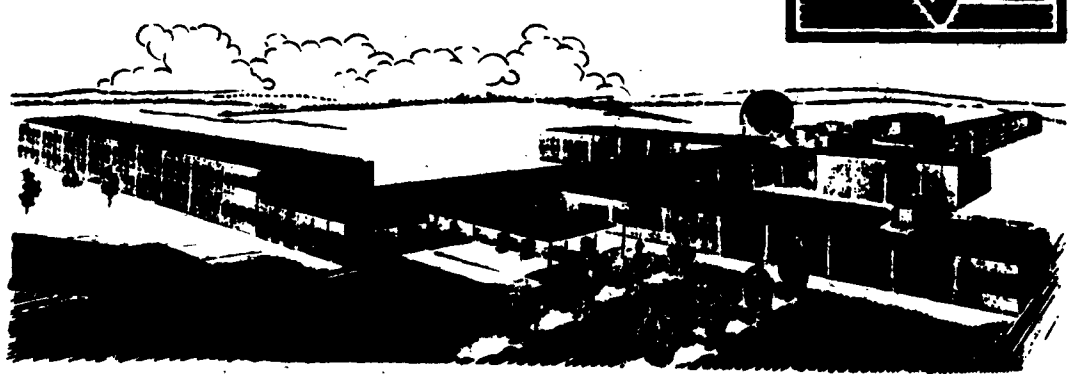

NOTICES

When Government drawings, specifications, or other data are used for any purpose other than in connection with a definitely related Government procurement operation, the United States Government thereby incurs no responsibility nor any obligation whatsoever; and the fact that the Government may have formulated, furnished, or in any way supplied the said drawings, specifications, or other data, is not to be regarded by implication or otherwise as in any manner licensing the holder or any other person or corporation, or conveying any rights or permission to manufacture, use, or sell any patented invention that may in any way be related thereto.

- - - - - - - - - -

Qualified requesters may obtain copies of this report from the Armed Services Technical Information Agency, (ASTIA), Arlington Hall Station, Arlington 12, Virginia.

- - - - - - - - - -

This report has been released to the Office of Technical Services, U. S. Department of Commerce, Washington 25, D. C. for sale to the general public.

- - - - - - - - - -

Copies of ARL Technical Documentary Reports should not be returned to Aeronautical Research Laboratory unless return is required by security considerations, contractual obligations, or notices on a specific document.

28-687, 300, 5-21-63

ARL 63-16

THE DESIGN AND INITIAL OPERATION OF A MAGNETIC MODEL SUSPENSION AND FORCE MEASUREMENT SYSTEM

EDWARD LEE TILTON, III
WILLIAM J. PARKIN
EUGENE E. COVERT
JAMES B. COFFIN
JOHN E. CHRISINGER

MASSACHUSETTS INSTITUTE OF TECHNOLOGY
AEROPHYSICS LABORATORY
CAMBRIDGE, MASSACHUSETTS

JANUARY 1963

CONTRACT AF33(616)-7023
PROJECT 7065
TASK 7065-01

AERONAUTICAL RESEARCH LABORATORIES
OFFICE OF AEROSPACE RESEARCH
UNITED STATES AIR FORCE
WRIGHT-PATTERSON AIR FORCE BASE, OHIO

FOREWORD

This interim technical report was prepared by the Aerophysics Laboratory, Massachusetts Institute of Technology, Cambridge, Massachusetts, on contract AF 33(616)-7023 for the Aeronautical Research Laboratories, Office of Aerospace Research, United States Air Force. The work reported herein was accomplished on Task 7065-01, "Fluid Dynamics Facilities Research" of Project 7065, "Aerospace Simulation Techniques Research". and covers the period February 1960 through May 1962. The contract was first monitored by Lt. George Luthringer and is presently under the monitorship of Lt. Stephen Koob of the Fluid Dynamics Facilities Laboratory of ARL.

Studies are still being conducted under this contract.

ABSTRACT

The design, construction and proof tests of a magnetic model suspension system capable of use in a M = 4.8 wind tunnel is described. The results indicate that the model can be suspended magnetically during the wind tunnel starting conditions, that the model can be angulated and lift and drag forces measured with the model at angle of attack.

TABLE OF CONTENTS

TABLE OF CONTENTS (Concluded)

LIST OF ILLUSTRATIONS

LIST OF ILLUSTRATIONS (Continued)

LIST OF ILLUSTRATIONS (Continued)

LIST OF ILLUSTRATIONS (Continued)

LIST OF ILLUSTRATIONS (Concluded)

LIST OF TABLES

CHAPTER I
INTRODUCTION*

It is probably no exaggeration to state that every engineer who has been engaged in wind tunnel testing has encountered support interferences and has thought of the advantages of supporting the model with magnetic fields. It can be shown that such a suspension is generally unstable. The control problem involves changes of relatively large amounts of current. These needs, coupled with the large size subsonic wind tunnels in operation 25 years ago, precluded the application of magnetic fields to model suspension.

The advent of supersonic testing tended to reduce the test section size (since the wall interference problem became less severe, if not negligible) and at the same time called for larger power consumptions. Thus the magnetic suspension system became more attractive. Further, the state of the art of automatic control systems had advanced rapidly and the gas filled electron tube was developed to the point that many amperes of current could be controlled quickly and efficiently.

The first published work that the authors are aware of on this problem, indicating a response to the favorable environment, came from the ONERA. Tournier and Laurenceau[1] reported in 1957 that they had constructed and operated a magnetic suspension unit and gave some results of sting-free drag measurements on several configurations.**

---

* The work on the magnetic suspension system has been continued at MIT under USAF Contract 33(616)-7023 monitored by Lt. G. F. Luthringer and Lt. S. J. Koob of the Aeronautical Research Laboratories, Office of Aerospace Research.

During the present investigation the magnetic balance system has attracted wide attention. A group at the Von Karman Facility of AEDC, Tullahoma, Tennessee also looked into the feasibility of this device, and prepared the Bibliography included at the end of this report.

** The authors have been informed by private communication from NACA, (now NASA) Ames, California, that a model magnetic suspension system was built and bench tested in 1952 - 3, but that it was never used with a wind stream. This work was based upon the work of E. C. Okress of Westinghouse (see J.A.P., May, 1952).

Manuscript released by the authors in August 1962 for publication as an ARL Technical Documentary Report.

Interestingly, the magnetic suspension of objects supported quite near to the magnet had been worked out before 1940. In 1937 F. T. Holmes described a magnetic suspension system[2] that was essentially a magnetic bearing. This technique was used in the development of the ultra centrifuge by Beams, Parker and others at the University of Virginia (Ref. 3 for example). All of these systems described above generated forces by direct current. Alternating currents have also been used to provide magnetic forces; Gilinson, Garcia, and Aronson[4] developed magnetic gyroscope suspension. The application to the gyroscopic suspension also requires that continuous position information be available. Likewise, when a magnetic suspension system is used for aerodynamic testing, some form of data must be provided which can be interpreted in terms of the aerodynamic forces, as indicated by Kuhlthau.[5]

The ONERA efforts were well received by MIT personnel because they, as well as others, had observed a curious flow interference at high Mach and low Reynolds numbers that had been attributed to sting interference. Hence a preliminary internal proposal was prepared, and as a consequence, some calculations were made for an exact copy of the French System. In subsequent correspondence the ONERA gave MIT permission to copy their balance.

John Chrisinger (Capt. USAF) became interested in these proposals and volunteered to undertake this work as a thesis for the degree of Aeronautical Engineer. The initial work indicated that an exact copy would not satisfy the expected needs. Subsequent studies[6] verified that reasonable scaling laws existed and provided for the design of five coils and the design of the cores for the lift and lateral magnets. Tilton and Schwartz[7] static tested these units and found that " . . . The design expectations have been verified, and that the three magnetic units are capable of producing the forces necessary to keep the model in equilibrium. The cooling system suffices to keep the temperature of the units within the range of 95 - 100°F."

The basic system considered by ONERA included two lift coils on a single horseshoe core (See sketch 1). The yoke is parallel to the relative wind; the legs are normal to the relative wind and in line with local gravity. The pole faces and the coils are, naturally, out of the wind. Thus the wind vector and the gravity vector define the plane of symmetry. The lateral plane is perpendicular to the plane containing these two vectors. Since gravity is unidirectional and invariant (for this discussion) the lift coils (#1 and #2) are required to produce only an upward force. Similarly, the drag coil need only pull forward on the model since whenever the wind is on, the drag force acts as a natural bias. The drag coil (#5) is an air core solenoid. It remains to provide resistance in the lateral plane. Resistance is accomplished by lateral coils (#3 and #4). These coils can in principle either attract or repel if the model contains a permanent magnet, or an electrical steel element which has been magnetized by the lift magnets. The system as described can now produce forces on the model but is impractical because there is no control for the current in the coils. This difficulty is resolved by installing position sensing elements. In the sketch, element #1 provides position data for coil #1, etc. For purposes of discussion, position sensor #1 can consist of a light source and a collimating lens in the right hand box and a focusing lens and a detector in the left hand box. As the model is placed in different positions in the beam of light, varying amounts of light fall on the detector. Thus position information is generated. Sketch 1 does not show the error signal shaping networks, or the magnet power supply. The use of a Schlieren to visualize the flow is complicated because the usual light path is obstructed by the lateral coils. However, there is a clear path at 45° to the plane of symmetry. A roll control system is not shown.

An alternate configuration is currently in use in France. In this system the magnets are arranged in the form of a V (Sketch 2). Four coils carry the weight. These are disposed symmetrically and at 45° with respect to the gravity plane. This configuration has the advantage of symmetry, the conventional Schlieren can be used, and there

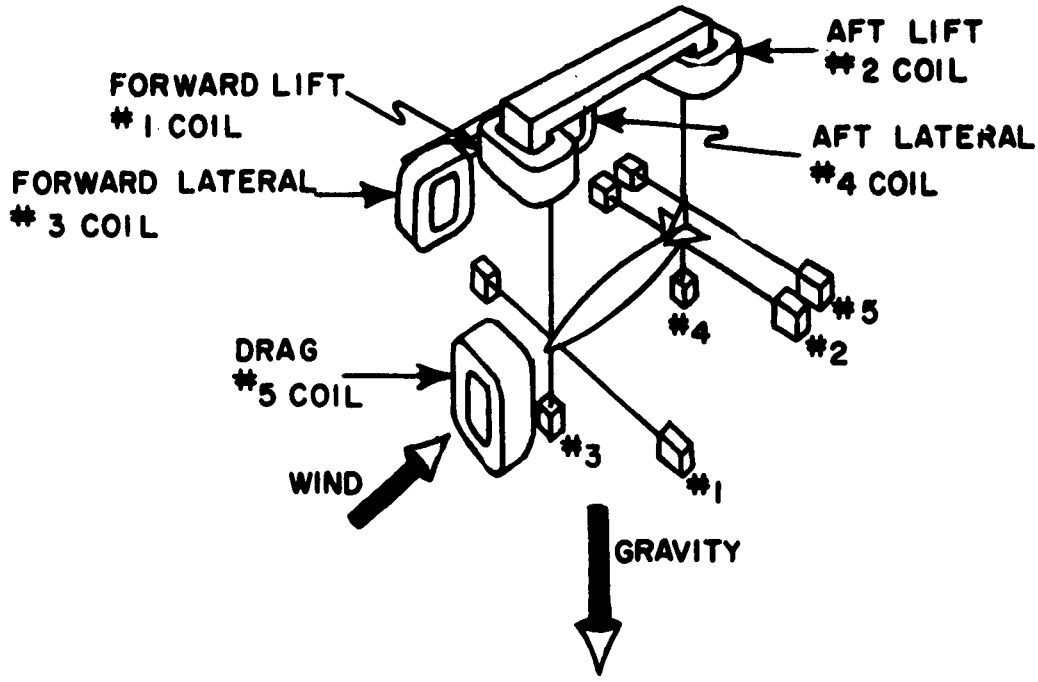

Sketch 1

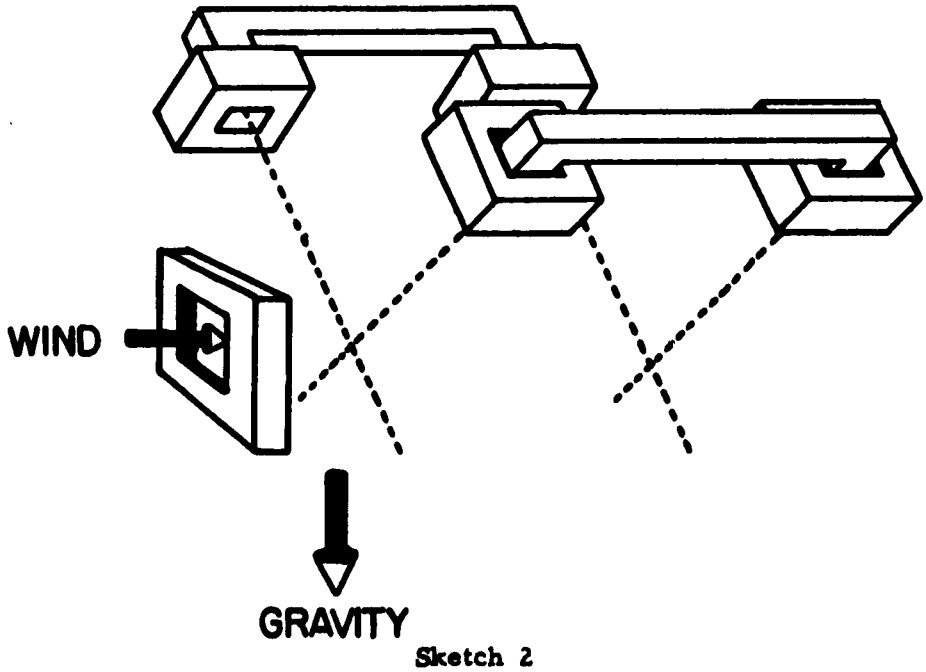

Sketch 2

are no problems of lateral bias. However, a cursory investigation indicated that, as a measuring apparatus, the advantages gained by this geometry were overcome by the increased complexity of the data reduction.

The magnetic suspension system described in this report was also built to accommodate the wind tunnel starting loads rather than to use a mechanical holding device. Note that in addition to this starting load capability, the magnetic balance was designed to operate continuously and to provide lift, drag, side force, pitching moment and yawing moment data as functions of angle of attack and yaw. The balance system as described has proved that it is capable of meeting these requirements. Within the scope of the authors' knowledge, this balance is unique in this regard.

The report that follows covers the design and fabrication of the cores, coils, power supplies, optics and control system of the magnetic syspension system. It is intended that descriptions be complete enough to permit straightforward construction of a copy of this magnetic system.

CHAPTER II
DESIGN OF THE SYSTEM

A. GENERAL REQUIREMENTS[1]

The basic design requirement for the magnetic balance system is that it be capable of continuous operation in conjunction with the 4 by 4 inch NSL hypersonic tunnel. The units should be at least capable of supporting the following static loads at the indicated current values and model locations:

Drag Solenoid	Lift Units	Lateral Units
10 oz at 30 amps	10 oz/leg at 30 amps	2.5 oz/leg at 15 amps
nose at 4 inches	at 4 inches from	4 inches from
from solenoid.	pole face.	pole face.

Further, it is expected that the response time will be fixed by the starting characteristics of the wind tunnel. The starting operation produces a transient dynamic loading of 3 – 5 times the static loading However, by reducing the total pressure from 100 psia to 28 – 30 psia it would seem that a reasonable limit would be approximately 50 amperes for the design current. Figure 1 shows the variation of impact pressure during starting as recorded by Figler at the NSF. It will be noted that these sharp rises and drops take place in times of 0.15 seconds. If one uses rectified 3 phase 60 cps alternating current then the longest possible wait for full power will be about 0.027 seconds.

---

[1] It is possible for high gas velocities and strong magnetic fields to interact and change both the gas velocity profile and the magnetic field. It can be shown that these changes are not significant if the Hartmann number Ha, and the magnetic Reynolds number Rm, are each much less than one.[8]

$$Ha = BL \frac{\sigma}{\mu}$$

$$Rm = \mu_0 UL$$

where B is the magnetic field strength, L is the characteristic length, σ is the conductivity of the gas, μ is the permeability of the gas, μ_0 is the permeability of a vacuum, and U is the gas velocity.

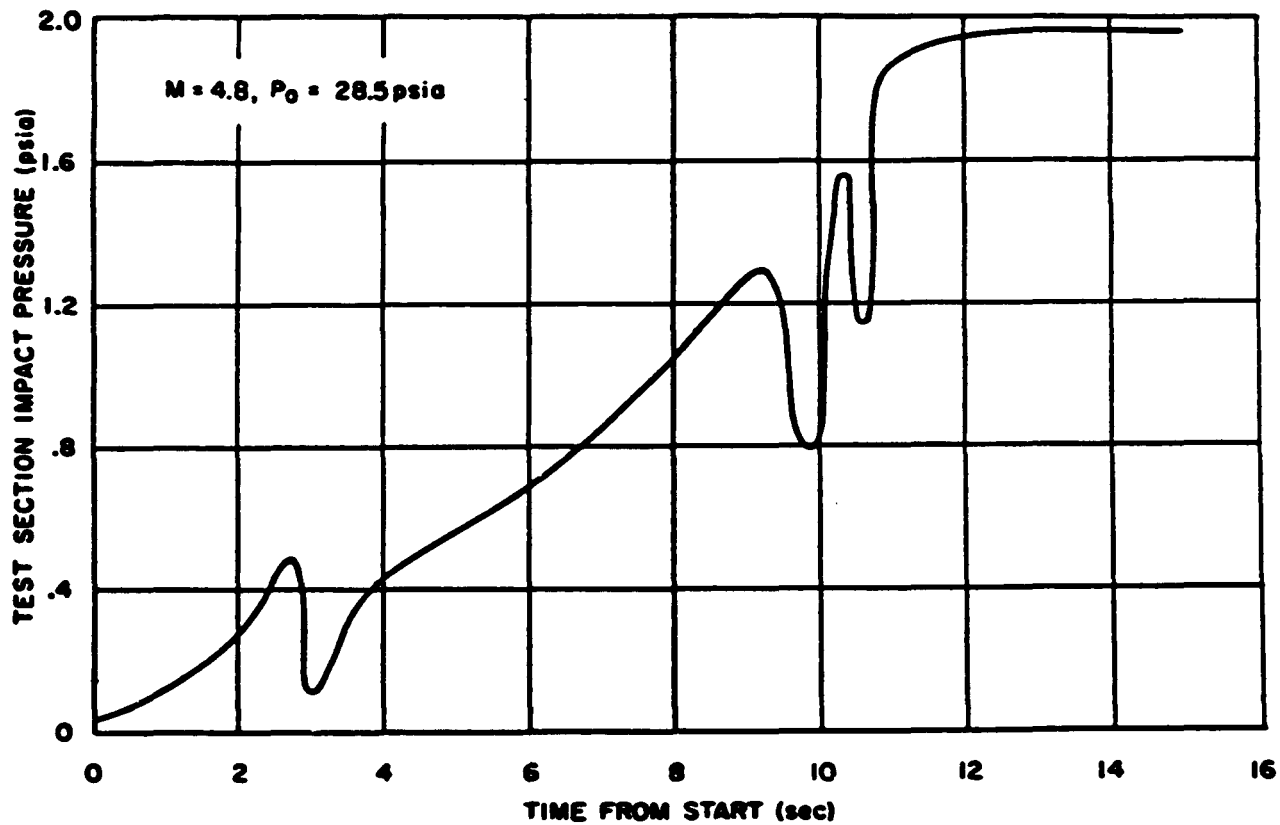

Figure 1. Typical start in NSF - (4" x 4") tunnel

Further the maximum pressure jump corresponds to about 3.6 ounces of force on the usual sized model. Consequently it is required that the system be able to stabilize a sequence of ±3.6 ounce step functions at 0.3 second intervals.

After the design parameters have been selected, the size and configuration of the magnetic units necessary to meet these requirements must be determined. The solutions of magnetic circuit problems are frequently treated as being analogous to those of electric circuit problems. Analogy is only true in a gross way. Whereas the current flow in an electrical circuit is physically restricted to move only in the high conductance paths provided, a significant portion of the flux flow of a magnetic circuit will invariably occur exterior to the design loop (a condition known as flux leakage). Also, while the resistance of an electrical circuit is constant (excluding temperature effects), the permeability, and hence the reluctance of the magnetic path is a variable. The comparative degree of mathematical complexity of the two types of problems can best be understood by realizing that the electric circuit problem is essentially one-dimensional in nature, while the magnetic circuit problem is one of three dimensions, due to the presence of the spatial magnetic fields.

Most important is a knowledge of the approximate number of ampere-turns (NI) required to produce the design forces at the given operating distances. For most isolated magnetic circuits which utilize a magnetic field to generate a force, the NI required to accomplish the given function can be determined by any one of three methods. These methods are: the application of magnetic field theory; the use of experimental data; the use of handbook type formulae which have been derived from the first two methods. The drag solenoid and two horseshoe electromagnets associated with the magnetic suspension system, however, are not isolated units, but must produce fields which are "centered" on the same region in space, i.e., the location of the model to be suspended. Hence, it can be seen that each of the three units exerts a three-dimensional influence of unknown size on the other two units. Accordingly, an evaluation, or plot, of the theoretical field

strength in the vicinity of the model can only be accomplished through the use of a lengthy and complex three-dimensional graphical iteration analysis. The use of handbook relationships,[10,11] is only applicable when the units are magnetically isolated, and furthermore, the length of the air gap is a relatively small dimension, i.e., less than the width of a pole piece. Hence, the mutual influence of the magnetic fields upon each other, and the large air gaps unavoidably present in this system, preclude the use of this approach. Likewise, the many formulae available for calculating the tractive power of the drag solenoid, ranging from simplified to sophisticated (Refs. 12 and 13), may be rendered invalid by the influences of the two horseshoe magnets.

As stated, experimental data can be used to estimate the required NI for each of the three magnetic units. The experimental data can be measured after construction of a static test apparatus to hold the three magnetic units and the model in the same spatial relationship as that to be employed in the wind tunnel installation. Additionally, the apparatus must provide an accurate means for measuring all of the forces and moments which may be imposed upon the model when the magnetic units are energized in any desired combination and intensity. A direct current power source must be employed which permits independent control and measurement of the current being supplied to each of the five coils in the three magnetic units.

The experimental data approach was used as the basic method of analysis.[6] A test apparatus was employed which was constructed entirely of non-magnetic materials and which fulfilled the above requirements. It is shown in Fig. 2. The five forces to be measured were transmitted to five spring scales through the use of strings and pulleys. The desired model position, established with respect to the magnetic units, was maintained by adjusting the position of the spring scales. This adjustment was made by rotating the threaded pins which served as anchor points for the scales, as shown in Fig. 3. Fishing tackle swivels isolated the strings and scales from this rotary motion. As may be noted in Fig. 2, the pulley constraints on the supporting strings were well removed from the model (38 inches). This permitted

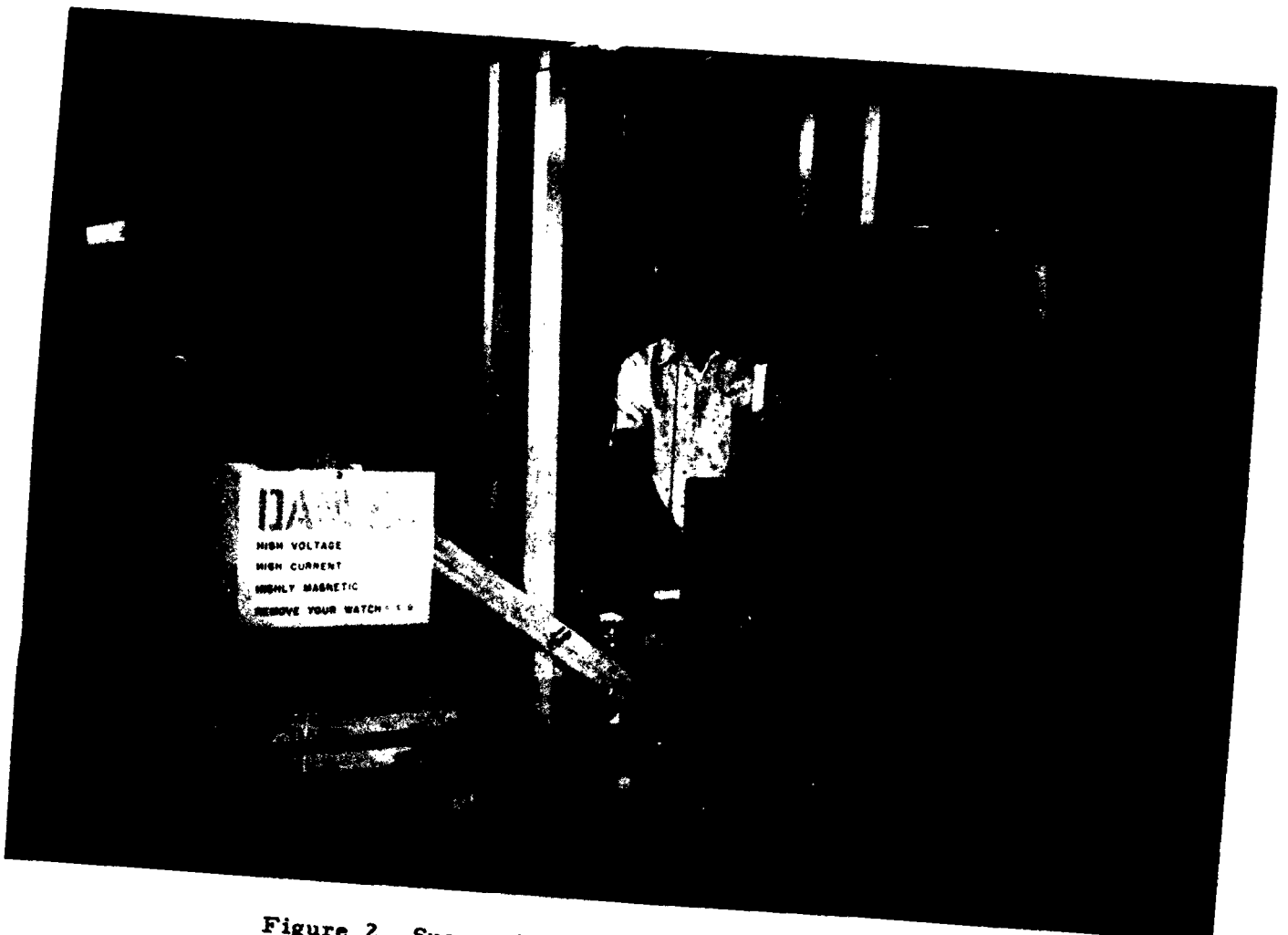

Figure 2. Suspension system static test apparatus.

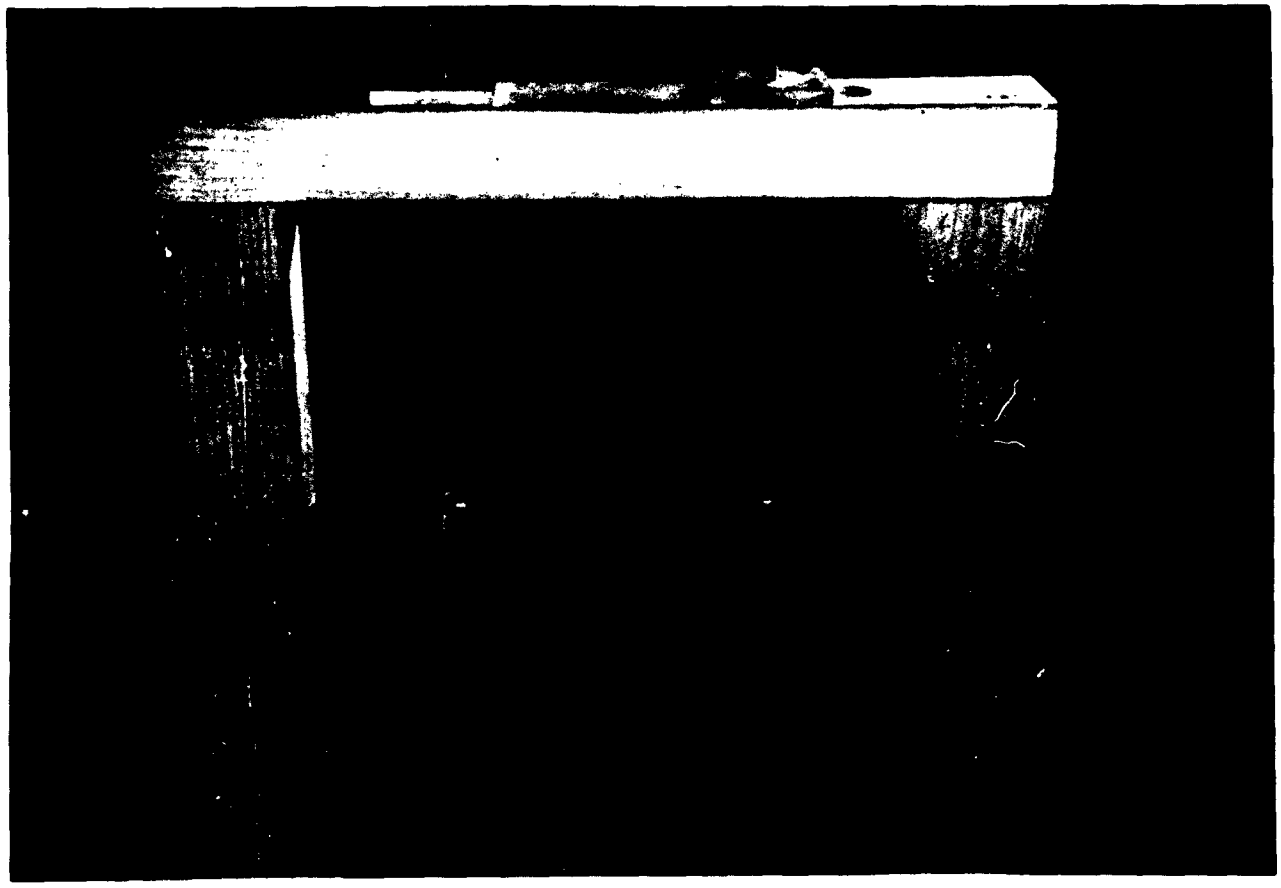

Figure 3. Adjustable support pins and scales.

considerable latitude in the positioning of the model without compromising the required orthogonality of the string supports. The orthogonality was required to insure independent force readings in the three directions.

As shown in Fig. 4, the suspension magnet was mounted in a horizontal plane, while the lateral magnet was mounted inverted in a vertical plane. This configuration was used in order to measure both repulsive and attractive forces generated by the lateral magnet, as well as the attractive forces of the other two units. The repulsive force measurements were obtained by noting the decrease in tare values registered on the lateral magnet scales, the units mounted directly over the magnetic model in Fig. 2. The drag solenoid was mounted in a ventilated box whose position was adjustable along the axial direction (see Fig. 4).

The direct current required to operate the five coils of the three magnetic units was generated by a 200 ampere capacity arc welder. Its output was fed to a control panel (Fig. 5), from which the five coils were independently energized at any desired current level. Switches were incorporated in the circuitry of the lateral magnet which enabled the operator to select any combination of polarity for that unit.

The model to be supported must be constructed in whole or in part of ferromagnetic material. (Materials of this type are broadly categorized as "magnetically soft" or "magnetically hard." (Ref. 14, Table 1, p. 27) The magnetically soft materials have high permeabilities, but low residual flux densiti s – i.e., they are easily magnetized, but retain only a very small degree of this magnetization when the magnetizing force is removed. The magnetically hard materials are conversely more difficult to magnetize, but have high residual flux densities when the magnetizing force is removed. Permanent magnet materials are "magnetically hard.") Both types of material were to be investigated, as each might prove to have unique features which surpassed the other material, dependent upon the model configuration and/or test conditions. It was furthermore decided that a standard size for the ferromagnetic material should be selected. This ferromagnetic material would then be used as an inner core, to be enclosed by non-magnetic material which would be shaped to the desired contours of the model to be tested. The standard configuration for the model core was chosen to

Figure 4. Magnetic units and model in position for test.

Figure 5. D. C. power control panel

be a circular rod with a diameter of one-half inch and a length of six inches.

For the soft magnetic material, an alloy called electrolytic iron was selected. For the hard magnetic material, a permanent magnet alloy composed principally of aluminum, nickel, cobalt, and iron was selected. The intrinsic flux density versus magnetizing force characteristics of these materials are given in Fig. 6. (For an excellent discussion of common magnetic property terms, including tabulated values and typical graphs, refer to Ref. 14, Chapter I.) In particular, note that the normal flux density and the intrinsic flux density of most ferromagnetic materials does not significantly differ until the onset of saturation conditions. Ref. 15 is another source of magnetic material and design information, convenient because of its condensed form.

One restriction would seem to arise from the upper operational temperature of the 4" by 4" wind tunnel (1000°F). If the ferromagnetic model is subjected to high temperatures, either through the use of a high temperature gas, or as a result of eddy current heating, the continuous running time of the system will be restricted. While the magnetic properties of any ferromagnetic material tend to decrease with increasing temperature, an abrupt decrease occurs at a given temperature known as the "Curie Point." At this temperature the material becomes merely paramagnetic. For pure iron, nickel and cobalt, the respective Curie points are 770°, 358°, and 1130°C.[9] The so-called electrical steels, which contain high percentages of nickel, have Curie points of 500°C and higher. Alnico V, a permanent magnet alloy with an exceptionally high residual flux density, has a relatively high Curie point due to the large percentage of cobalt in its composition. However, when heated to temperatures in excess of 538°C, it suffers an irreversible loss in its residual flux density. Hence, this lower figure represents the useful maximum temperature for this alloy. The maximum total temperature in the 4" by 4" tunnel is less than 600°C and since the model recovery temperature will be somewhat lower, and it cools itself by radiation, it is quite likely that the problems associated with loss of magnetic properties will not be severe.

In the remainder of this chapter the design considerations of the several parts of the magnetic balance system are, in the order to be discussed, the power supply, the magnets, the control system, structural and cooling considerations for the electronics, the magnets, and the optics, and finally a brief discussion of reliability is presented.

B. POWER SUPPLY AND ITS CONTROL CIRCUIT

After the output of the position sensing circuit is modified by the compensating circuit the signal is sent to the power supplies. The power supplies can be thought of as high power gain, direct current amplifiers with an input impedance of approximately 10,000 ohms. An input signal of zero to ten volts will drive the power supplies from zero output to full output. Five power supplies are needed (two lift, two lateral, and one drag) for the present system and, while alike schematically, they differ in output voltage and current requirements. The two lift coils each have a resistance of 2.8 ohms and a current requirement of approximately zero to 50 amps. The two lateral coils each have a resistance of 1.27 ohms with a current requirement of approximately 30 amps. The drag coil has a resistance of 4.9 ohms with a current requirement of approximately zero to 50 amps.

The power supplies are basically grid controlled rectifiers (thyratrons) connected in a 6 phase half-wave-star configuration. This arrangement was selected because of the power levels involved, the low ripple requirements in the output and the fast response time. For the lift and drag power supplies type C16J thyratrons were used. Type C6J thryatrons were used in the lateral power supplies. With C16J thyratrons connected in the 6 phase half-wave-star configuration it is possible to draw up to 96 amps continuously and be within the tube ratings. This is adequate for the 50 amp requirements of the lift and drag coils. With C6J thyratrons it is possible to draw up to 38 amps continuously which satisfies the 30 amp requirement of the lateral coils. Some series resistance was added to the lift and lateral coils to bring the operating voltages into better regions for the thyratrons and also to improve the time constants of the coils.

The following table lists the capability of the various power supplies.

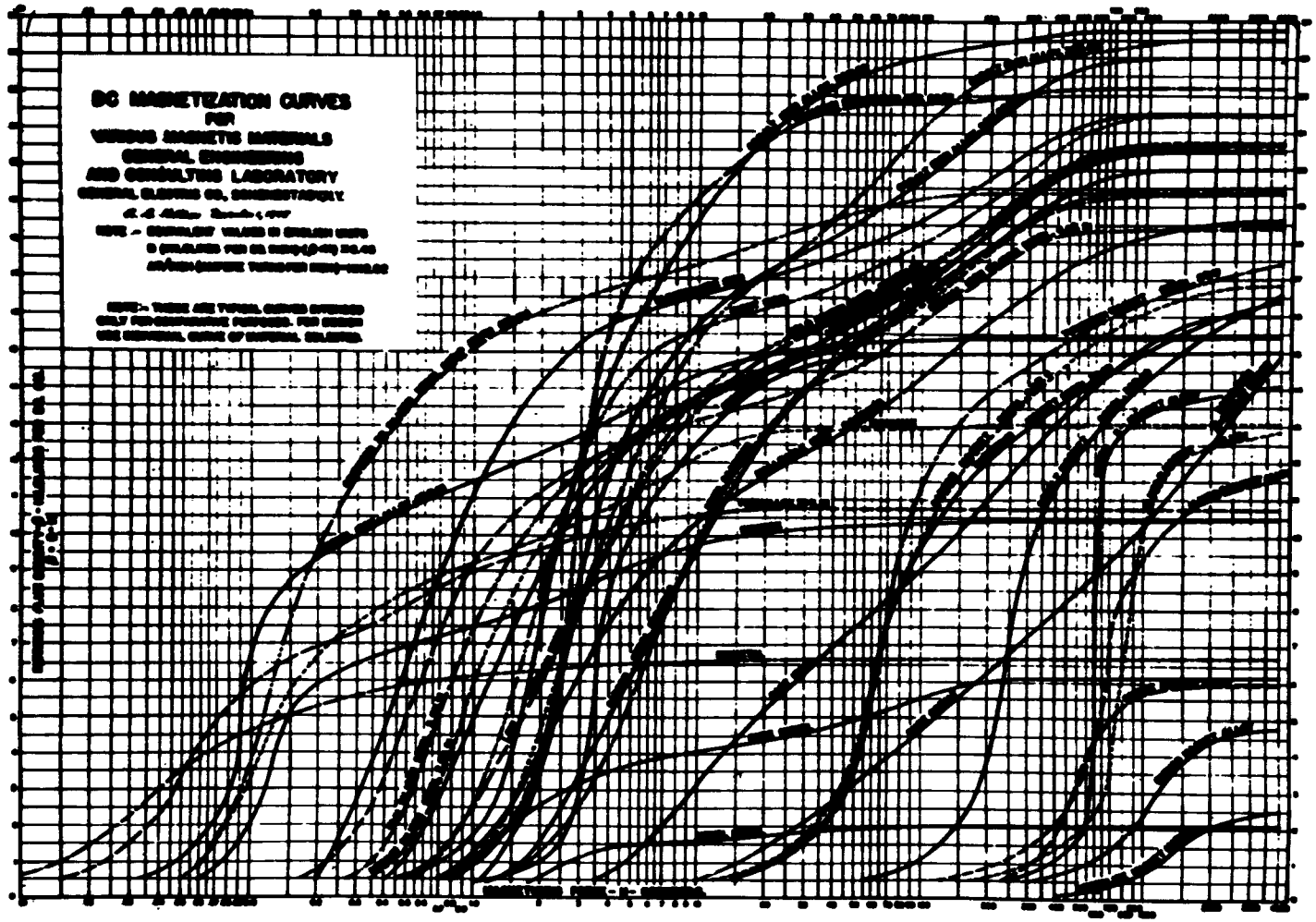

Figure 6. D.C. magnetization curves for various magnetic materials.

	Max. Volts	Max. Amps
Drag Power Supply	250 V.	96 A.
Lift Power Supplies (each)	132 V.	96 A.
Lateral Power Supplies (each)	117 V.	38 A.

In addition to the five electronically controlled power supplies there is a need for one more power supply for the bias windings on the lateral coils. The bias windings enable the model to be repelled as well as attracted. This allows the model to be placed and held in a desired position in spite of the absence of side forces. Gravity eliminates the need for bias windings on the lift coils. Each of the two lateral coils has a bias winding. These are connected in series allowing the use of just one power supply. This power supply is regulated with a maximum output voltage of 30 volts and a maximum output current of 50 amps. Commercial units are available to supply this need.

Circuit Description

A single phase schematic of the power supply is shown in Fig. 7. The purpose of the control tube is to convert a zero to 10 volt positive DC signal voltage to correctly phased firing pulses on the grids of the C16J thyratrons. This is achieved by placing an AC bias voltage on the grid of the 2050 control thyratron that is retarded by 90° with respect to its plate voltage (Fig. 7). This AC bias voltage is suppressed with a DC bias voltage until the control tube does not fire (Fig. 8a). Any positive input signal voltage will override the negative DC bias voltage and drive the AC bias voltage into the critical grid voltage region of the control tube causing it to conduct (Fig. 8b). As this positive signal voltage increasis in amplitude, the control tube will fire earlier in the positive plate voltage cycle and therefore conduct over a longer portion of the positive cycle (Fig. 8c). When the 2050 control tube conducts, there will be a voltage drop across its cathode resistor which overrides the output tube bias; this causes the C16J output tube to conduct and deliver power to the load or coil. It should be observed that the voltage appearing across the control tube cathode resistor is a series of positive pulses at a frequency of 60 cycles that are in phase with the plate voltage of the output tube. A simple single phase half-wave-circuit has just been

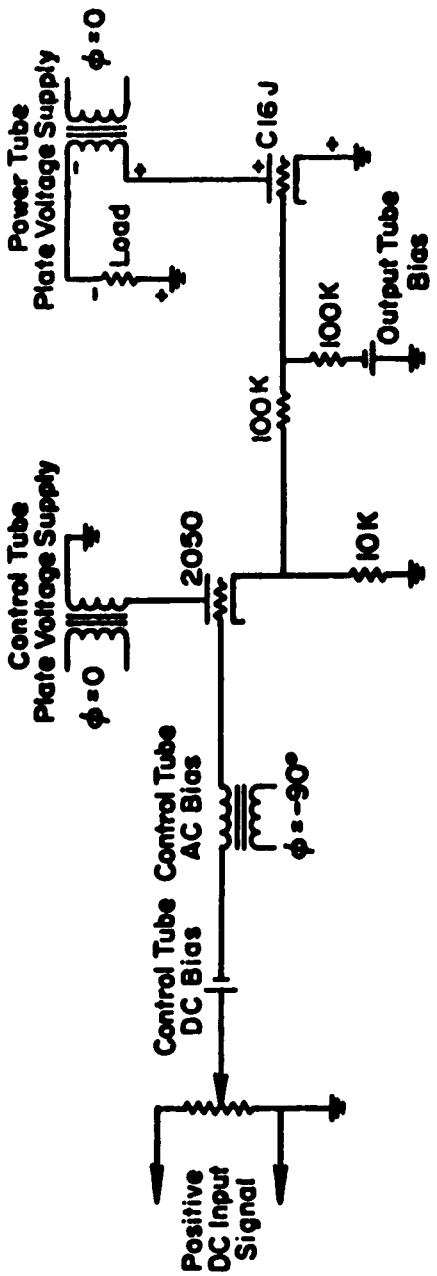

Figure 7. Power supply schematic

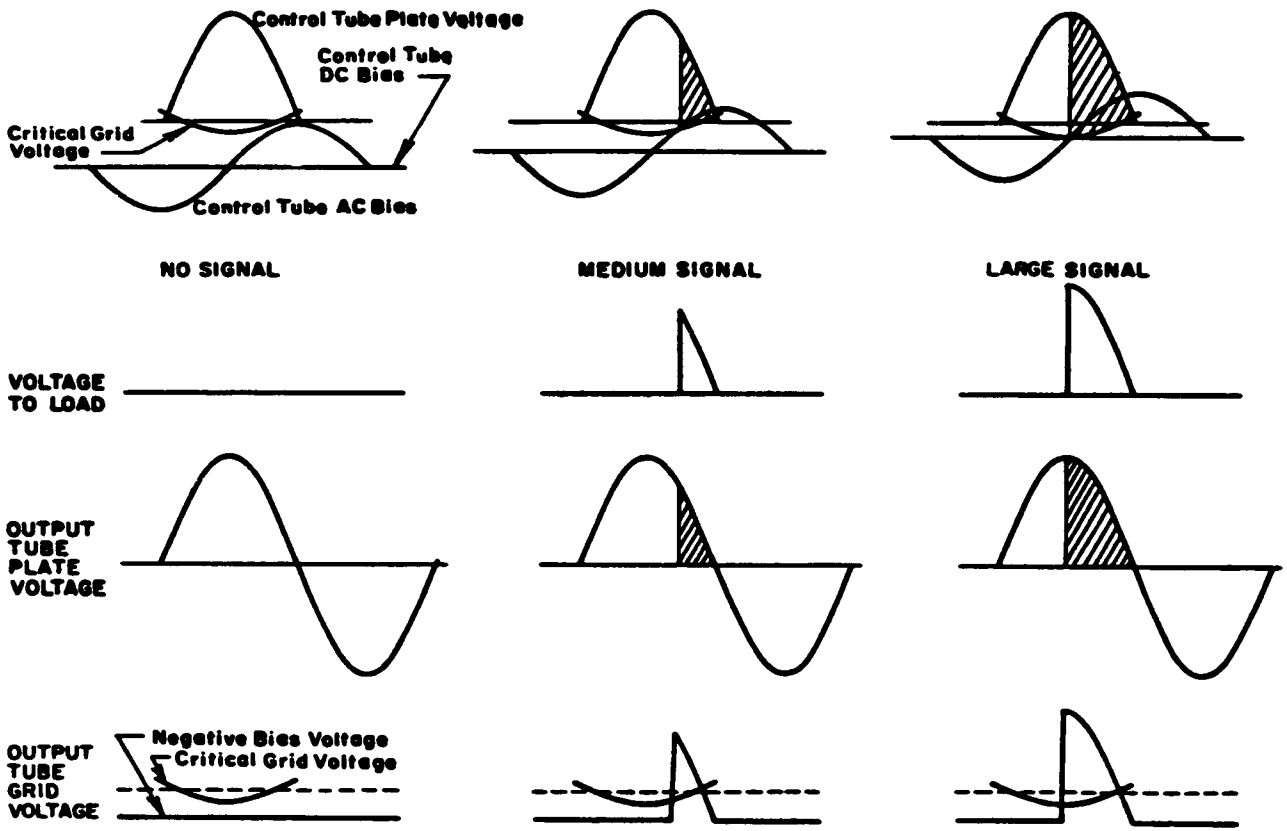

Figure 8. Control operation for power supply

described and this type of circuit would not be very desirable for our purposes because of the large ripple voltage in the output. A partial schematic of the circuit used in the present system is shown in Fig. 9. The six-phase star secondary configuration is energized from delta connected primaries which are connected to a 440 volt three phase power line. This arrangement is effectively a three phase full wave rectifier system with a ripple frequency of 360 cycles in the output. There is complete control of output voltage from zero to approximately 1.35 times the r.m.s. value of each secondary winding. With the inductive load of the magnet incorporated in the system, the ripple in the output current has proven negligible. A diagram of the wave forms is shown in Fig. 10a in order to clarify what is happening in the output circuit of the system. It can be seen from Fig. 9 and 10a that if one tube fires early or late in its respective phase there will be a larger ripple component in the output and an unequal sharing of the load in the output tubes. If for example the phase "b" output tube were firing early in its phase, most of the average current would be carried by this tube and this would lead to its destruction. This process could be cumulative if precautions were not taken. It is for this reason that control thyratrons are used to generate large trigger voltages in order to fire the output tubes. Under these conditions the output tube characteristics do not have to be matched and any change in output tube characteristics under load is unimportant. The firing characteristics of the type 2050 control tubes must be very closely matched in order to drive the output tubes properly. This close matching is accomplished with the circuit and not by selecting tubes. (To demonstrate the range of these controls, a 2050 thyratron was closely matched with a 2D21 thyratron with no circuit changes other than a tube matching socket.) The DC current control signal for the supplies as installed in the system is shown in figures 10b - f. The actual circuit used is shown in Fig. 11.

It is more convenient at times to think of a six phase system as a three phase full wave rectifier circuit. For each of the three major phases there are five balancing or matching controls: "180 degree

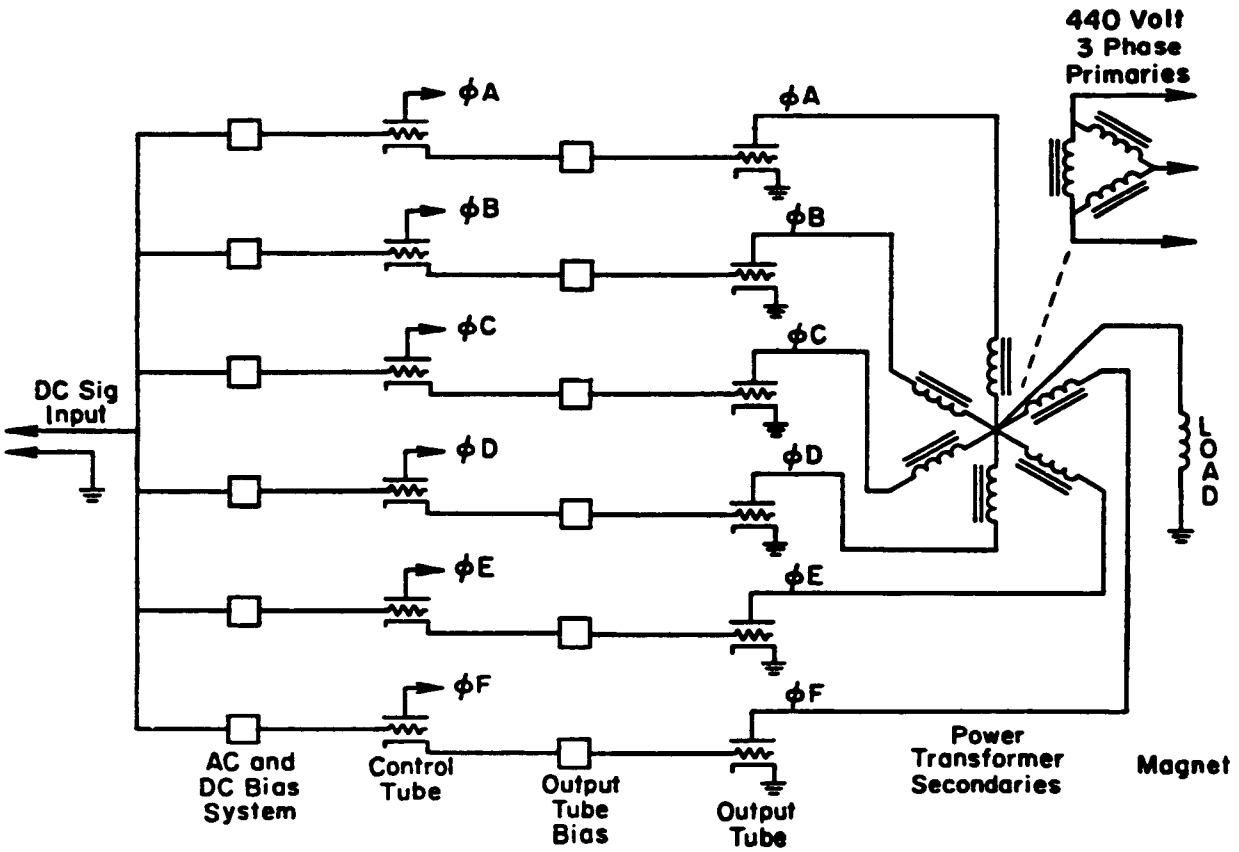

Figure 9. Six-phase half-wave-star secondary configuration and its relation to the system

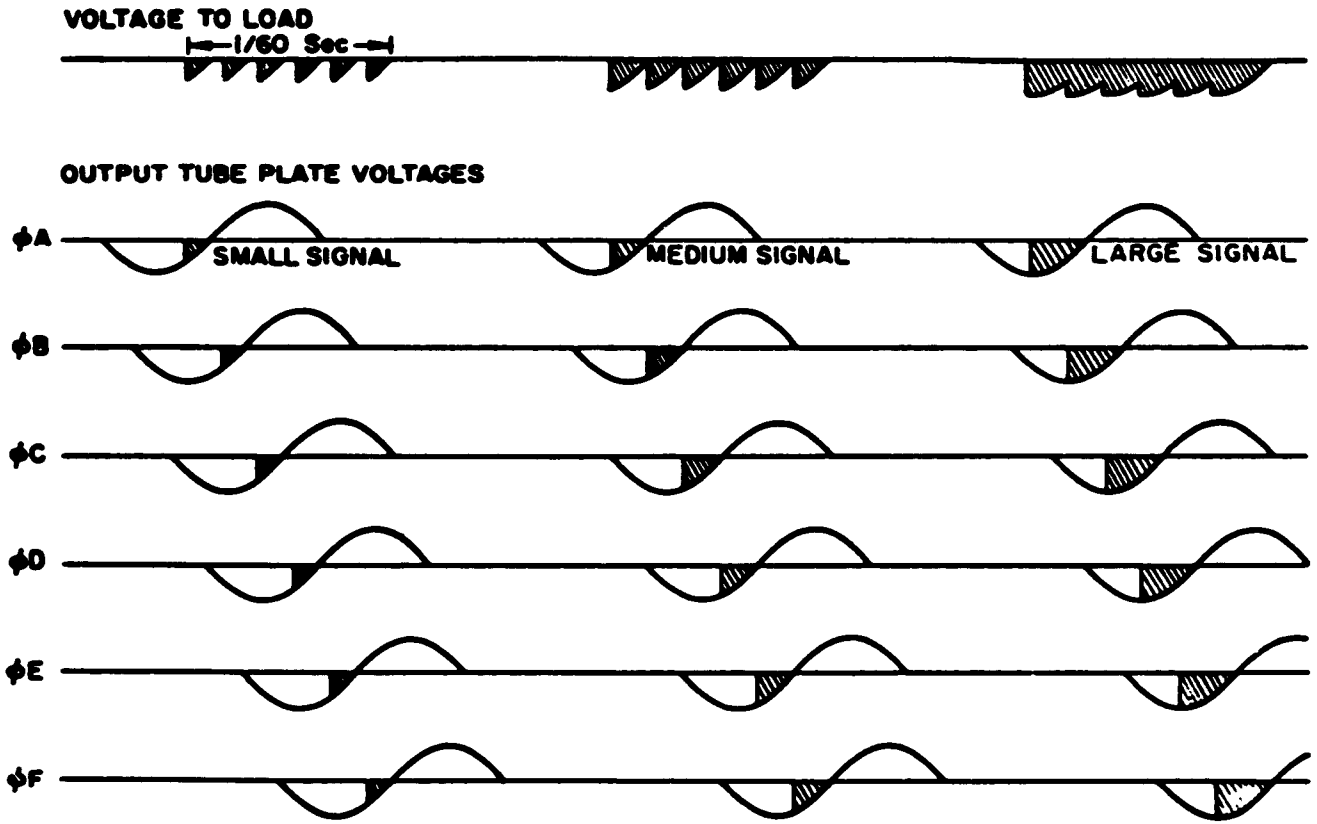

Figure 10a. Power supply voltage wave forms

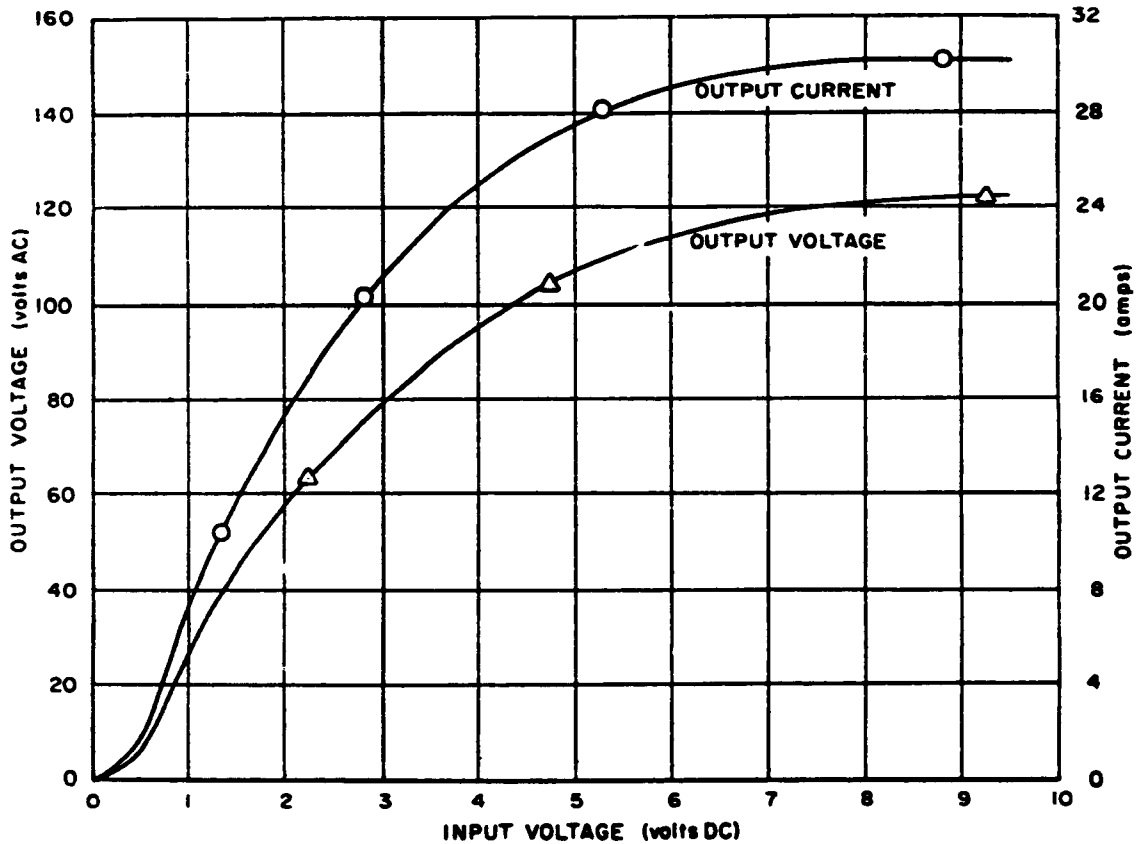

Figure 10b. Lift 1 Output voltage and current versus input voltage

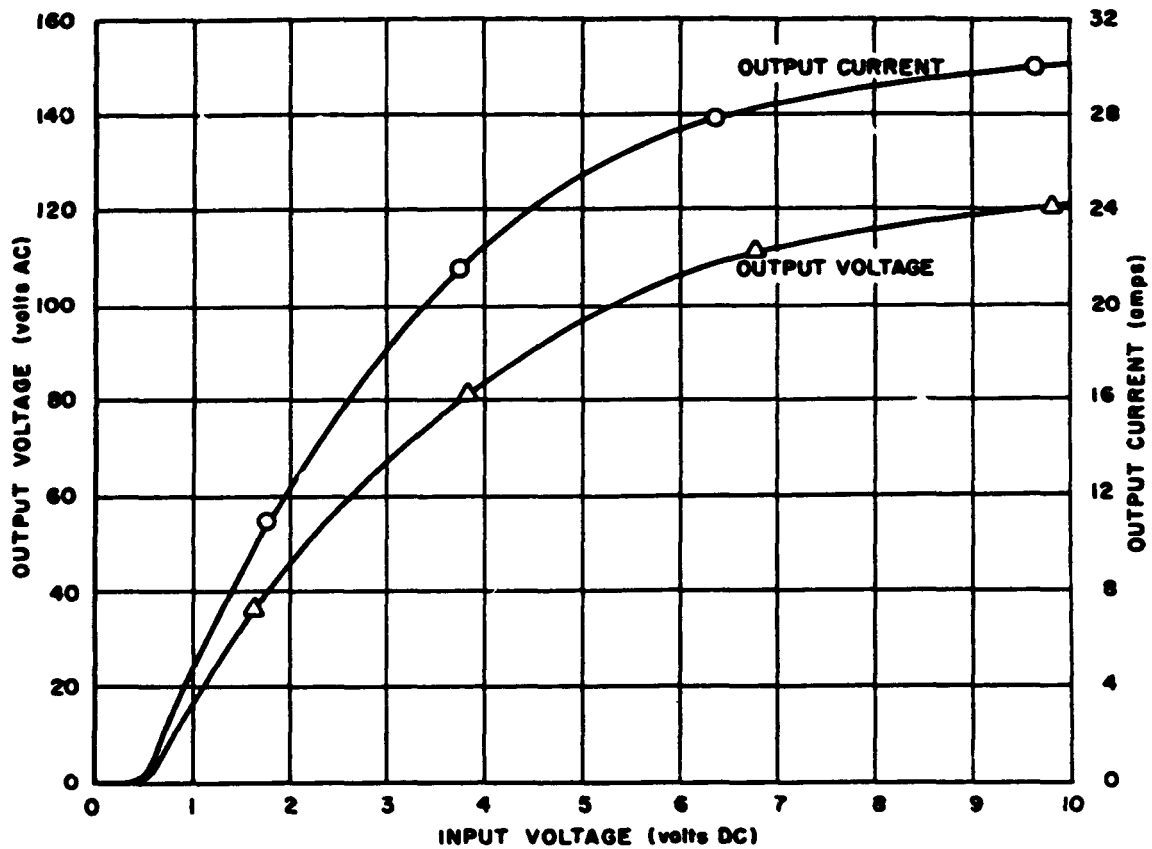

Figure 10c. Lift 2 Output voltage and current versus input voltage

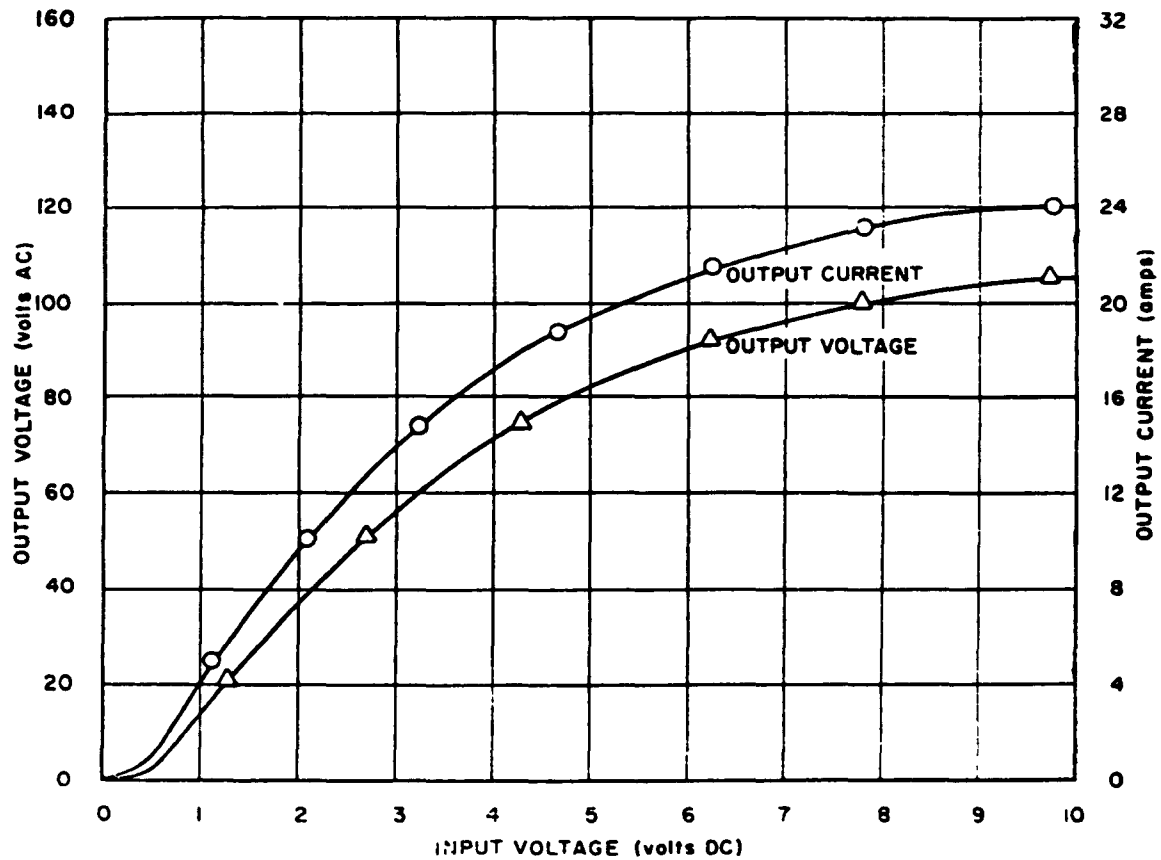

Figure 10d. Lateral 3 Output voltage and current versus input voltage

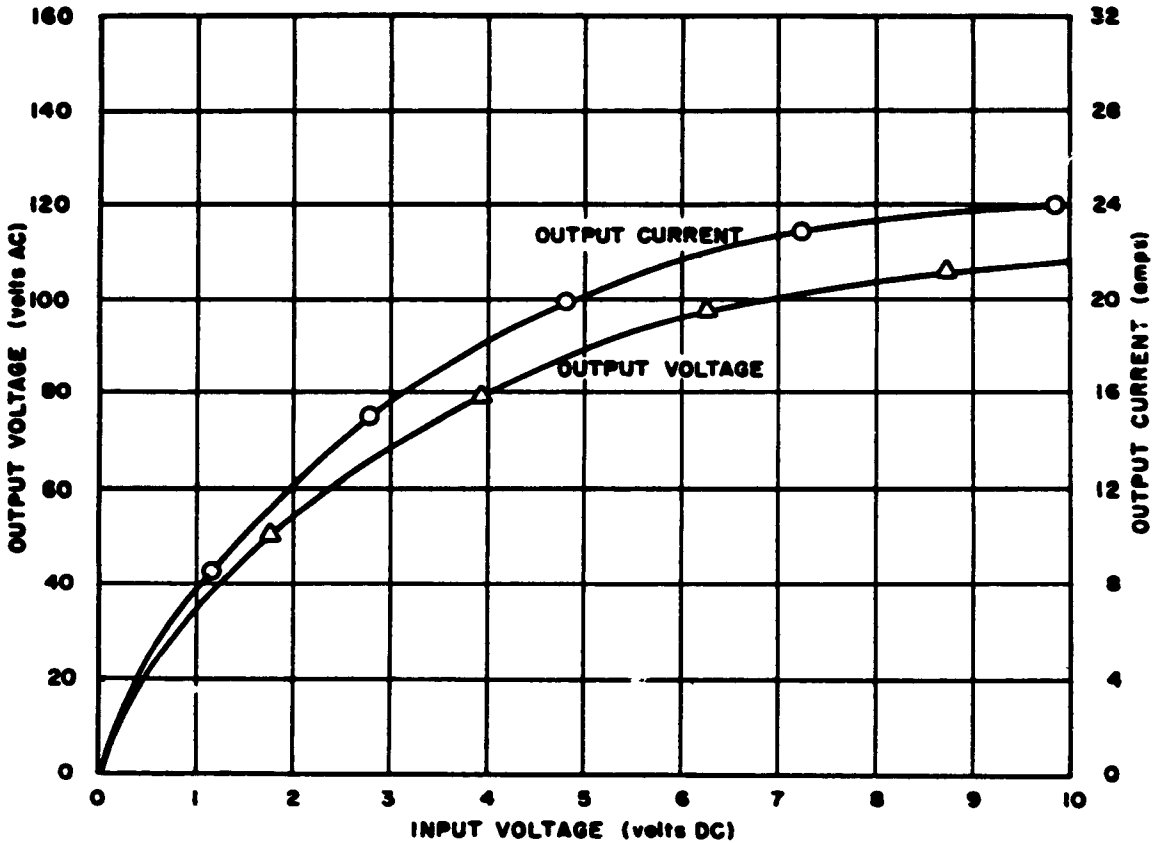

Figure 10e. Lateral 4 Output voltage and current versus input voltage

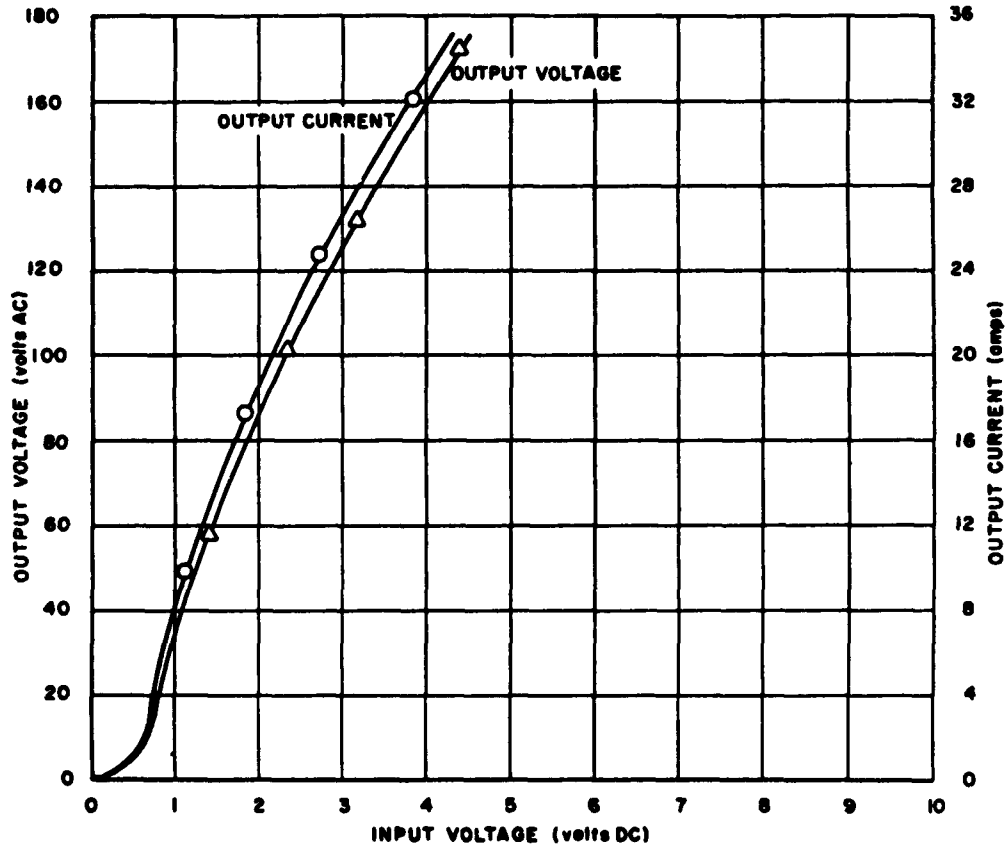

Figure 10f. Drag Output voltage and current versus input voltage

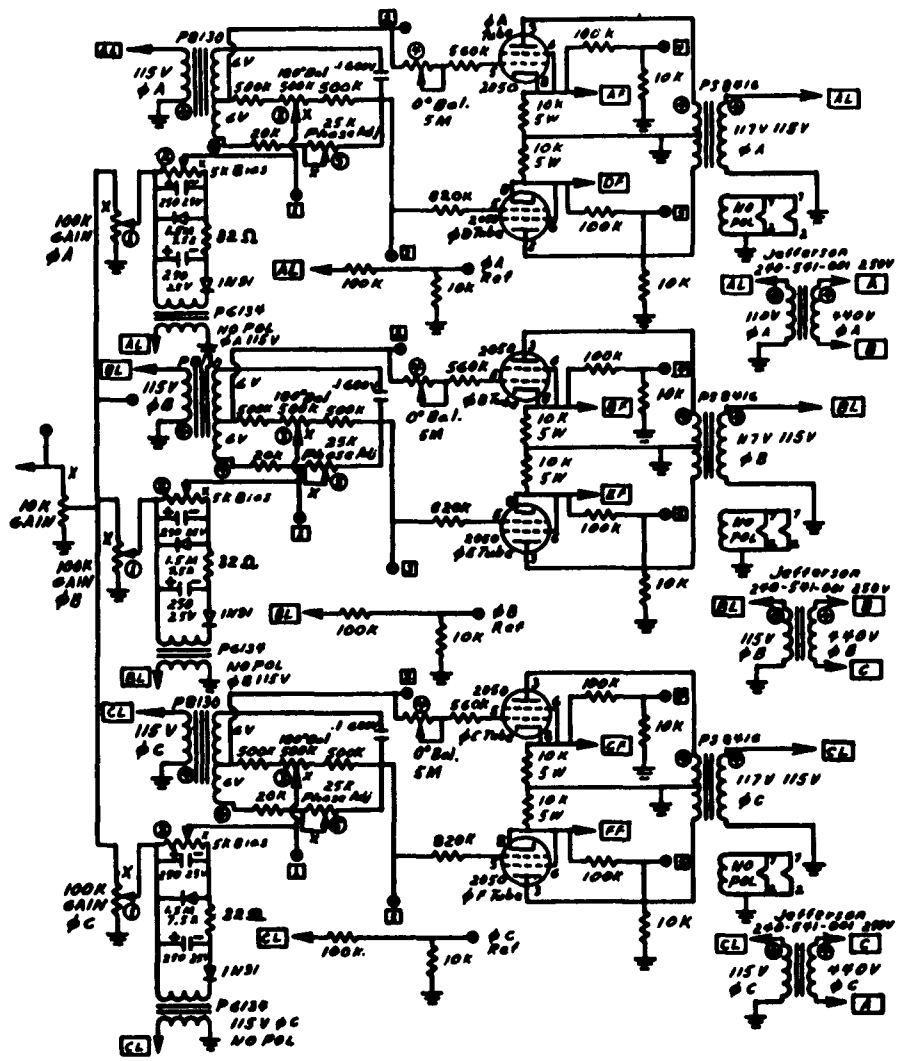

Figure 11a. Magnetic balance power supply circuit - control circuit chassis.

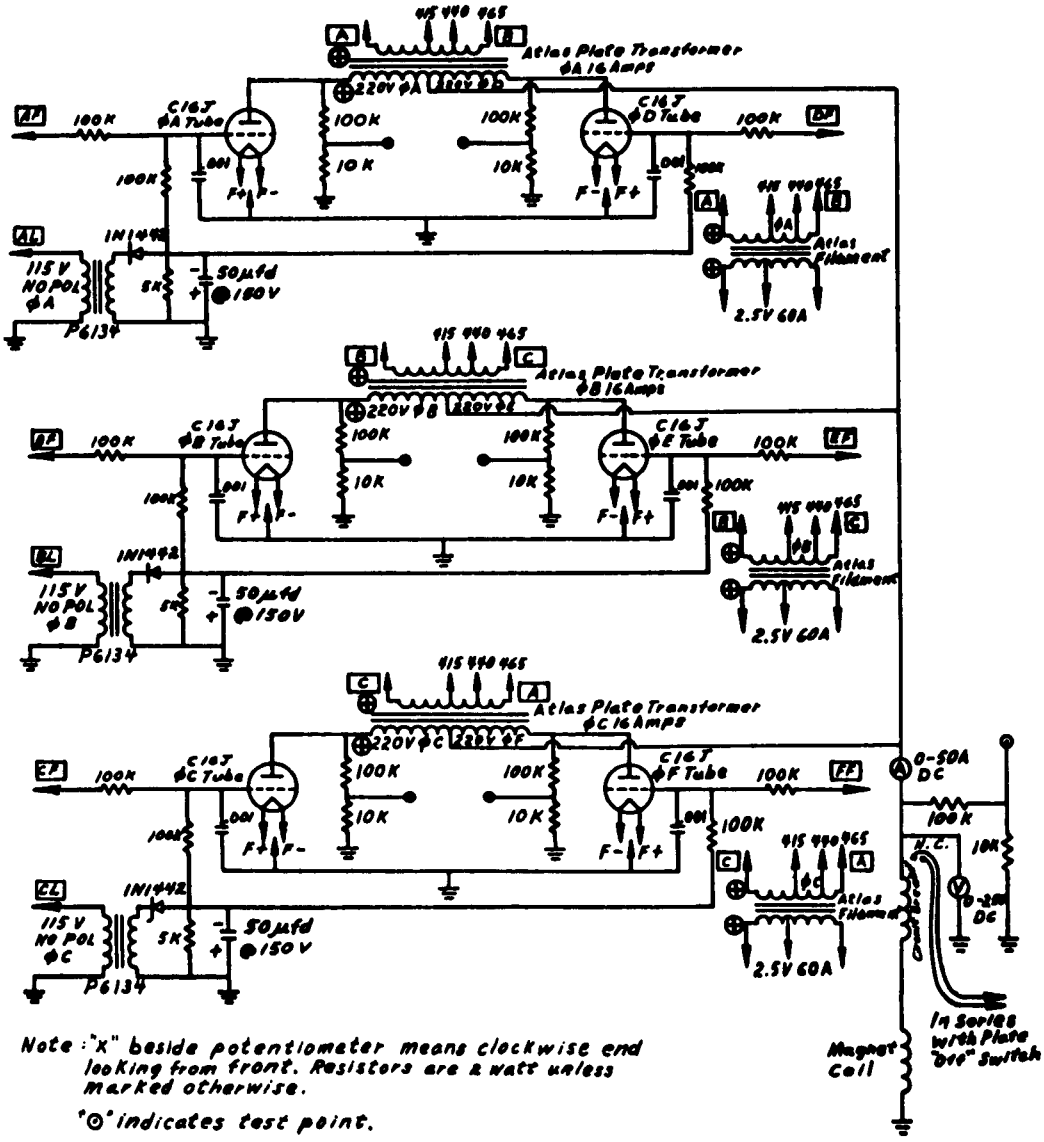

Figure 11b. Magnetic balance power supply circuit - power supply chassis.

balance" which allows matching of firing points for small signals; "zero degree balance" which allows matching of firing characteristics for large signals; "phase adjust" which shifts the AC bias signal on the grids of the control tubes 90 degrees with respect to the plate voltage of the control and output tubes; "bias adjust" which suppresses the AC bias signal and sets the firing threshold level of each major phase; and "phase gain" which matches the overall sensitivity or gain of each of the three major phases. All balancing and matching of tube firing characteristics is done on the control tube chassis. There is a master gain control on the input to set the gain of the complete power supply. These sixteen controls are mounted on the front panel of the control chassis with all the necessary test points for adjustment and testing. All test points are standard coaxial BNC connectors and any test points that could have high voltages have built-in attenuation resistors to minimize the possibility of subjecting personnel and test equipment to dangerously high voltages. Making use of the alignment procedures listed in Table I and a dual beam oscilloscope, the three major phases that make up the six phase system can be adjusted in approximately thirty minutes. After these adjustments are made, the potentiometer shafts are locked and should not have to be adjusted for many months of operation. All bias power supplies are energized from the power line and the bias supplies in each major phase are energized by their respective phases. This reduces the possibility of having plate voltage with no bias voltage to hold the tubes at cutoff. The bias voltage on the output tubes is not critical so long as it is well below the cutoff value, as any pulse from the control tubes is large enough to drive the tubes to conduction. The DC bias supplies for the control tubes are critical and must be regulated with Zener diodes. All the transformers must be phased before wiring and the small cross placed by each winding on the diagram indicates the start of the various primaries and secondaries. The phasing of the transformers, the wiring, and the subsequent oscilloscope checks, all require close attention to every detail.

The control circuit was built on a 28 inch wide chassis with an 8 3/4 inch by 30 inch wide panel. It weighs approximately 70 pounds

(Figs. 12 and 13). There are five control circuit chassis in the system. The power supply, consisting of C16J or C6J thyratrons, three plate transformers, 3 filament transformers and miscellaneous power supply AC control circuitry, was constructed on another 28 inch chassis with a 21 inch by 30 inch panel. It weighs approximately 375 pounds (Figs. 14 and 15). There are five power supplies of this type in the system.

The AC power control circuit that activates the filaments, fans, plate supplies, and time delays is shown in Fig. 16. The 60 second time delay is necessary to allow the thyratrons an adequate warm-up period prior to applying plate voltage. The power supplies are equipped on the primary side of the line with fuses and on the output side with circuit breakers. With this arrangement it is possible to protect the system from either an excessive power or current overload. The output circuit breaker opens the primary side of the power transformer. This eliminates the problem of opening a high value direct current to an inductive load. These current trip circuit breakers on the output are continuously adjustable from 10 amps to 100 amps. All switches, controls, pilot lamps, relays, etc., are heavy duty industrial components. All cooling of the components in the electronic cabinets (which includes the power resistors in series with the lift and lateral coils) is done with air and only the coils and optical system in the tunnel are water cooled. All pilot lamps have a "push to test" circuit and are identified on Fig. 16 as "T." Because of the high voltages and power available in the system there are warning lights located on the back and front of the various chassis and cabinets that indicate when the main circuit breaker to the system is "on." All chassis and assemblies in the system are connected with flexible rubber jacketed cable and "AN" type connectors. There are provisions in the system for turning the power supplies on and off independently or simultaneously with a master "on" and "off" switch. There are a number of master "on" and "off" controls in various locations in the system for convenience of operation.

C. MAGNETS – COILS AND CORES

As indicated in the introduction it was deemed necessary to base the design upon experimental data due to the overall complexity of the

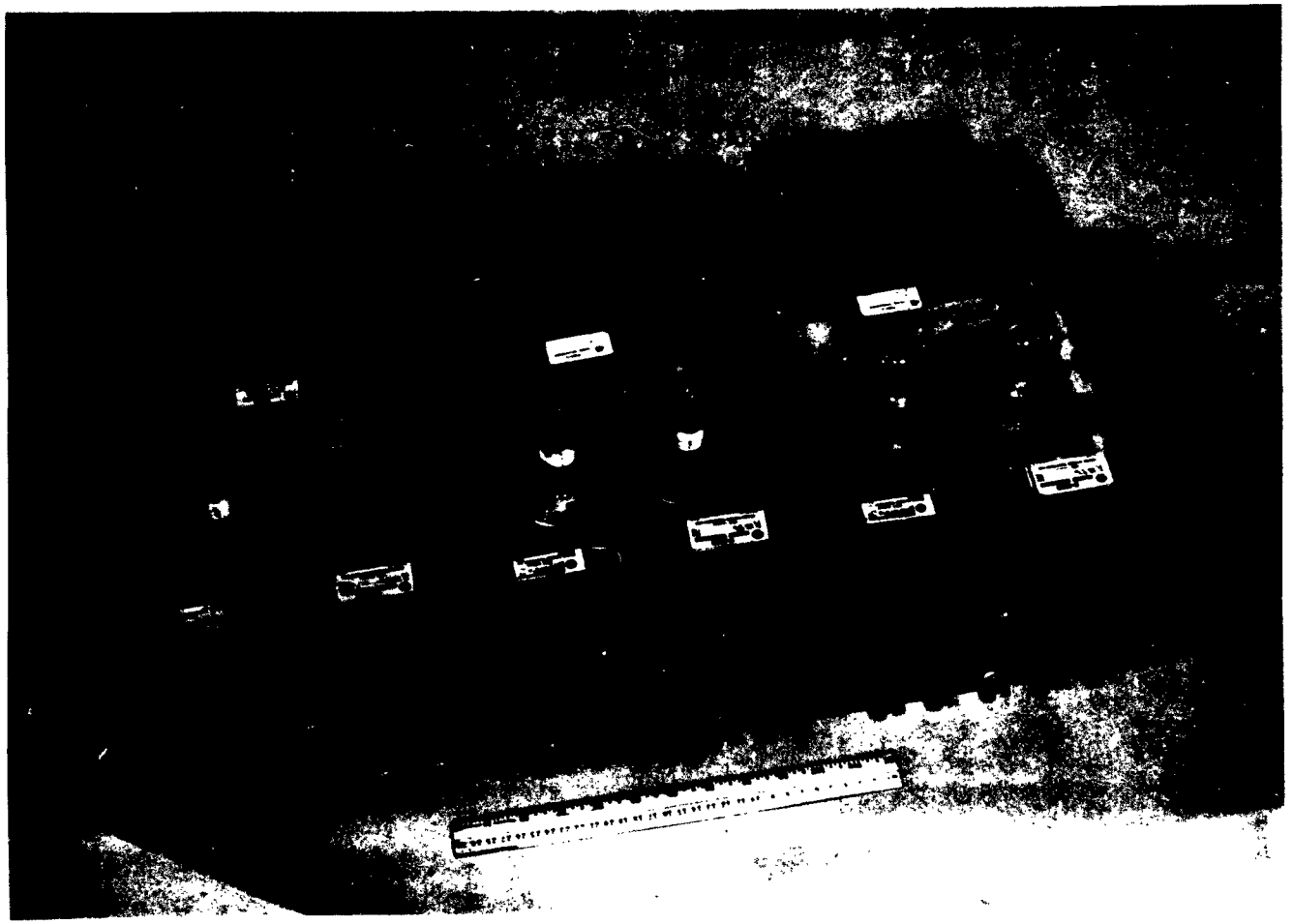

Figure 12. Control Chassis

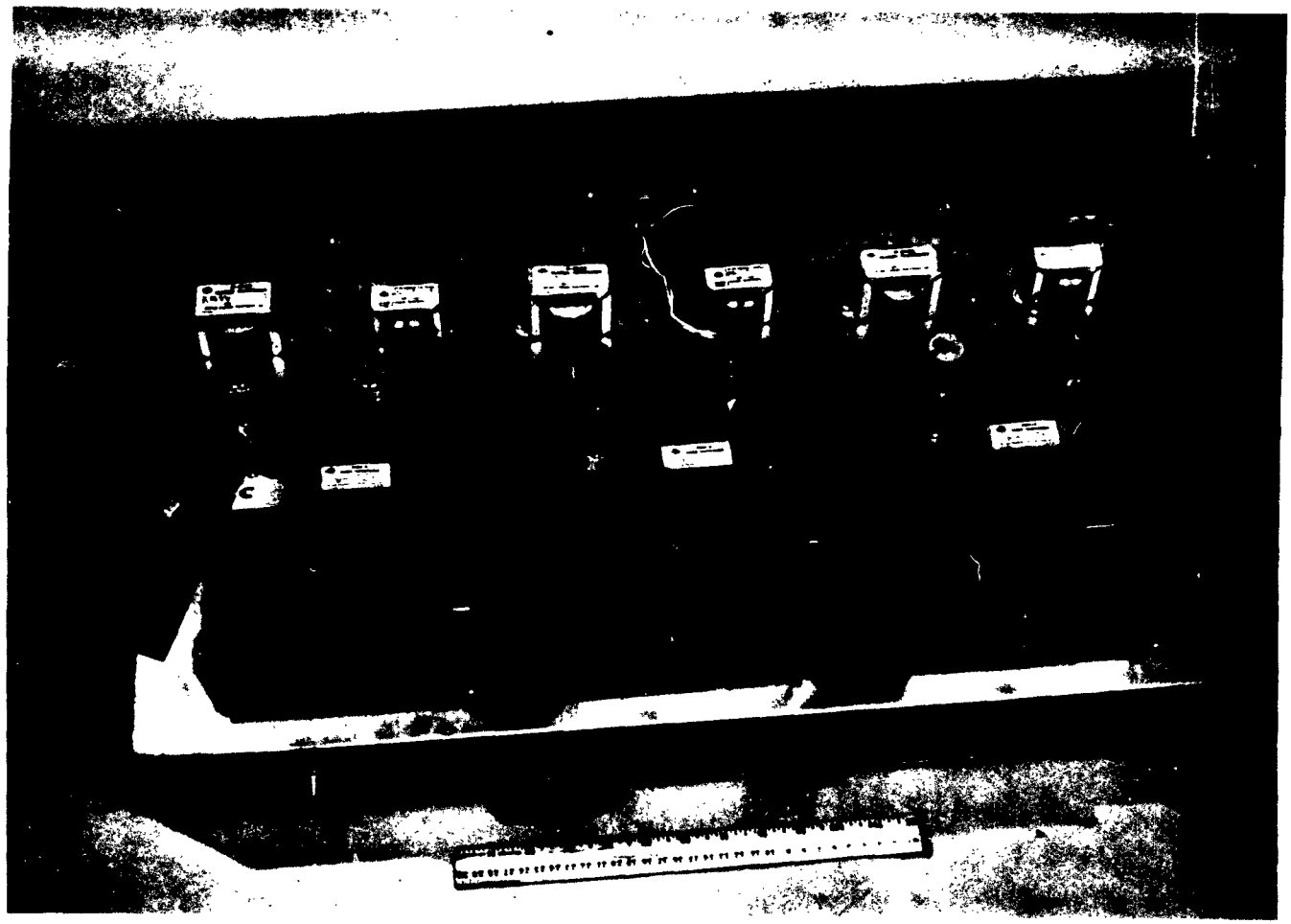

Figure 13. Control Chassis

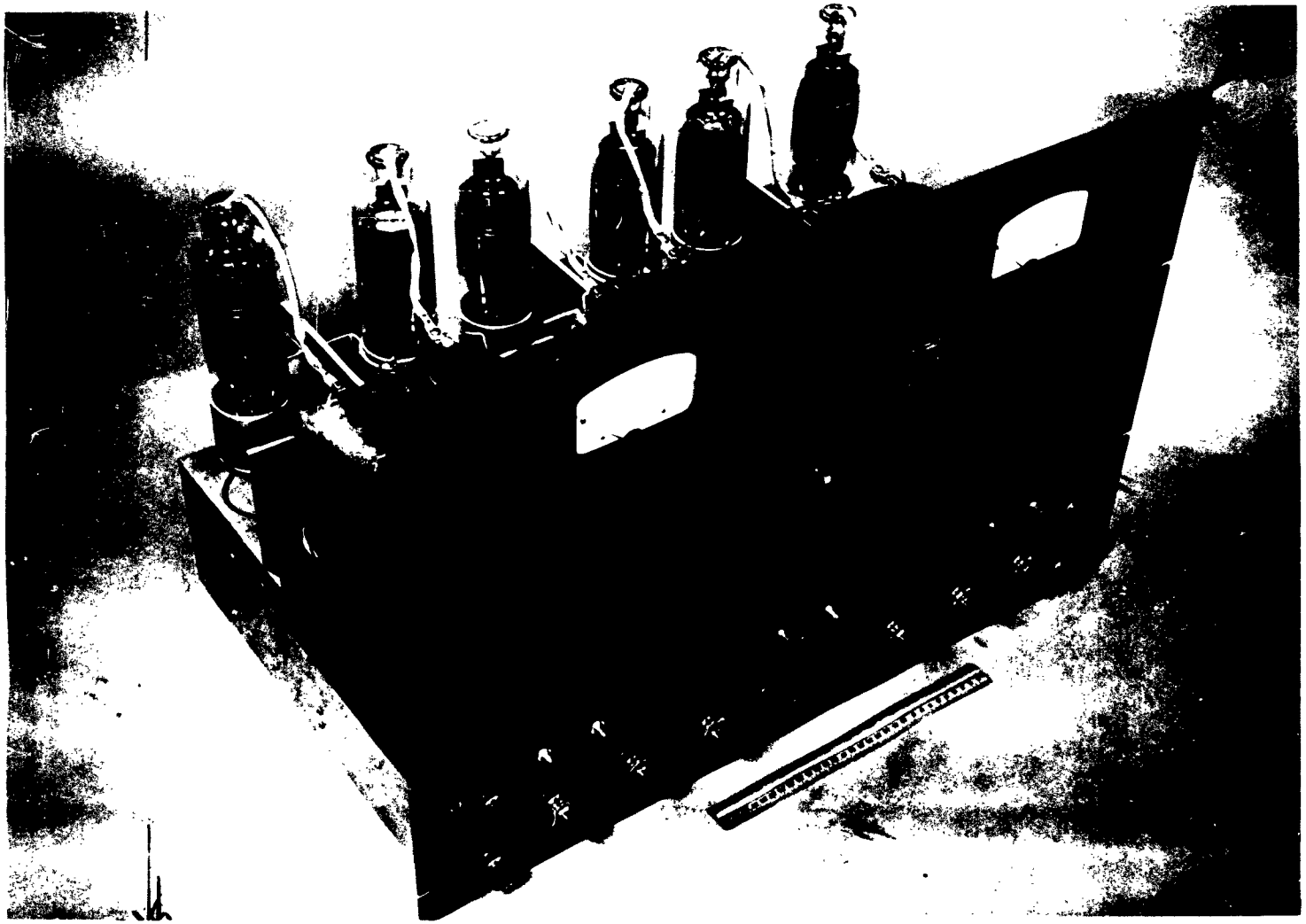

Figure 14. Power supply chassis

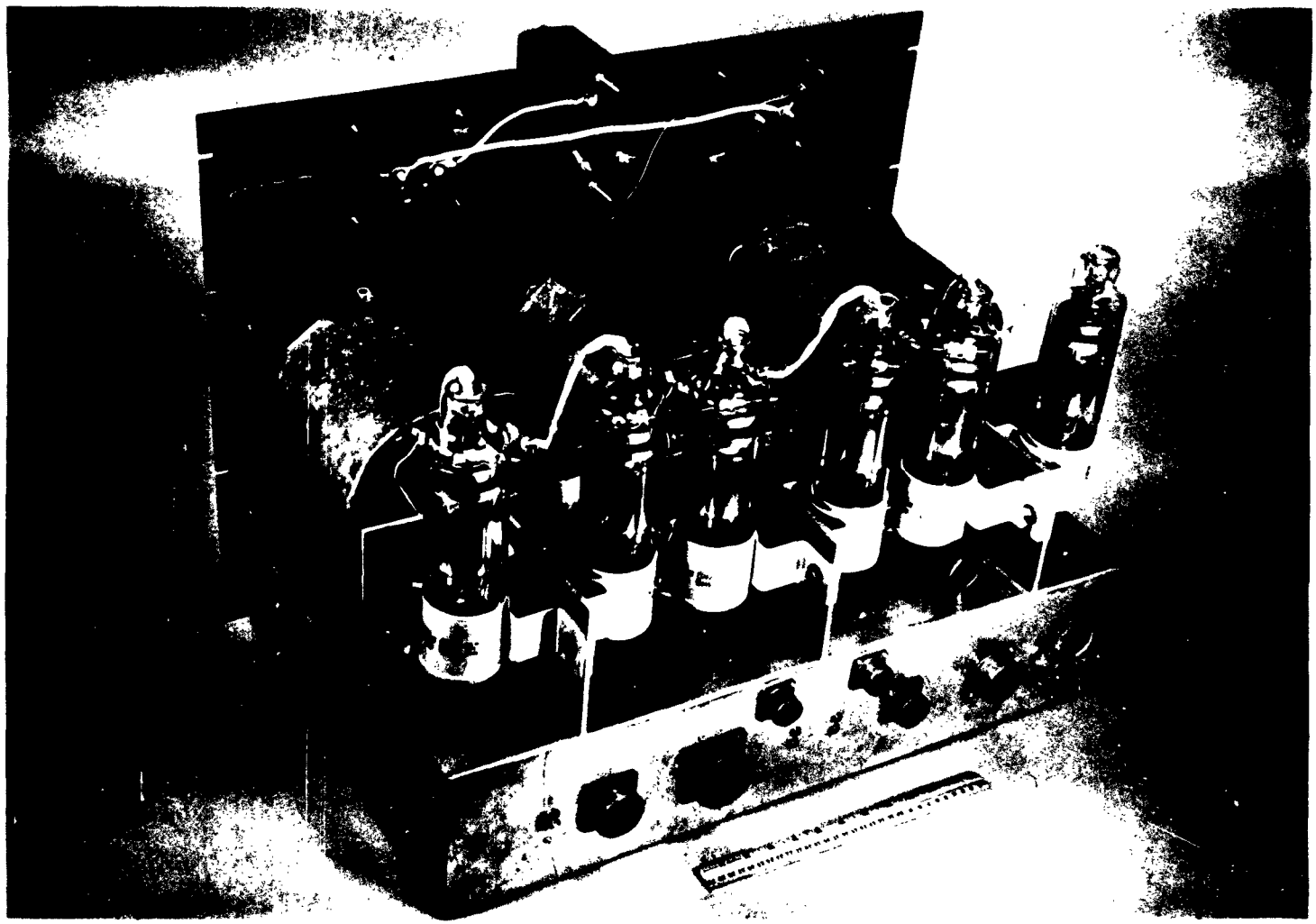

Figure 15. Power supply chassis

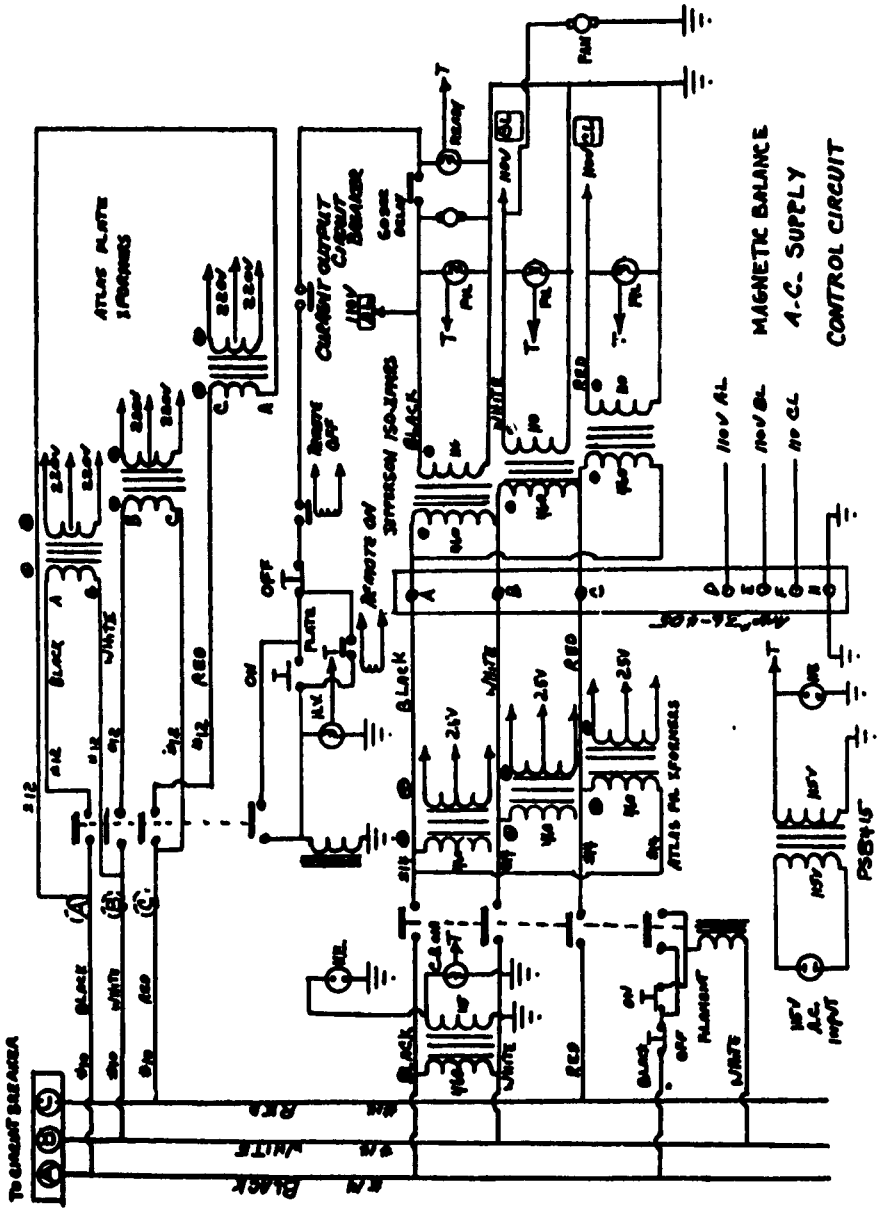

Figure 16. Magnetic balance AC supply control circuit

TABLE I

BALANCE PROCEDURE

1. Warm up system for 30 minutes.
2. Adjust bias volts for 6.5 volts.
3. Set master gain to zero, and phase gain controls for maximum.
4. Place 22 1/2 volts on input.
5. Plug external sync on scope into "ref A" (10v/cm. sens.).
6. Plug upper beam of scope into main supply output.
7. Plug lower beam of scope into "Test" (0.1v/cm. sens.).
8. Adjust sweep for 2 millisec/cm.
9. No output tubes should fire.
10. Adjust master gain control for 0.1 volts on "Test."
11. All output tubes should be on threshold of firing, adjust "phase adj" and "180° bal" for this condition.
12. Adjust master gain control for 0.2 volts on "Test."
13. All output tubes should be firing reliably and evenly matched. Adjust "phase" adjust and "180° bal" for this condition. Repeat steps 9, 10, 11, 12, and 13 until system is balanced for both conditions.
14. Adjust master gain control for large output. If output of tubes is not evenly matched, adjust phase gain controls for tube balance. Repeat steps 9, 10, 11, 12, 13, and 14 until system is balanced for all three conditions.
15. Pulses from output tubes should be identified on scope face with grease pencil to make above adjustments easier.

problem. Accordingly, a magnetizing assembly with physical and magnetic characteristics of the same order of magnitude as the proposed suspension magnet was borrowed. The general configuration of this unit is shown in Fig. 17.

The magnetizing assembly was first checked to determine its yoke and pole flux density characteristics. The results are shown on Fig. 18. The leakage flux of this unit was calculated and found to be 84 percent of the measured value.

With the magnetizing assembly mounted on the static test stand, as a replacement for the less powerful magnet of Fig. 4, the force data graphically presented on Fig. 19 was obtained. Note that the force versus NI curve for the Alnico V model is essentially linear for the major portion of the NI range investigated. The "leveling off" tendency of the curve is a saturation effect. Figure 6 shows that all of the permanent magnet materials have relatively low saturation values. The force curves for the electrical steel models are essentially quadratic as theoretically expected.

The force data presented on Fig. 20 was obtained with only one of the poles energized, and served to confirm the earlier assumptions made regarding the ability of a horseshoe magnet to produce moments as well as forces. Operating restrictions on the direct current source used with the magnetizing assembly were responsible for the difference in maximum NI values plotted on Figs. 19 and 20.

Using an electrical steel model, a series of force readings was also taken with the model located at four inches and at six inches from the magnetizing assembly. This information is presented on Fig. 21. To make the data applicable to operating distances other than four, five, and six inches, the three curves were reduced to the general relationship which is given on Fig. 22.[1] The theoretical change in the force

[1] Empirically $Fd^{4.6} = 0.0625\ (NI/pole)^2$

F = attractive force in ounces

d = perpendicular distance in inches

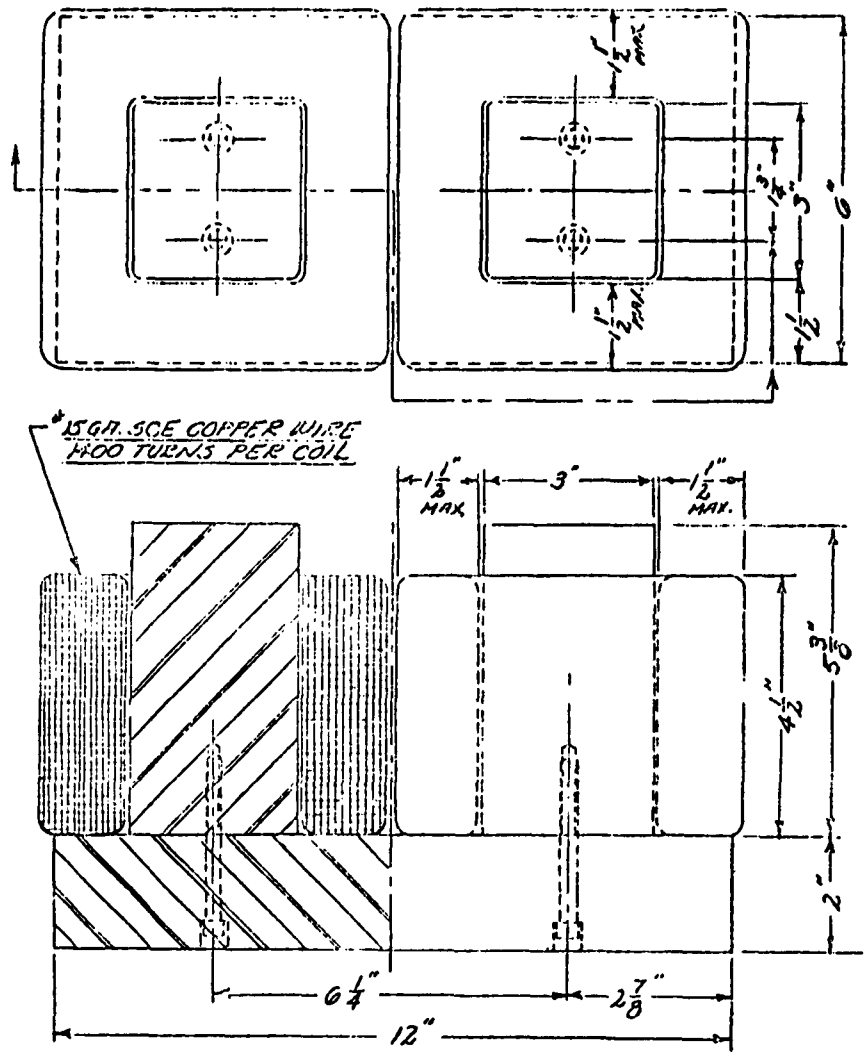

NOTE: ALL MATERIAL (EXCEPT WIRE) IS STEEL

RATED FOR 110 V.-9 AMPS. MAX.- NOT DESIGNED FOR CONTINUOUS USE

SCALE ½ SIZE

MAGNETIZING ASS'Y.
INDIANA STEEL PROD. CO.
FROM DWG. No. 27203B

Figure 17. Magnetizing assembly

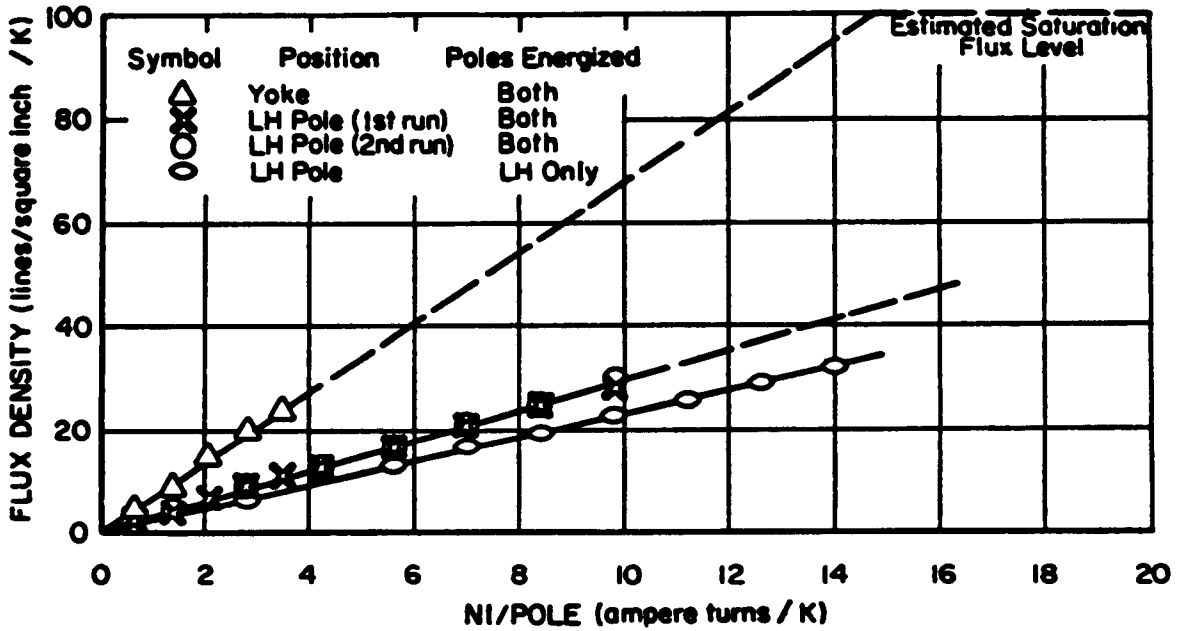

Figure 18. Flux density versus ampere turns per pole for the magnetizing assembly

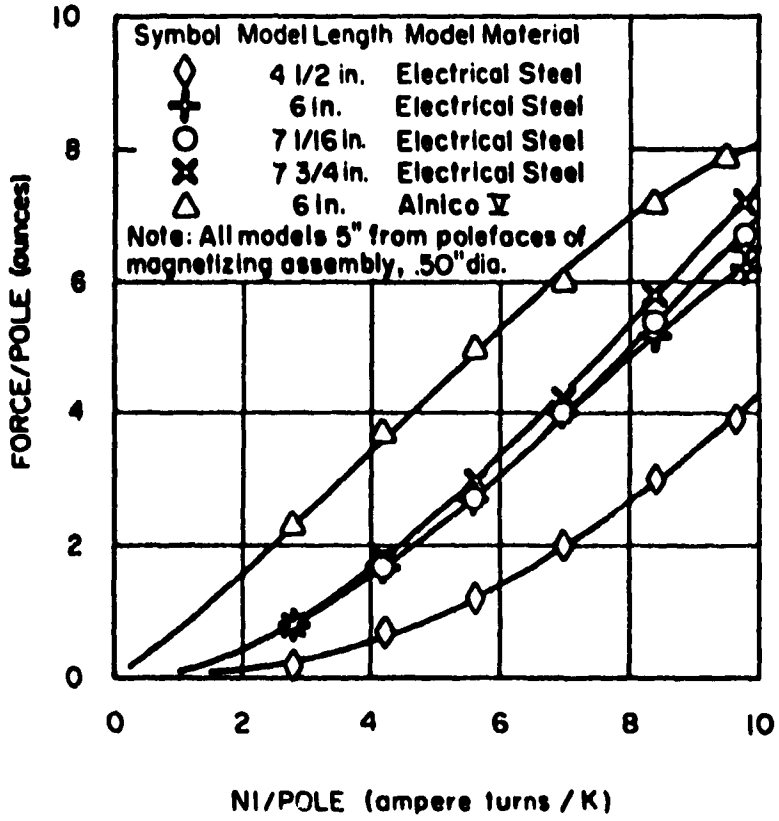

Figure 19. Suspension force versus ampere turns per pole for various models

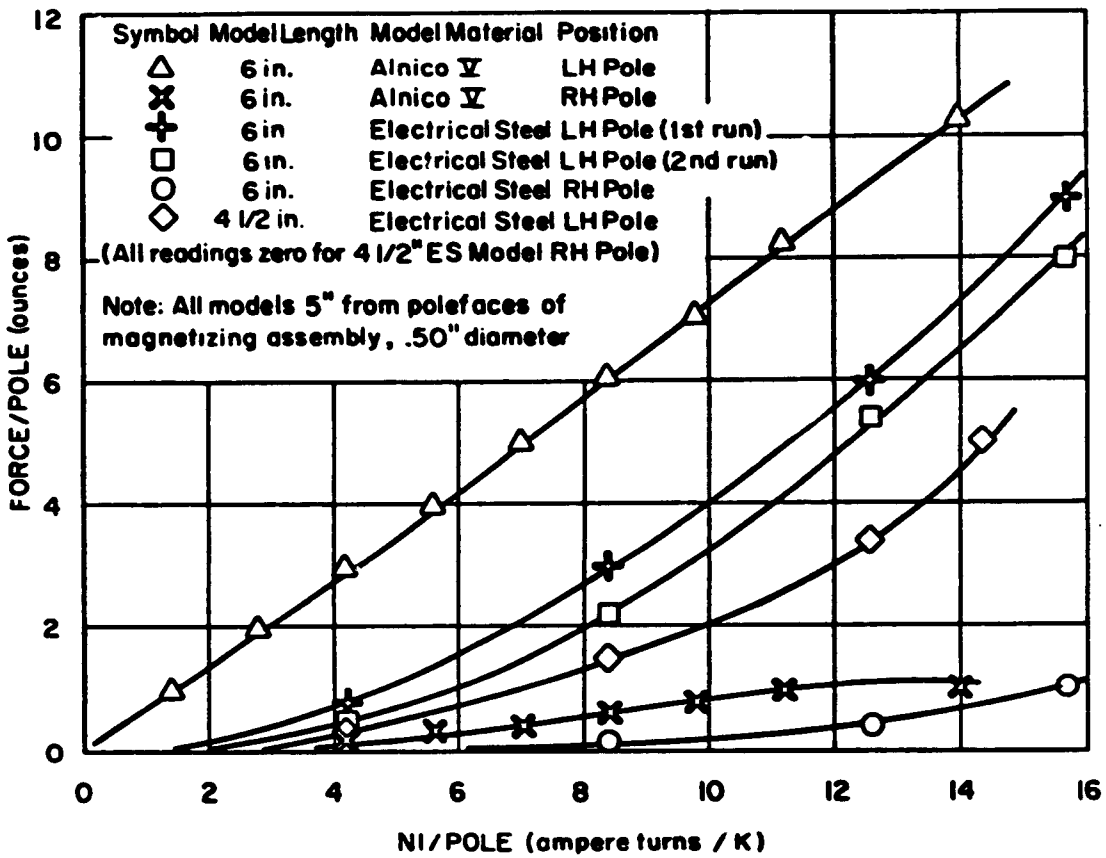

Figure 20. Suspension force versus ampere turns per pole for various models - LH pole only energized

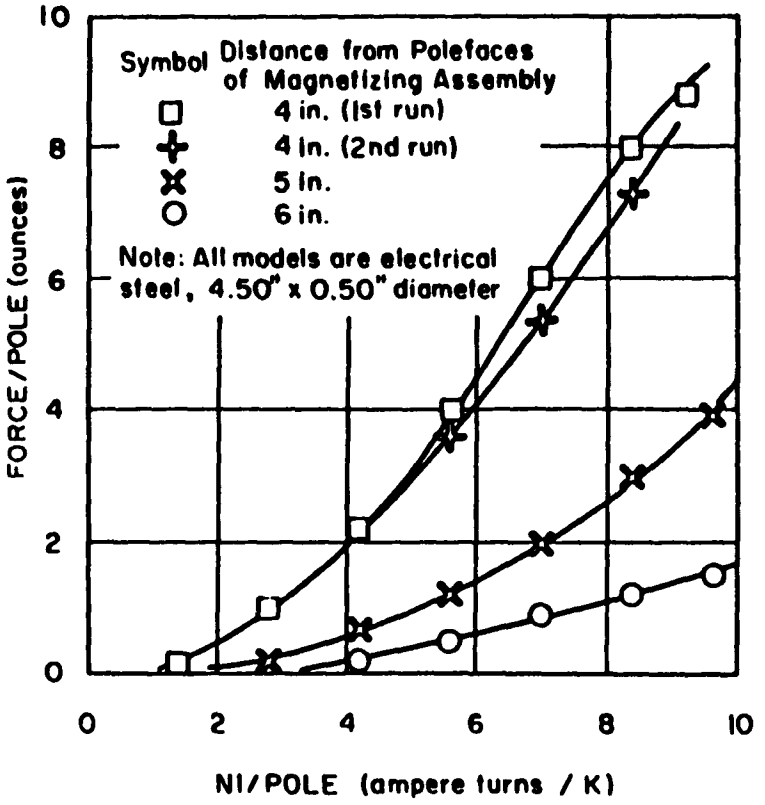

Figure 21. Suspension force versus ampere turns per pole for different distances

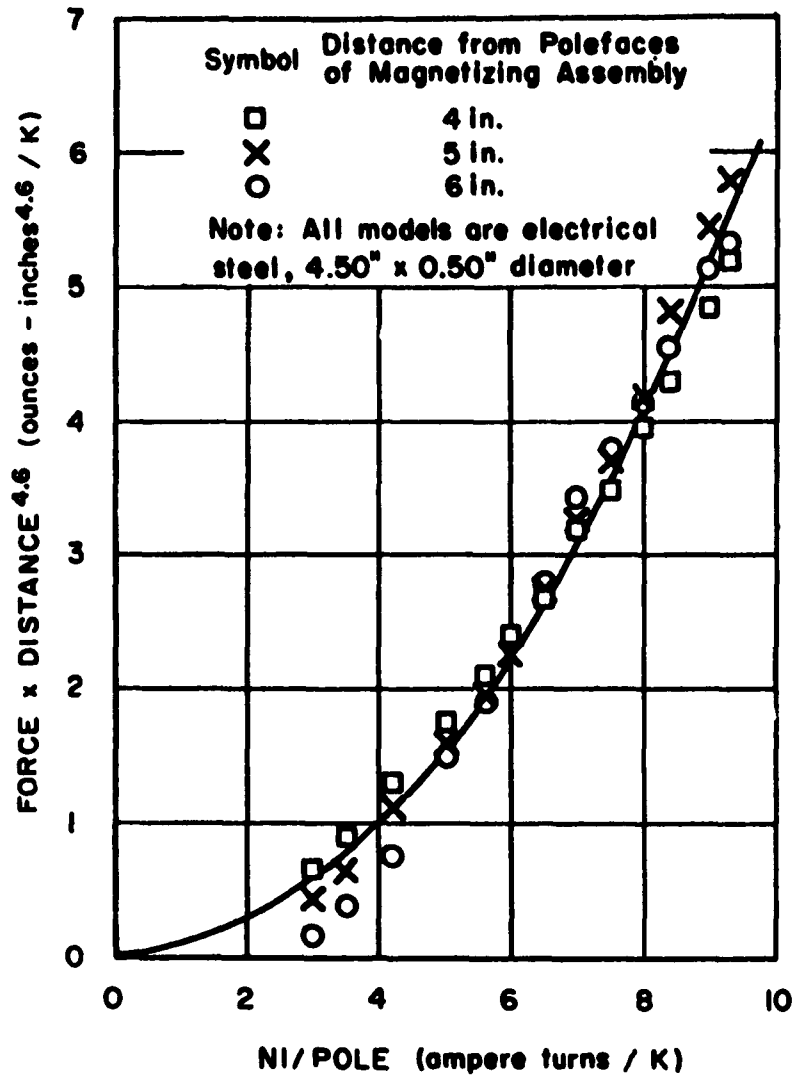

Figure 22. Suspension force × (distance$^{4.6}$) versus ampere turns per pole

level on a "soft" magnetic material, due to a change in the operating distance, is a fourth power exponential. Therefore, the experimentally determined exponential value of 4.6 seems to be quite reasonable. The additional increment is probably caused by a change in leakage properties.

The magnetic force exerted on a model is strongly influenced by the length of the model. Experimental data pertinent to this relationship is shown on Fig. 23. By reference to Figs. 17 and 23, it can be seen that the force curve leveled off when a model length was about one and one half the center-to-center distance between coils.

Design of Lift Magnet

It was specified that the suspension magnet should produce a force per leg of at least 10 ounces when acting on the standard ferromagnetic model. This figure was selected after considering likely total model weights and potential dynamic effects. Extrapolating the curves of Fig. 19, and considering the beneficial effect to be gained by tapering the legs of the horseshoe magnet core, a design figure of 20K NI per leg was selected. Making use of extrapolated flux density information from Fig. 18, the suspension magnet core was designed as shown on Fig. 24. The leakage flux for this tapered leg design was calculated and found to be 12 percent less than the value for a comparable unit with legs of uniform cross-sectional area. Furthermore, as the ferromagnetic model lengths are likely to be restricted to approximately the standard length chosen (six inches), the "spread" of the pole faces beyond this value should be held to a minimum as indicated by the previous discussion of Figs. 17 and 23.

A number of factors had to be considered in the design of the coil winding. As previously discussed, 30 amperes was selected as the maximum design current value. This determined a minimum N value per leg of approximately 670. Calculations of the heat to be dissipated at maximum power revealed that internal liquid cooling of the coils was mandatory. Various dimensional considerations dictated a maximum coil thickness of approximately one and one half inches.

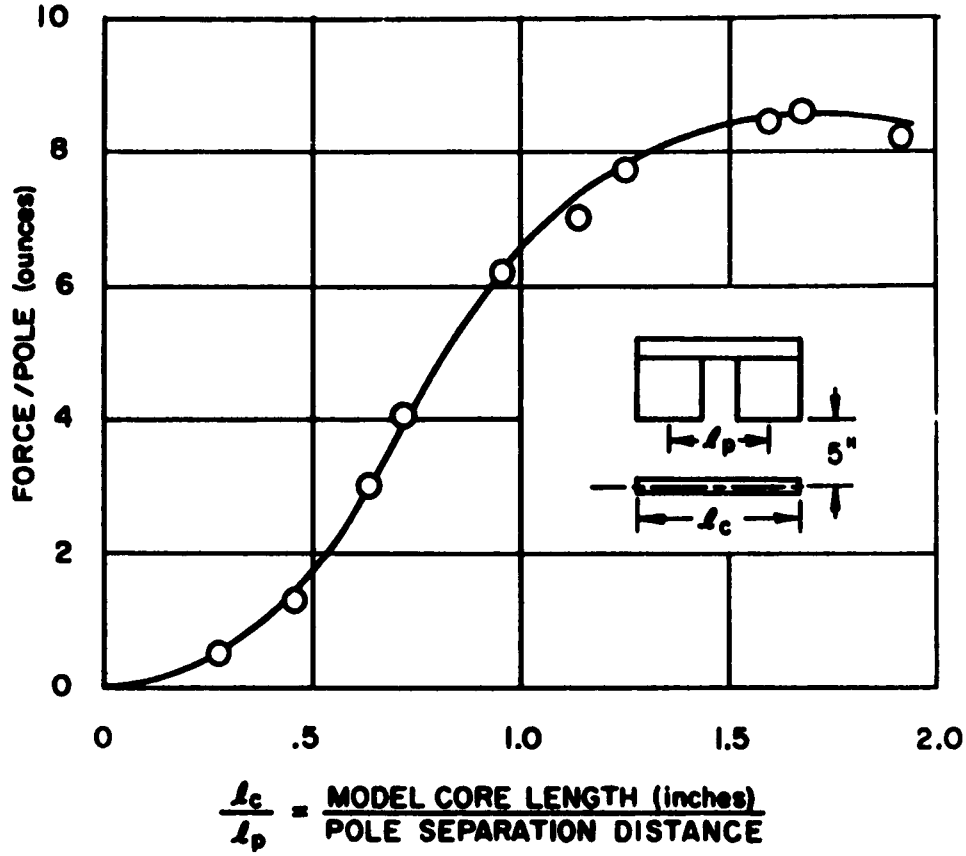

Figure 23. Suspension force versus model length.

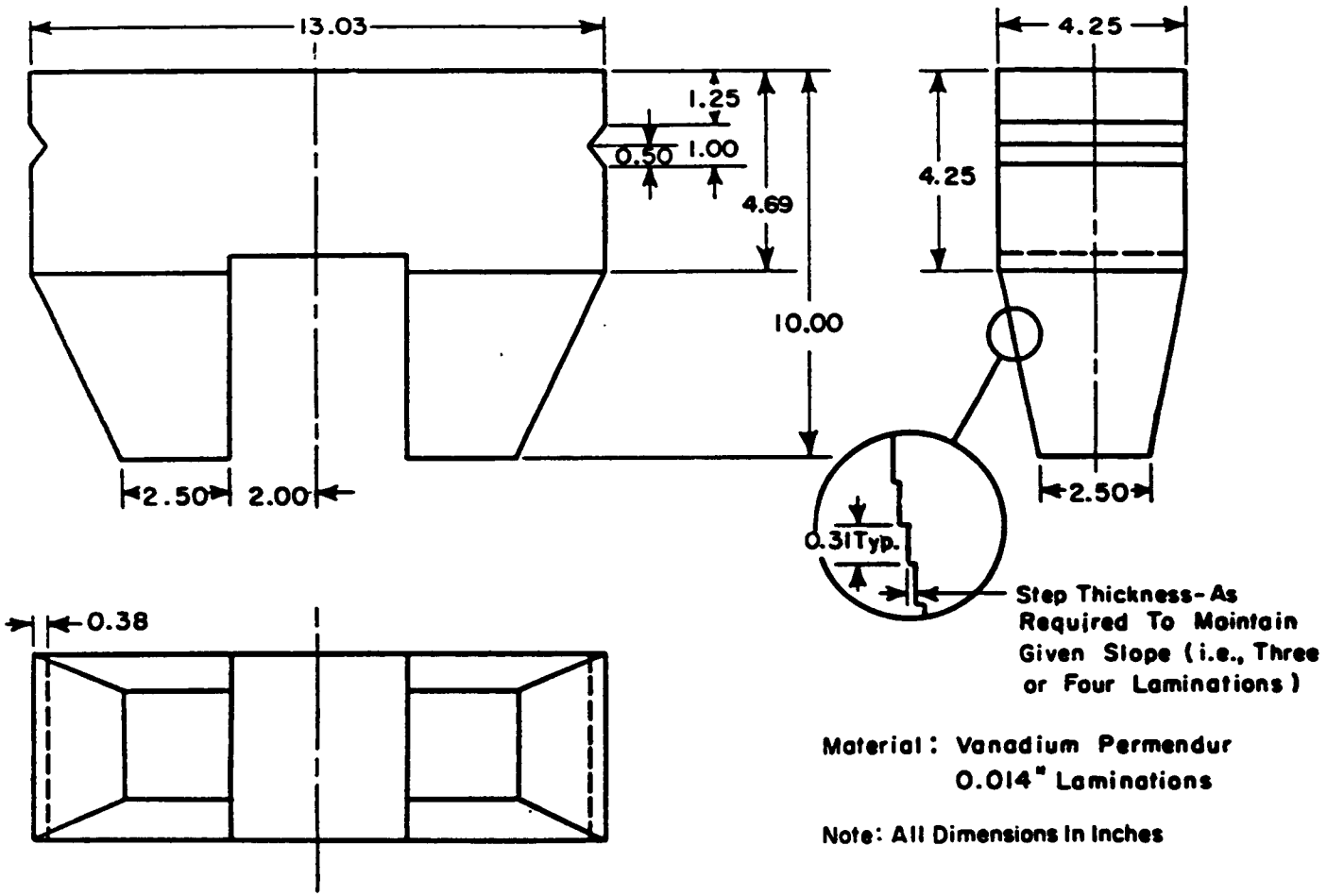

Figure 24. Suspension magnetic core.

Design of the Lateral Magnet

The purpose of the lateral magnet is to prevent lateral displacements of the model in a horizontal plane, and also to prevent rotation of the model about a vertical axis. To accomplish this, each coil must be separately energized and controlled by a feed back loop system nearly identical to those provided for the suspension magnet coils. However, since this unit does not operate against a steady force field, such as gravity, its force requirement is necessarily zero whenever the model is properly positioned. Hence, the input voltage reference signal does not contain the primary component specified for the suspension magnet system. Accordingly, considering that each lateral magnet pole can operate separately and does so about a zero voltage point, movement of an end of the model away from the desired position in a particular direction will develop a particular polarity of the nearest pole. Conversely, a movement in the opposite direction, from neutral, will develop the opposite polarity in the same pole. Hence, it is apparent that if the model is a permanent magnet, either an attractive or a repulsive force can be developed as required, and likewise a correcting moment. If the model, however, is composed of soft magnetic material, it would appear that development of a repulsive force would be impossible – and such would be the case without the influence of the suspension magnet. With the model being suspended, however, a strong induced polarity is present. Hence, the electrical steel model will react to the force field, or fields, of the lateral magnet in the same qualitative way as that discussed for the Alnico magnet model.

As was discussed above, it was impossible to determine a logical estimate for the magnitude of the maximum force and moment capability required of the lateral magnet. Hence, by an arbitrary decision, an initial lateral magnet was constructed with one fourth of the NI capacity specified for the suspension magnet. Its performance was unfortunately submarginal due to early saturation of the yoke. Used in conjunction with the magnetizing assembly and the two types of models, however, large enough lateral forces of both an attractive and a repulsive nature were developed to experimentally establish the feasibility of generating the required lateral forces.

For the design of the final lateral magnet, it was again arbitrarily determined that the NI capability should be one fourth that of the suspension magnet. The magnet core was designed accordingly, and is shown on Fig. 25. It was specified that the coil bank be wound with a double winding, so that each bank would contain two simultaneously wound coils of 442 turns each. By using the double coil winding it was felt that additional experimental information could be gained during future operations of the unit. As a further example of the potential use of the double winding, two different N values, and consequently I values, can be used to produce the same NI product. By this means, then, the effect of such a change on any of the system parameters can be determined.

The cooling system design for the lateral magnet will be discussed later.

Design of the Drag Solenoid

It is well known that an air core solenoid will produce a tractive force on a cylindrical ferromagnetic plunger which is centered in the radial plane of the solenoid, but whose center of mass is axially displaced from the mean radial plane of the coil. Such devices normally operate with some portion of the plunger enclosed by the coil. When the plunger is completely removed from the enclosed volume of the solenoid, the reduction in tractive force is severe, and for most solenoid operations, is considered to go to a zero value.[16]

The tractive force produced on a plunger positioned outside the solenoid is not zero, however, but only relatively small. If sufficient NI capability is incorporated in a solenoid which surrounds a wind tunnel, a tractive force can be produced which will effectively counter the air drag force on a model located a few inches downstream from the solenoid.

To determine adequately what cross section dimensions of the drag solenoid would give the most effective force capability, it was felt that a variety of drag solenoid models should be used in the static test apparatus. Accordingly, five coils were constructed with various combinations of mean diameter and numbers of turns. These coils are shown in Fig. 26. Three of them had 102 turns each, with mean

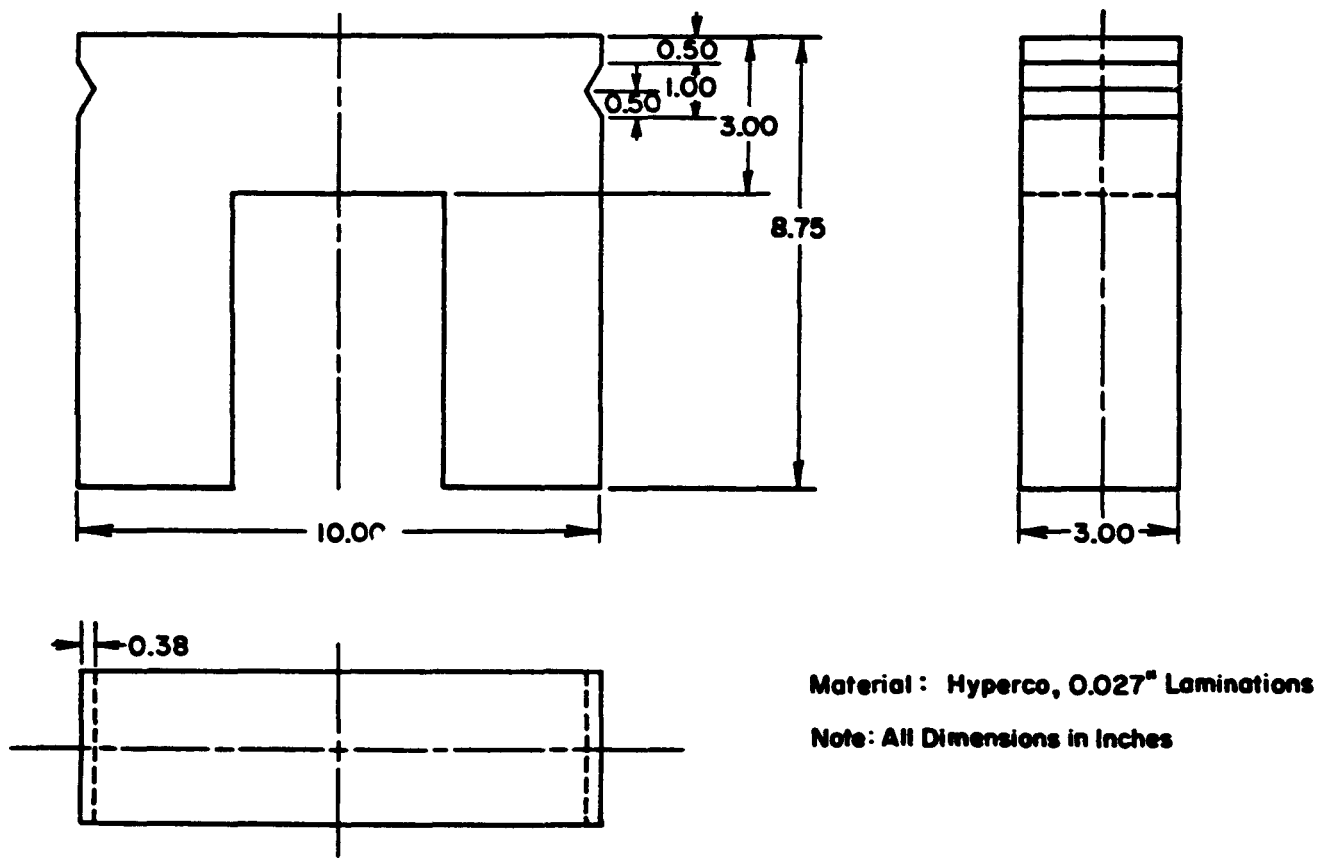

Figure 25. Lateral magnet core

Figure 26. Initial drag solenoid coils.

diameters of 8.5, 9.5, and 10.5 inches respectively. The other two each had a mean diameter of 9.5 inches, and had turn values of 54 and 192 respectively. They were operated over a range of 0 – 50 amperes. Significant drag solenoid forces were produced, however, on the electrical steel model when the magnetizing assembly was used to produce substantial suspension forces (and hence a high induced polarity condition). The magnetizing assembly was available on a short-time loan basis and had to be returned before a detailed experimental investigation of the drag solenoid design problem could be completed. Figures 27 and 28 present some of the data taken. The curves in Fig. 29 correspond to single turn coil theory.

As indicated earlier in this report, it was assumed that the design drag force should fall in the range of 8 to 16 ounces. Using the data presented on Figs. 27 and 28, and more significantly, the knowledge that the French ONERA drag solenoid was claimed to produce a force of approximately 11 ounces at an NI value of 23K, while using a model roughly comparable to the ones to be used with this system, a design value of 30K was selected for the drag solenoid. The internal dimensions of the drag solenoid were selected to be of sufficient size so that the unit may be used with either of the nozzles currently available for use with the 4" by 4" tunnel. An N value of 1000 turns was used and the same type wire was utilized for winding as for the other magnetic units.

Table II gives a summary of the magnet properties.

D. CONTROL SYSTEM

The magnetic balance will be useful as a wind tunnel tool only if the model can be controlled accurately and aerodynamic data can be obtained from the system. Since no physical supports touch the model, several requirements must be imposed on the control systems to insure the accuracy of the information which is taken from the model or from the electromagnets. The basic requirements are:

1) Model transient amplitudes during starting and stopping the wind tunnel must not exceed the limits of the optical system. Therefore, the control systems must be fast enough to accommodate the starting shock.

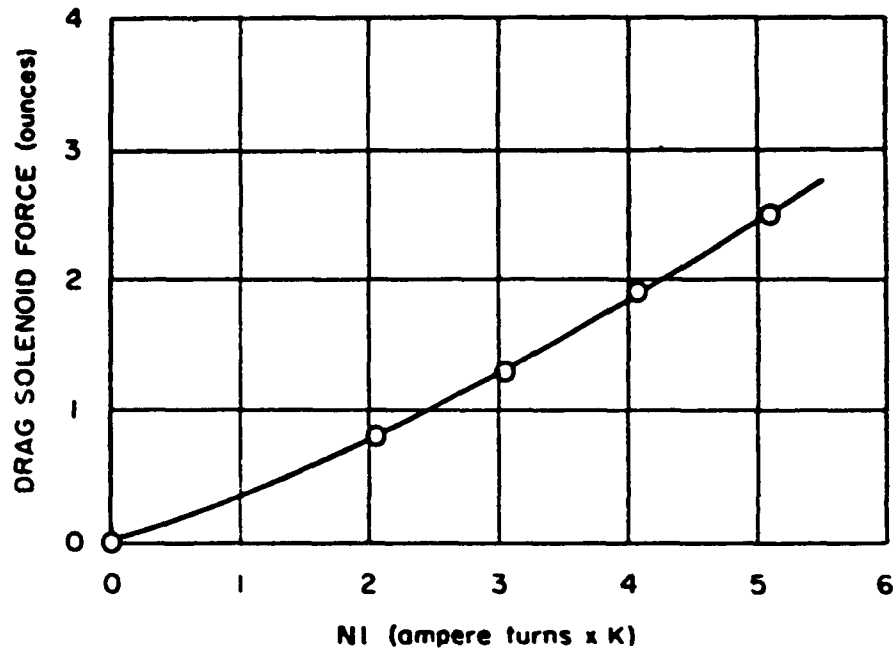

Figure 27. Drag force versus ampere turns in drag solenoid. Data taken with initial drag solenoid (102 turns-9 1/2" mean diameter). Model was 6" x 0.50" diameter Alnico V magnet, with near end of magnet located 3 1/2" from near face of drag coil. The magnetizing assembly had no significant effct on the counter drag readings.

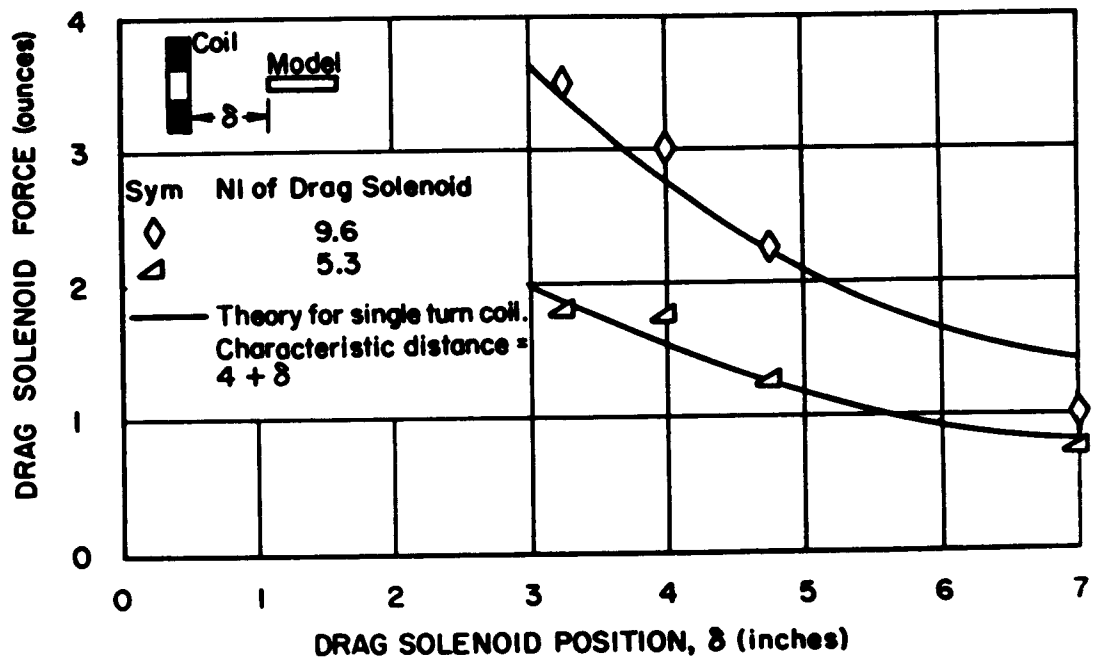

Figure 28. Drag force versus separation distance. Data taken with initial drag solenoid (192 turns - 9 1/2" mean diameter). Model was 6" x 0.50" diameter electrical steel and was positioned 5" from the magnetizing assembly. The magnetizing assembly was energized at 8.4K per leg. Separation distance was measured between near end and near face of model and coil respectively.

TABLE II
SUMMARY OF MAGNET PROPERTIES

Lift System

Core –	Laminated Vanadium Permendur
Flux –	26,760 NI/leg
Turns –	892/coil (two coils)
Force –	10 oz at 4" distance for 6" long model
Current –	30 amps

Lateral System

Core –	Laminated Hyperco
Flux –	6,690 NI/leg
Turns –	446/coil (four coils)
Force –	2.5 oz/leg at 4" distance for a 6" long model
Current –	15 amps

Drag System

Core –	Air
Flux –	30,000 NI
Turns –	1000
Force –	8 – 16 oz at 4" from face
Current –	30 amps

2) The model must be held in the uniform part of the flow and must not oscillate or drift beyond specified limits during steady-state conditions. This allows accurate determination of forces and moments.

Supporting an object with a DC magnetic field is analogous to hanging an object on a spring with a negative spring constant. At the point in the field where the magnetic force just balances the gravity force a condition of unstable equilibrium exists. A slight displacement in either direction will result in the object being accelerated in that direction.

To achieve stability at a given position in the field the currents in the magnet coils must be controlled. Since, in this case, model position information is available from the optical system as an electrical signal, this signal, after suitable operations with a compensation network can be used to govern the amount of current in the magnet coil.

For purposes of discussion consider a "rate plus proportional" control system. Its electrical output is proportional to model position and the time derivatives of model position. This system develops a steady-state position error for steady-state loads and controls the small perturbations about the steady-state position. The major disadvantage of this control system is that changes in steady-state loads result in changes in steady-state position. As it is important to control the model position with respect to the wind stream and the magnets, position errors cannot be tolerated. Thus the simple control system needs integral as well as rate and proportional control. Since the model position is integrated over time the model is held at a predetermined position regardless of load. In other words, the integrator provides a bias current that reduces the steady-state position error to zero. This modified system was chosen to be the basis for the control system. In the following discussion the optical position sensors are discussed first. This discussion is divided into optical and electrical elements. Then the model control system is discussed.

The Optical Model Position Sensing System

Five optical systems are required for error signal information. The two lift and the two lateral optical systems are identical in

construction and in their operational characteristics. The drag optics use a different technique and therefore some of the components of this system differ from the lift and lateral optics.

1. Optical Components

a. Lift and Lateral Optical System

In the early ONERA system the model was located in a parallel light beam which was collected and focused on a photoelectric cell (Fig. 29). Under these conditions the optical system would be sensitive to model position perpendicular to the optical axis and insensitive to model movement parallel to the optical axis. Unfortunately the range of model displacement perpendicular to the optical system shown in Fig. 29 is limited, which makes the range of pitch and yaw angles very small.

A second type of system that was used initially in the M.I.T. experiments is shown in Fig. 30. The diameter, or height of the beam, is equal to or larger than the model diameter or height which allows a large displacement of the model in the light beam. The light beam is masked in a manner which allows no ambiguity in light output to the photocell within the optical system field of view. It can be seen in Fig. 30 or Fig. 31 that as the model moves down, less light will fall on the photocell and when the model moves up, more light will fall on the photocell.

The optical mask presently in use is a combination of those shown in Figs. 29 and 30. The beam width was reduced to about the model diameter, but the system incorporated a tapered mask. This compromise reduces the maximum angle of attack range but provides increased output from the bridge. The compromise configuration is also less sensitive to the perturbations of the light path due to the heated jet of air and the shock waves.

The photocell is electrically connected to a bridge circuit and the bridge is adjusted so that the output will be zero when the model is centered in the optical system. Under these conditions the pitch angle of the model will be zero.

It is possible to achieve positive or negative angles of pitch by a number of methods. One could unbalance the bridge circuit with a

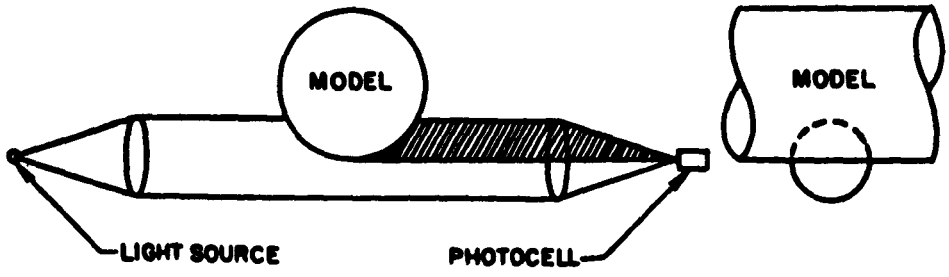

Figure 29. Early ONERA optical system.

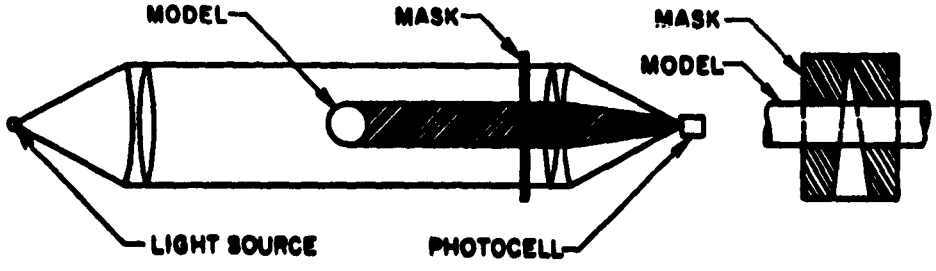

Figure 30. MIT system of optics.

Figure 31. Angular orientation of model.

variable resistor in one arm of the bridge which would shift the zero point in the optical system to some new position. Alternatively the bridge could be balanced for zero output when the model is centered in the optical system and then positive or negative voltages are added to the output of the bridge circuit. This method effectively shifts the zero point of the optical system. If a positive angle of pitch is desired, then the zero point of the forward lift optical system would be shifted up (Fig. 31) and the zero point of the aft optical system would be shifted down. In practice the model is angulated by changing the reference voltage of the integrator in the control system. In operation, this method is effectively the same as one which employs movement of the zero point of the optical system. The lateral optical system is identical in construction and operation, and is shifted 90° about the wind tunnel axis with respect to the lift optical system.

It was found necessary to fold the optical system of Fig. 30 in order to fit within the available space. The wind stream comes within a few inches of the lift and lateral electromagnet pole faces (See Fig. 32) which makes it impractical to collect and focus the light beams on

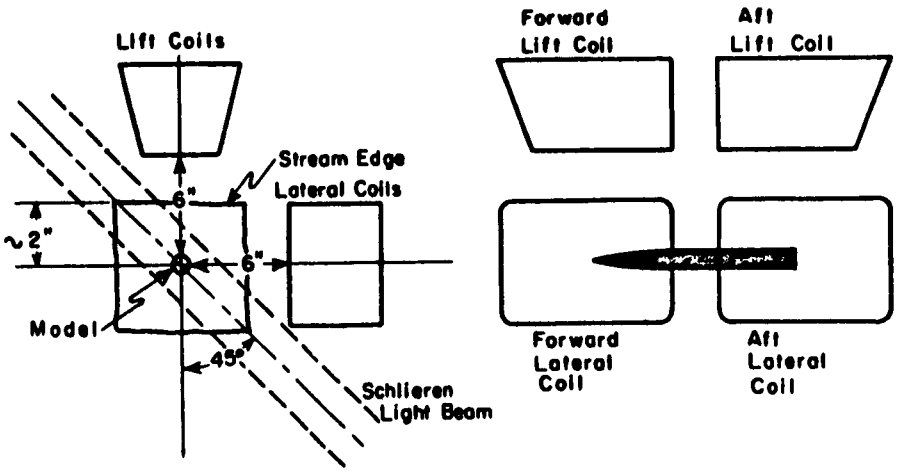

Figure 32. Geometry of optic installation

photocells in the distance available. The final form is shown in Fig. 33. The light from the bulb is collected and collimated by the lens. This parallel light beam passes by the model to a front surface mirror, which is covered by a suitable mask for model position control. The light is then reflected back past the model as parallel light and collected by the same lens and focused on the photoelectric cell.

As shown in Fig. 33, the light beam striking the mask can be rectangular in shape. Round achromatic lenses were purchased and cut to a rectangular shape by a local optical firm at low cost. Because of the high temperatures in the vicinity of the lens it is important that all cemented components use a high temperature thermosetting cement. By using rectangular shaped optical systems it is possible to have both lift optical beams and both lateral optical beams separated by a short distance when using small models. The system shown in Fig. 33 performs best when the photocell and light source have the smallest possible separation and the light source is a high intensity point source. With a need for a well defined parallel light beam with a practical finite light source, the focal length of the lens should be as long as available space permits.

The lenses used in this system have a focal length of 5 3/4 inches. In order to position the reflected light on the photocell the mirror is fully adjustable in horizontal and vertical tilt with spring loaded screws. The light source used in the optical systems is a Chicago miniature lamp, model number CM8 634. The lamp envelope is 0.175 inches in diameter and 0.46 inches in length. For operation with 6 volts at 0.200 amps the life expectancy is approximately 500 hours.

It is desirable to use a small photocell because of the folded optical system and yet have the photocell wired to a bridge circuit as one of the elements. A low impedance bridge circuit is necessary in order to keep electrical pickup problems down and reduce the output loading effects on the bridge.

The Clairex type CL3A cadmium selenide photocell satisfied the above requirements and was used in the bridge circuit. Unfortunately this cell is temperature sensitive and must be mounted in a location or holder where the temperature is relatively constant. Temperature

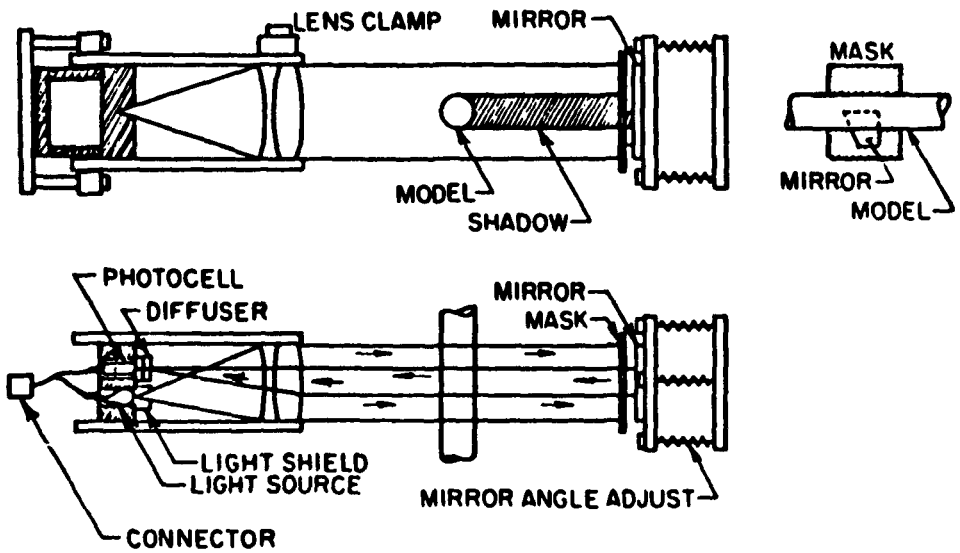

Figure 33. Folded optical system

control of the photocell is discussed in another section of this report.

The light source assembly and the mirror assembly are independently clamped on rigid supports and are fully adjustable in two directions. This facilitates the use of various model shapes and sizes.

The system shown in Fig. 33 is very sensitive to vibration as any displacement of the image on the photocell will result in a large output signal. This problem is eliminated by placing two opal glass light diffusers over the entire face of the photocell. The point source image falling on this surface is diffused and falls on a larger area of the photocell than the active area. Under these conditions any displacement of the image due to vibration, or shock wave effects is greatly reduced. Nonuniformities in the active area of the photocells are also canceled out with this technique.

Optical alignment of the system is easily accomplished by looking through a hole in the side of the cell holder and adjusting the mirror until the light source image falls on the opal glass. Once this is done, the output of the bridge circuit is observed and the mirror is adjusted until the bridge output indicates the photocell is receiving maximum illumination.

In order to reduce internal reflections in the optical system, the interior of the light-source-photocell-lens assembly was painted flat optical black and a light shield with a small aperture was placed in front of the light source.

The above optical system is reliable in use and is unaffected by normal room illumination. The system is efficient optically and provides more than adequate illumination with the various masks.

b. Drag Optical System

The location of a drag optical beam is shown in Fig. 34. As the model is forced back due to drag forces, less light is allowed to pass to the photocell and the drag bridge produces an output signal to the amplifiers. Unfortunately with this simple system the model misses the drag optical beam as the model angle changes. Therefore, a two beam or double pass optical system (Fig. 35) is required to allow larger

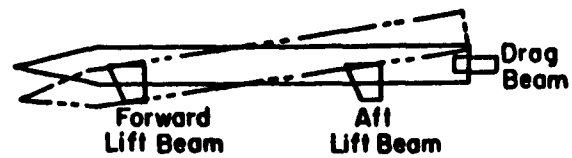

Figure 34. Influence of angle of attack on single element drag optics.

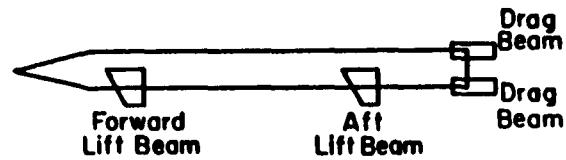

Figure 35a. Double drag optics.

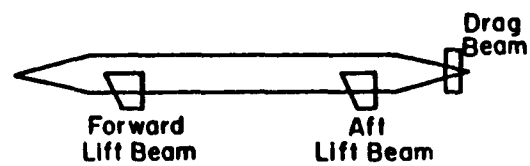

Figure 35b. Drag optics for pointed base model.

model angles. A method of doing this is shown in Fig. 36. The light source is located at the focal point and on the optical axis of a 5 3/4 inch focal length lens. This parallel light beam then passes by the model to a prism and is reflected twice. The return beam is displaced, inverted, and made parallel to the first beam. This parallel light is collected by a second 5 3/4" focal length lens and focused on the photocell. The light source has a shield in order to reduce internal reflections and the photocell has the opal glass diffuser to reduce the problems of vibration and cell nonuniformity described previously. The shape of the optical beam is controlled by a mask located on the prism, and the design of this mask is determined by the model. If a model with a pointed aft section (Fig. 35b) is used in the wind tunnel, the drag optical system described above would be replaced with an optical system similar to the lift and lateral systems. It can be seen in Fig. 35b that as the model is displaced axially the amount of light passed to the photocell is changed.

c. General Remarks

Many of the mechanical components of the drag, lift, and lateral optical systems are identical and all systems use the same type photocells and light sources.

Because of its location all material, hardware and support members of the optical system must be nonmagnetic. If this precaution is not taken, the magnetic field of the various magnets will be distorted, which would lead to an unpredictable system. All mirrors are front surface aluminized with a protective layer of silicon monoxide. The small rectangular block that holds the photocell and light source is clamped in position with set screws in the rectangular tube which holds the lens. All lenses are held in position within the rectangular tube with a clamping device (Fig. 37) which consists of a set screw and lock nut, brass pad, and a rubber pad which is in contact with the lens. With these methods adjustment or replacement of any portion of the optical system is easily accomplished.

A simplified schematic of the various optical systems and locations is shown in Fig. 38.

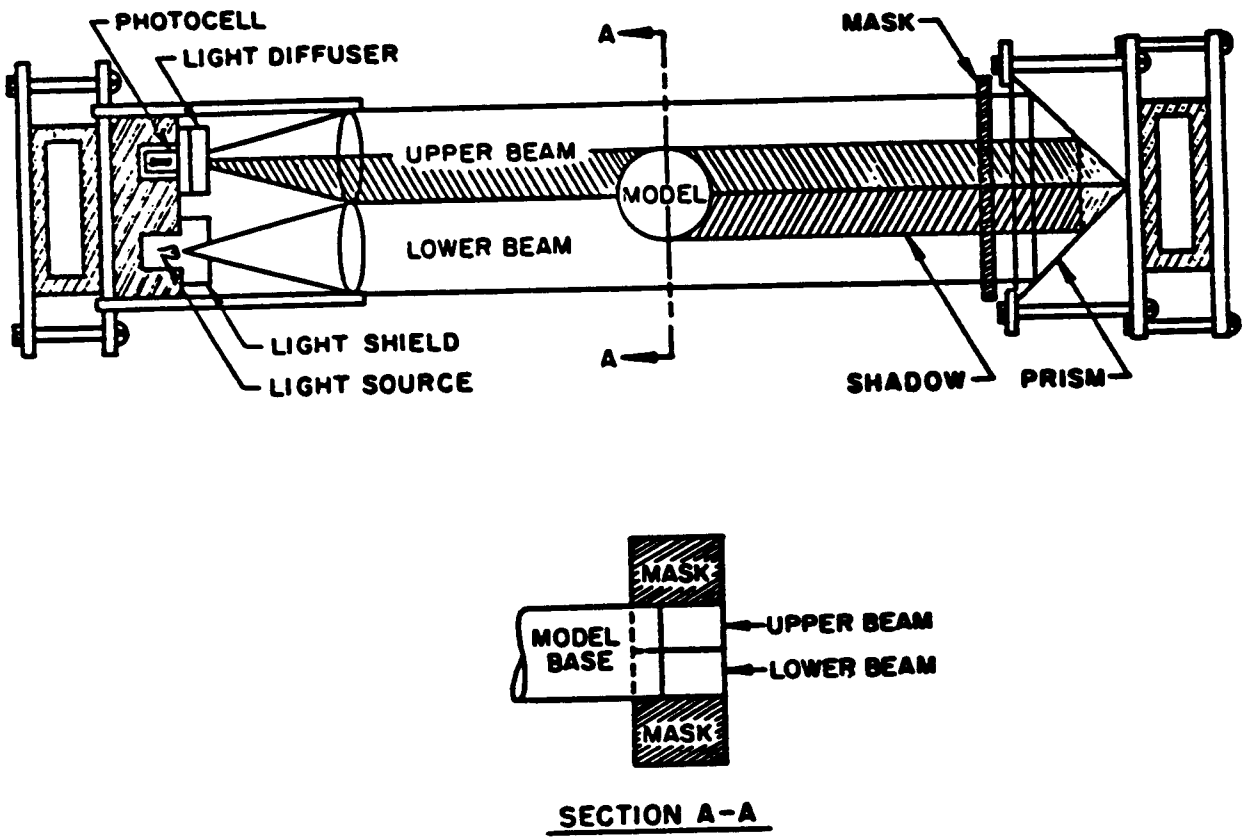

Figure 36. Side view of double drag optics

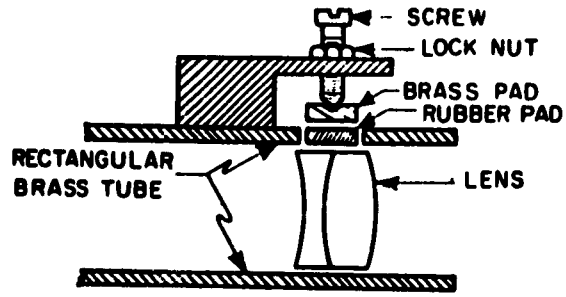

Figure 37. Lens holding assembly.

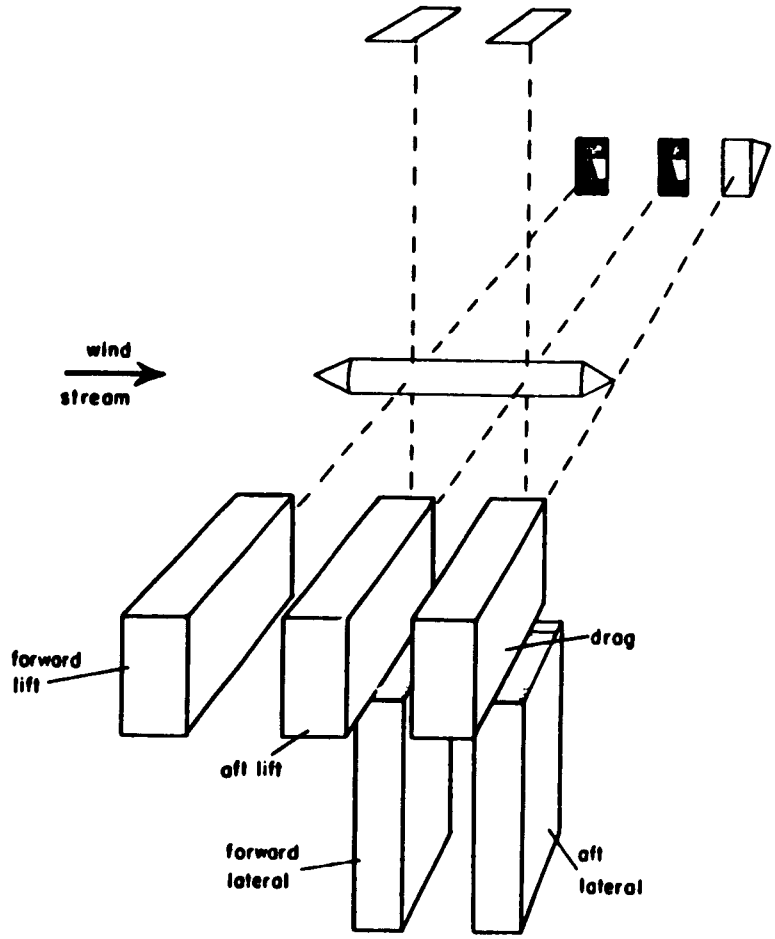

Figure 38. Schematic of lift, lateral, and drag optical systems.

2. Electrical Components

a. Photocell Bridge Circuit

The electrical output of the photocells must be modified before it can be useful as an input to the main power supplies. This is accomplished with a wheatstone bridge circuit and compensation networks consisting of Philbrick differential operational amplifiers which perform proportional rate and integral operations. The compensation networks will be discussed below.

The diagram of the bridge circuit is shown in Fig. 39. The nature of a bridge circuit requires either ungrounded power supplies for bridge excitation or ungrounded input and output connections. For this system it was decided to have a common grounded input and output connection. The photocell is connected to the bridge circuit with approximately 20 feet of insulated coaxial cable. Precautions were made to prevent the braided shield of this cable from touching ground at any point along its length in order to eliminate ground loops. The ground connection is made only at the cabinets which contain the bridge circuits and compensation networks. The coarse balance adjustment is a conventional single turn rheostat and the fine balance adjustment is a 10 turn rheostat with indicating dial. The power supply for the bridge excitation is a 90 volt battery, and a separate battery is used for each of the five bridge circuits. The bridge circuit, batteries and adjustment potentiometers are located in a shielded chassis in order to keep AC pickup and noise in this circuit at a minimum.

b. Bridge Balance Procedure

To balance the bridge circuit electrically (zero volts output) the model is mechanically held on the wind tunnel axis with no pitch or yaw angle. The fine balance rheostat is set to its midrange position and the bridge is then balanced for zero output with the coarse balance rheostat. Zero output is indicated on a zero center galvanometer with a 50 microampere sensitivity which is mounted on a control panel in the bridge circuit cabinet. The bridge to be balanced is connected to the test circuit with a selector switch. A spring loaded push button switch is then pressed in order to connect the galvanometer to the output

of the bridge circuit. The galvanometer is a low impedance device and is used only to indicate a null position on initial setup. The spring loaded push button switch eliminates the possibility of leaving the low impedance galvanometer connected to the output of the bridge circuit during normal circuit operation. This galvanometer is also used to establish the zero output setting on the voltage sources for model angle control described in another section of this report. A diagram of the test circuit is shown in Fig. 40. In addition to the panel meter there is a portable meter for making adjustments in locations where the panel meter is not visible.

The sensitivity of the lift and lateral optical systems is approximately 100 volts per inch. The above sensitivities are measured at the output of the bridge circuit.

The optical system signals are arranged so that the magnets do not receive power when there is no model in the light beams.

c. Light Source Power Supply

The light source used in the optical system is a model CM8-634 Chicago miniature lamp. The power requirement for this lamp is 6 volts at 0.200 ampere.

The voltage applied to this lamp must be regulated, as any change in lamp voltage would change lamp intensity which would result in a photocell bridge circuit zero shift. The power to this lamp must also be ripple free, direct current. Due to the characteristics of this lamp, any AC component in the light source power supply will produce a modulated light output which would be received by the photocell. This flase signal would then appear as an output from the bridge to the compensation network with unpredictable results. A diagram of the power supply used to energize the five light sources is shown in Fig. 41. This regulated power supply has an output of 7 volts DC with an available current of 1.2 amperes and an AC ripple less than 200 microvolts. All five light sources are energized by this one power supply.

d. Model Angle Control and Power Supply

In order to change the model pitch and yaw angles, or reposition the model axially in the wind tunnel, positive or negative reference voltages must be supplied to the integrators in the control circuits.

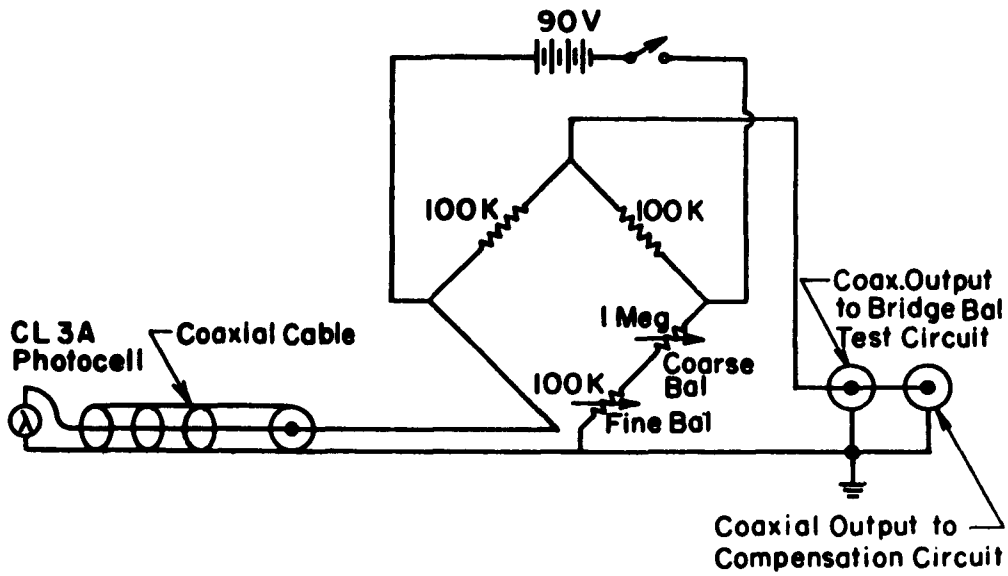

Figure 39. Photocell circuit.

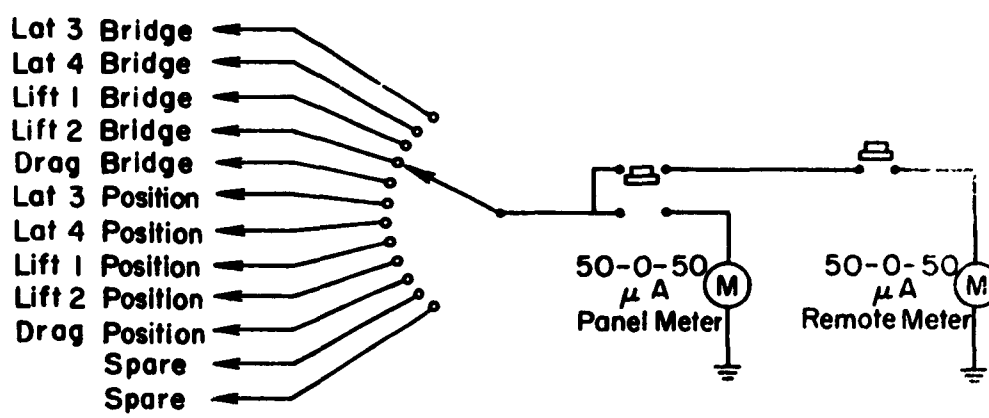

Figure 40. Bridge balance test circuit.

This is done electronically with differential amplifiers in the compensation networks. The model angle control circuit is shown in Fig. 42. The model angle controls are ten turn precision potentiometers with digital indicating dials. The two power supplies used to energize this circuit are the same type (Fig. 41) used to energize the optical system light sources. The system is initially set for zero output voltage when the potentiometers are positioned midrange.

Model Control Networks

1. Drag Control System

The configurations of the magnets and model are shown in Fig. 43. The drag solenoid controls longitudinal movement, the lift magnet controls vertical and pitch movements and the lateral magnet controls lateral and yaw movements. The five coils (one on each leg of the horseshoe magnets and the drag solenoid) are controlled independently by five compensation works that receive independent signals from the optical system as discussed above. The control of the sixth degree of freedom (roll) will not be discussed here.

The drag solenoid controls only one degree of freedom. Therefore the drag system was chosen as the starting point for design of the compensation networks, since it is the least complicated of the five systems.[17]

Several methods are available for determining the operational form of the stabilization networks. The root-locus method was chosen here because of its value in indicating time domain characteristics on the complex plane. A block diagram of the drag system is shown in Fig. 44. It is a one loop configuration with negative feedback.

Referring to Fig. 44 the force acting on the model is the aerodynamic drag minus the magnetic force due to current in the solenoid. If the magnetic polarization of the model is considered to be independent of the solenoid current* the magnetic force can be written as

$$F_M = \frac{AI}{(x_0 + x)^2} \qquad (1)$$

*The validity of this assumption will be discussed as part of the model calibration.

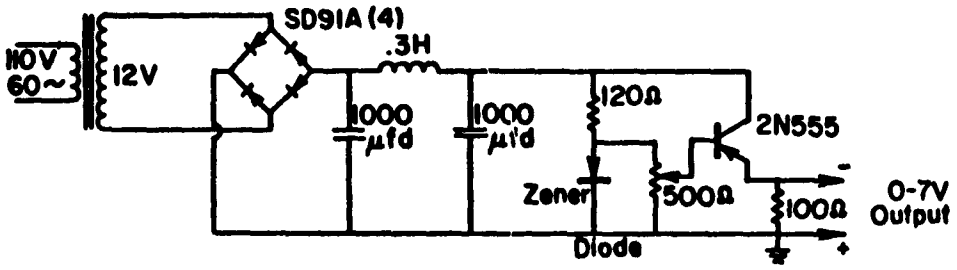

Figure 41. Light source power supply.

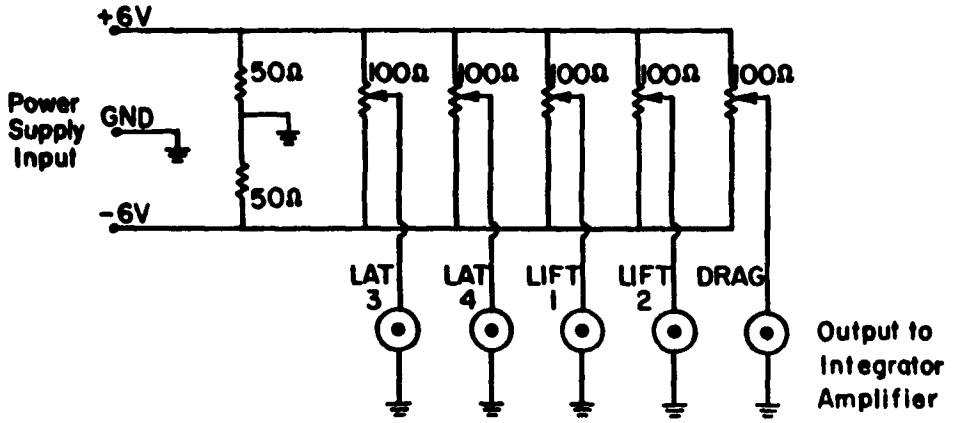

Figure 42. Model position control circuit.

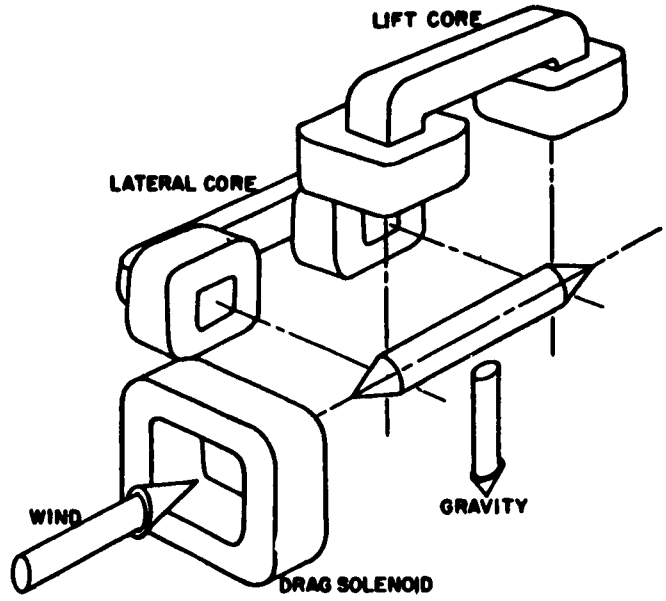

Figure 43. Magnet configuration.

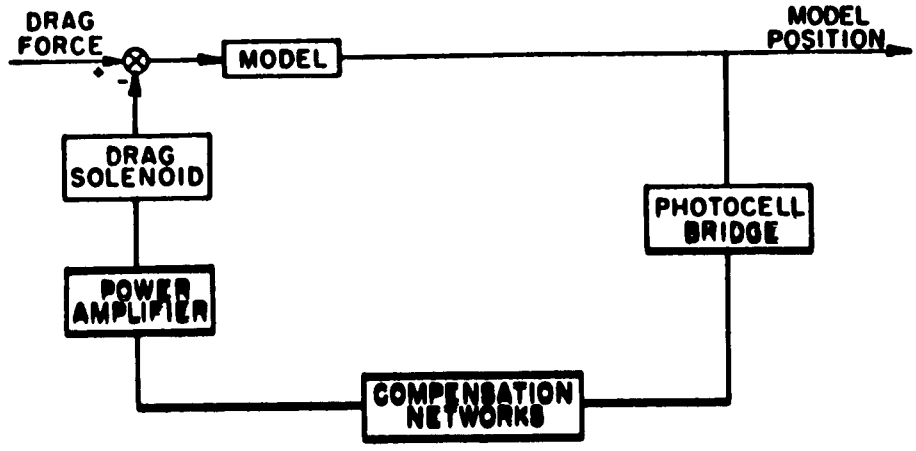

Figure 44. Drag system block diagram.

where I is the current and A is a constant. If x is much less than x_0 (small perturbations) then the binomial expansion gives

$$F_M = \frac{AI}{x_0^2}\left(1 - \frac{2x}{x_0} + \ldots .\right) \tag{2}$$

$$\cong \frac{AI}{x_0^2} \tag{3}$$

The current in the solenoid as a function of the voltage (V) across its terminals may be written in Laplace notation as

$$\frac{\bar{I}}{\bar{V}} = \frac{1/R}{1 + (L/R)\,p} \tag{4}$$

where the bar on the symbol indicates a variable in the Laplace domain and p is the Laplace variable. R and L are the resistance and inductance of the solenoid. Combining (2) and (3)

$$\frac{\bar{F}_M}{\bar{V}} = \frac{A/(x_0^2\,R)}{1 + (L/R)p} \tag{5}$$

If the basic configuration of the loop is now considered, there are two time integrations to obtain model position, a time integration in the feedback loop for integral control and a time lag in the solenoid. On a root locus plot these correspond to three poles at the origin and a pole on the negative real axis. This configuration is unstable for any value of open loop gain. To stabilize the system, the loci of the characteristic roots of the system must be forced to lie in the left half of the complex plane at the operating value of the open loop gain. This can be accomplished by operating on the model position signal in the feedback loop with a suitable compensating network. The form of this network can be determined by positioning zeros on the complex plane (Fig. 45) until the desired closed loop performance is indicated by the root locus. A detailed account of this analysis can be found in Ref. 17.

After the theoretical characteristics of the control system are determined an electrical network must be synthesized to perform the

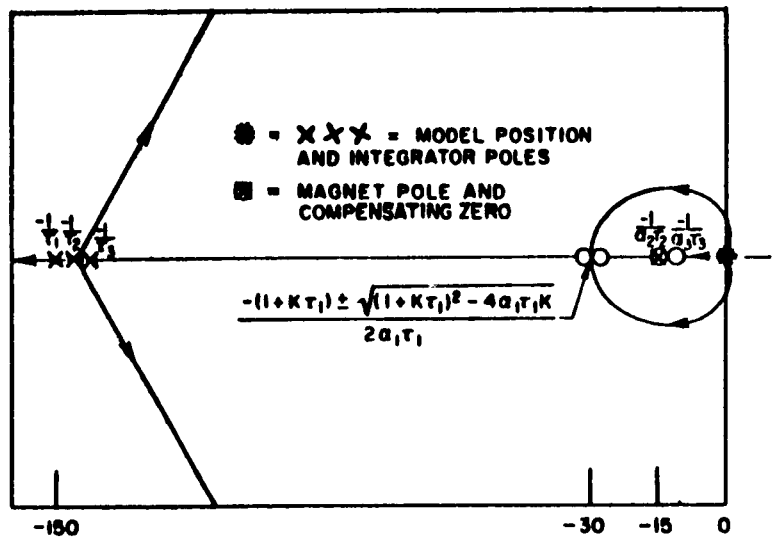

Figure 45. Drag system schematic root locus plot

operations on the signal from the optical system. The performance function of the network to be synthesized is:

$$P.F. = \frac{[\alpha_1 \tau_1 p^2 + (1 + K\tau_1) p + K] (1 + \alpha_2 \tau_2 p)(1 + \alpha_3 \tau_3 p)}{p(1 + \tau_1 p)(1 + \tau_2 p)(1 + \tau_3 p)} \qquad (6)$$

where the time characteristics (τ's, α's) are indicated in Fig. 45. The distribution of the operations is shown in the block diagram (Fig. 46). The network (Fig. 47) was synthesized with as much passive circuitry as possible to keep reliability at a maximum. Also, it was desirable to make most of the circuit components variable since the theoretical analysis did not take into account all of the physical characteristics of the system.

Figure 47 shows the necessary isolation of the control network from the optical system to avoid loading the photocell bridge. The isolation amplifier is followed by a lead-lag network and then an

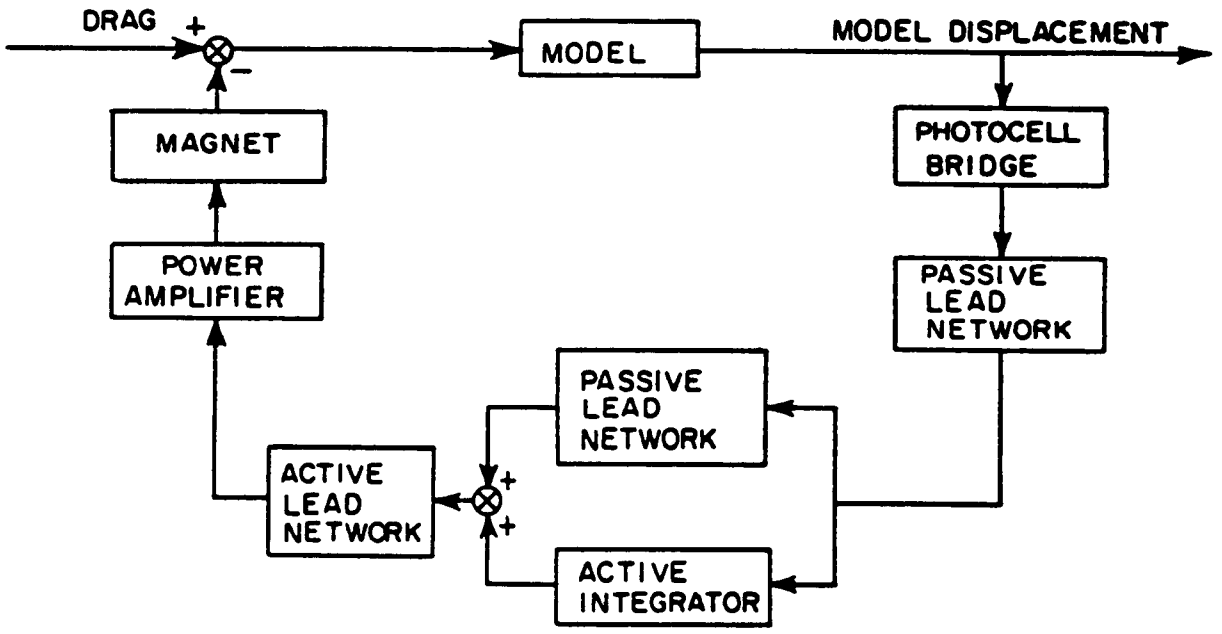

Figure 46a. Block diagram of the drag system

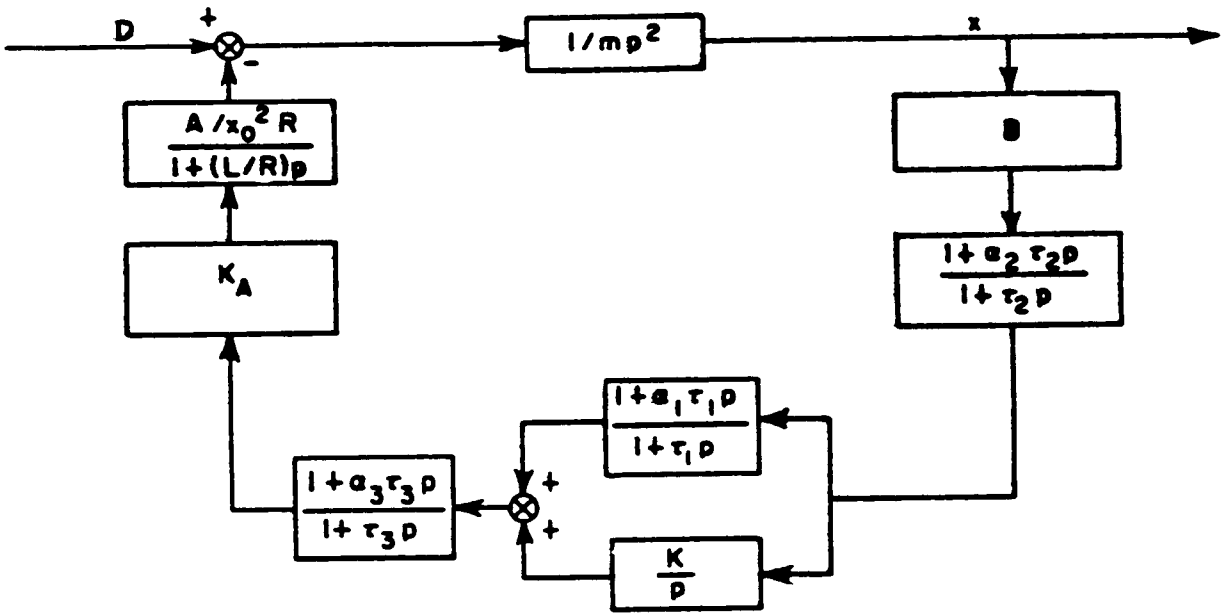

Figure 46b. Operational block diagram of the drag system

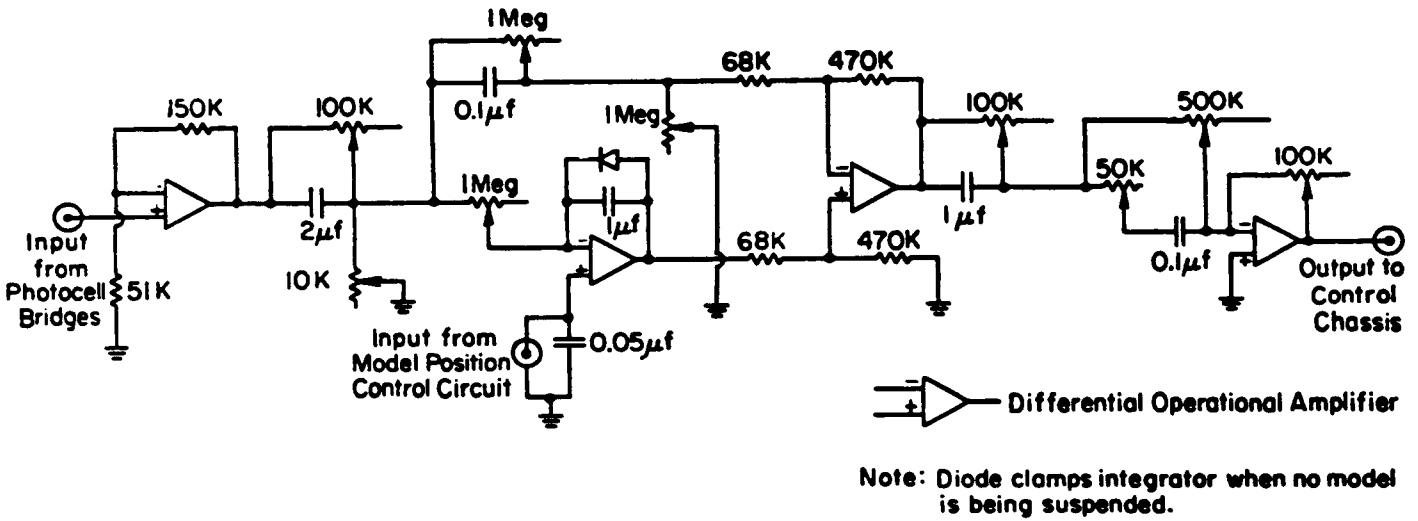

Figure 47. Compensation network (Identical for all 5 units)

integrator in parallel with a lead-lag network. The parallel combination generates two of the zeros on the root locus plot. This is followed by a summing amplifier and an active lead-lag network. The last lead-lag network was made active to sharpen the rate control since a passive network has a maximum α of about 20. All of the amplifiers are of the DC, operational, differential type (Ref. 18).

This control network was tested using the configuration in Fig. 48. The model was an Alnico V bar magnet, six inches long and one half inch in diameter. Gravity represented the drag force and no lateral restraint was necessary since the model tended to orient itself in the maximum magnetic flux density. Forces were applied to the model with weights and the network was found satisfactory after some adjustment of the variables.

2. Lift Control System

The lift compensation networks control the vertical and pitching movements of the model. The currents in the upstream and downstream lift coils are independently controlled by two circuits, one for each coil.

The form of these networks was arrived at mostly through an experimental procedure because of the complex nature of the lift control loops. There are three interactions between the two loops which make an analysis difficult. There is a force coupling on the model due to magnetic flux in the magnet core; there is a mutual inductance effect between the lift coils; and there is coupling through the angular inertia of the model. The latter coupling is responsible for most of the difficulty in controlling the lift mode.

Referring to Fig. 49, the following equations may be written to describe the motion of the model for small perturbations:

$$\bar{F}_{M_1} + \bar{F}_{M_2} + \bar{F}_{L_2} + \bar{F}_{L_2} = m p^2 \bar{z}$$

$$(\bar{F}_{M_1} + \bar{F}_{L_1}) \ell_1 - (\bar{F}_{M_2} + \bar{F}_{L_2}) \ell_2 = I p^2 \theta$$

$$z = z_1 - \theta \ell_1 = z_2 + \theta \ell_2$$

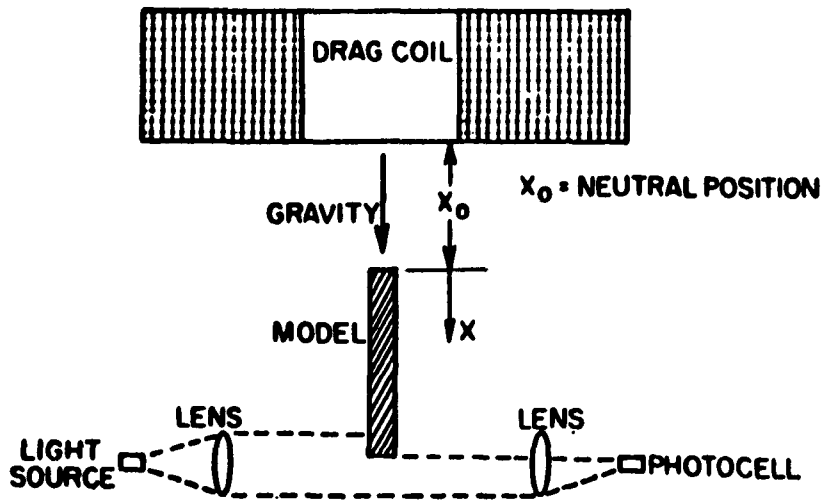

Figure 48. Schematic of optical system for detecting model displacement

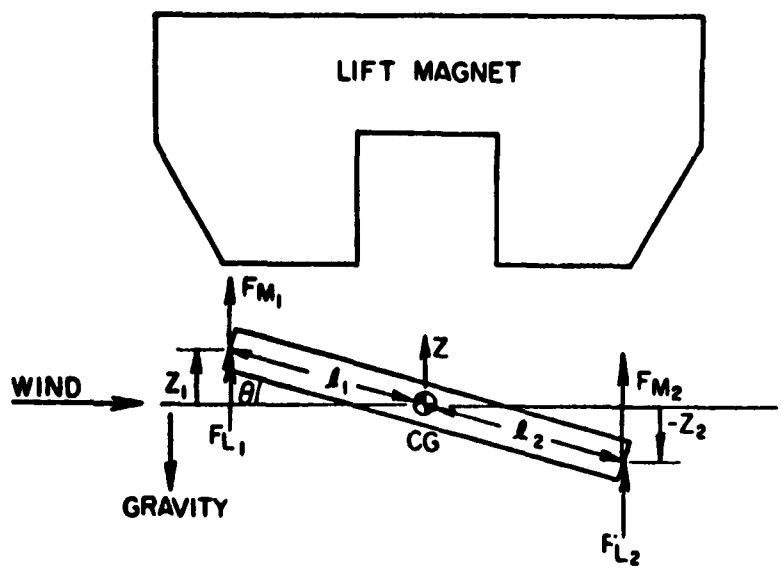

Figure 49. Model forces in lift degree of freedom

Using these equations the block diagram in Fig. 50 was drawn. As a first approximation the forms of the control networks are the same as in the drag system. If the differential equations for model displacement as a function of lifting force input are derived from Fig. 50, it is found that they are fourteenth order as compared to seventh order for the drag system. An equation of such large degree is difficult to interpret in terms of all the control network variables, and the coefficients of the characteristic equation are such that the usual approximations cannot be made. Therefore, two networks were constructed which were identical to the drag circuit. As in the drag network, almost all resistive elements were made variable and the initial settings of the component values were made the same as in the drag circuit. Since the time characteristics of the lift system are similar to those of the drag system, it was felt that this was a good place to start.

Preliminary stabilization of the model in the lift degree of freedom was accomplished by hand holding the model and adjusting the control circuit variables until it ceased to oscillate or diverge. After this point was reached it was possible to improve the model response to small perturbations by watching model displacement on an oscilloscope while varying the control circuit components.*

It appeared at this time that the lift circuits being used would give satisfactory model performance. However, the limit to which model performance could be improved had now been reached because perturbations in the lift degree of freedom were transferred to the uncontrolled lateral and drag degrees of freedom. Therefore, it was necessary to put the other units into operation for fixing the final settings.

---

* Originally an Alnico V bar magnet was being used for a model. It was observed, however, that if the model was left suspended it would gradually go unstable. It was then discovered that the magnetic strength of the bar magnet changed with time because of the strength of the field which suspended it. This change of strength resulted in a change of loop gain which increased until instability resulted. This effect was corrected by using a model made of electrolytic iron which has negligible hysteresis.

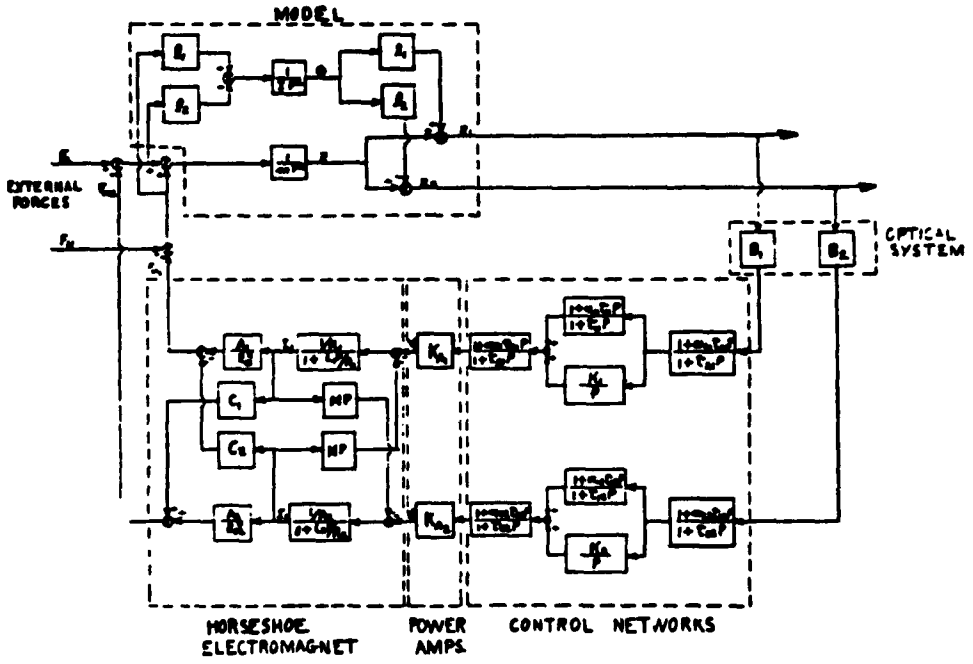

Figure 50. Lift system block diagram

3. Lateral Control System

The lateral magnet controls the side and yaw movements of the model. The control networks for this system are identical to the lift circuits. However, the lateral system differs from the lift system in one way. There is no gravity in the lateral degree of freedom. Since the power supplies will deliver only a negative voltage to the magnet windings some artificial gravity must be supplied. This was accomplished by winding two coils on each leg of the lateral magnet core. The current in one coil is controlled while the current in the other is constant. These two currents provide opposing fields, one attracting the model and one repelling it. Therefore, a constant lateral force bias is applied to the model.

Because of the need to both attract and repel the model in the lateral degree of freedom, the model must be magnetically polarized. Since a permanent magnet cannot be used for a model (See Lift Control System Section) the lateral system is dependent on the lift magnet to polarize the model. The polarization due to the lift magnet is always present because of the gravity force on the model. Since the weight provides the bias, it is important to realize that the lift should not exceed the weight. Thus the model could be expected to be tested in an inverted state.

4. Control System Equipment

The equipment used to construct the compensation networks consists of standard analog computer building blocks manufactured by George A. Philbrick Researches, Inc. Three model HK operational manifolds, housing twenty Model K2-W operational amplifiers (four for each network) are used to perform the compensating operations. The power for these units is supplied by a Model R-100A regulated dual power supply and by a Model R-100B regulated dual power supply. The networks are wired in plug-in modules (five for each network) which plug into the manifolds. Figure 51 shows the compensation networks in the relay rack on the right. The rack on the left contains the bridge networks, balancing circuit, and model position controls.

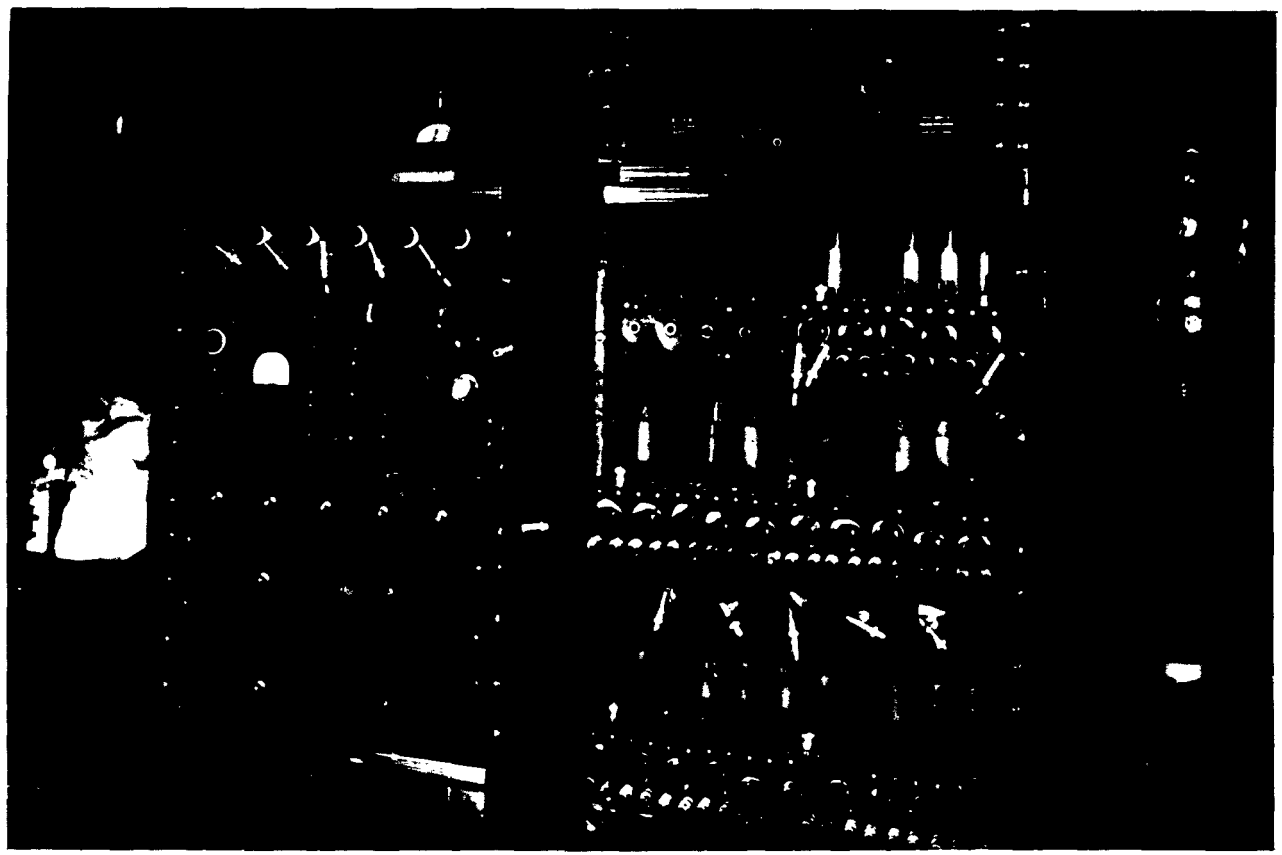

Figure 51. Control system equipment

5. General Comments on Control System Performance

The adjustment of the variables in the five control networks must be made while all units are operating. As was mentioned earlier, if one or more of the units is not operating the model motion will be transferred to the uncontrolled degree or degrees of freedom (excluding roll) and proper adjustment cannot be made. It should be noted here that when no wind or calibration loads are on the model there is no external force in the longitudinal or drag degree of freedom. Under this condition any small perturbation of the model will be transferred to the longitudinal degree of freedom and cause the model to sway like a pendulum in that mode with increasing amplitude until the model falls. To prevent this the longitudinal position control is used to move the model slightly forward of the center of the lift magnet. Due to the symmetry of the lift magnetic field the model will want to move back to the center of the magnet. Thus a small external load is provided by the lift system for the drag system in the downstream direction to prevent the swaying mentioned above.

The criterion that has been found most useful in adjustment is optimization of model position response. For example, if the lift system circuits are being tuned the forward and rear lift system optical signals are observed on a dual beam oscilloscope. A voltage step or impulse is added to the control signal at the input to either one of the lift power supplies. The variables are then adjusted to give the desired model response to this perturbation. It should be pointed out here that the number of variables is large and random knob turning during the critical phases of adjustment does not bring satisfactory results. However, satisfactory adjustment can be obtained by observing what each adjustment does to the pole and zero positions on the root locus plot of Fig. 49. Although this plot applies to the drag system only, it has been found helpful in the tuning of all five systems. In general, the circuits can be tuned to give a critically damped model position response in all five degrees of freedom.

As indicated above, model position changes can be made by varying the reference on the integrator amplifier in the control circuit.

Since the amplifier is of the differential type, the integrator drives the model to a new position where it is held independent of any external forces.

Aside from the control system effects, model performance is also influenced by interactions due to the model not being magnetically saturated. When the field of one magnet changes it changes the strength of model polarization. This change in polarization produces a gain change in the other systems and results in transient position disturbances in all degrees of freedom. These interactions can be significantly reduced by suitable cross-over networks between the five control circuits. However, the additional circuit complexity can be avoided by making the ferrous model core smaller. This brings the material closer to saturation and reduces the interaction effects. However, a decrease in core size will require more magnet current to counter the same external forces. Therefore, the limit to which the model core can be reduced is governed by the amount of power that can be dissipated in the magnet windings by the cooling system and the current limitations of the power supplies.

E. STRUCTURAL AND COOLING CONSIDERATIONS

Electronics

1. Structural Considerations of the Power Supplies

The power supplies and the electronic chassis were designed to be tools in the overall system and therefore not require excessive attention to maintain good operating characteristics. Thus the chassis were designed to be free of mechanical failures.

All of the basic chassis were constructed of cadmium plated steel. The power supply chassis measured 30" by 18" by 6" ; the electronic control chassis measured 30" by 18" by 3" . Both the power supply and control chassis were equipped with bottom plates to minimize the shock hazard to personnel and to help control the flow of cooling air. All the self mounting components such as transformers, relays, meters, and terminal boards, were securely fastened to the

chassis with screws, lock washers, and nuts. Non-self mounting components such as resistors, condensers, semi-conductors and the like were securely mounted to terminal strips to fix their position and eliminate accidental shorts within the chassis. Reliable electrical connection of the components to the circuit was insured by using a combination of pretinning, solid mechanical joints, and solder. As a consequence, no electrical connection problems have occurred to date. The cable connections required between the control chassis and the power supplies and from the power supplies to the coils are accomplished with rubber jacketed multi-conductor stranded copper wire. All connectors used in the system are amphenol AN series. This type of connector was chosen because it offered good electrical properties as well as the ability to clamp mechanically each cable so that any strain imposed on the cable would be countered at the mechanical connection rather than at the electrical connection. The signal inputs to the power supplies were carried in coaxial cable equipped with Amphenol BNC series connectors rather than the AN series. All of the power and control chassis are mounted in three 36" by 66" by 24" relay racks (Fig. 52). The relay racks have vertical support members in the front and back and adjustable horizontal support members that carry the installed chassis. This horizontal support is necessary since each of the power supplies weighs approximately 385 pounds and each control chassis weighs approximately 75 pounds. This means that the total equipment weight in each relay rack is nearly 1000 pounds. The lift system elements are shown in Figs. 53 – 56.

2. Cooling Considerations

a. Power Chassis

Each power supply has a fan which draws air through the front panel and exhausts the air up through six ring holes in the top of the chassis (Figs. 53 and 57). Thus the air flow cools not only the interior of the chassis but also the C16J thyratron tubes which are mounted above the ring exhaust (Fig. 56). The control chassis are cooled by free convection as only a small amount of heat is dissipated there.

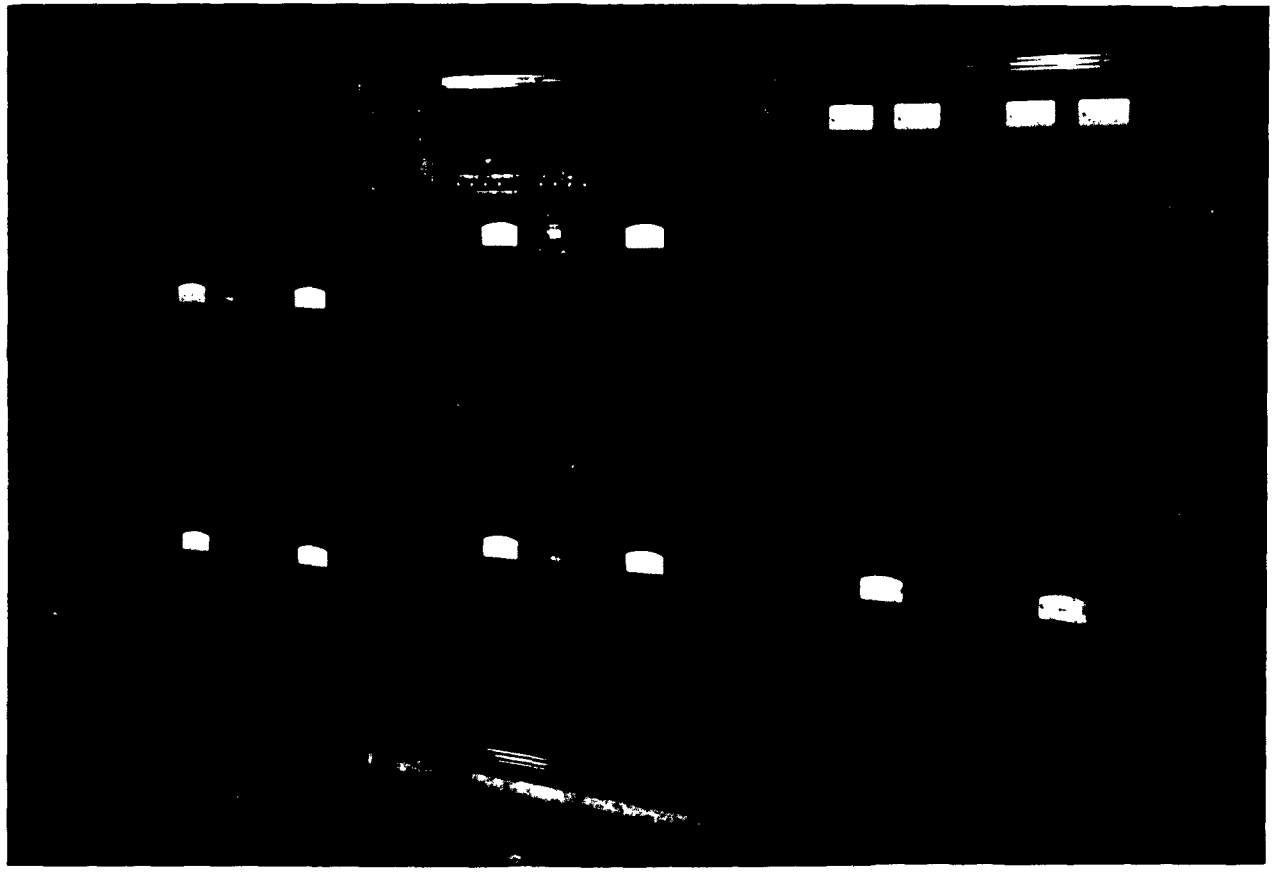

Figure 52. Control chassis and power supplies

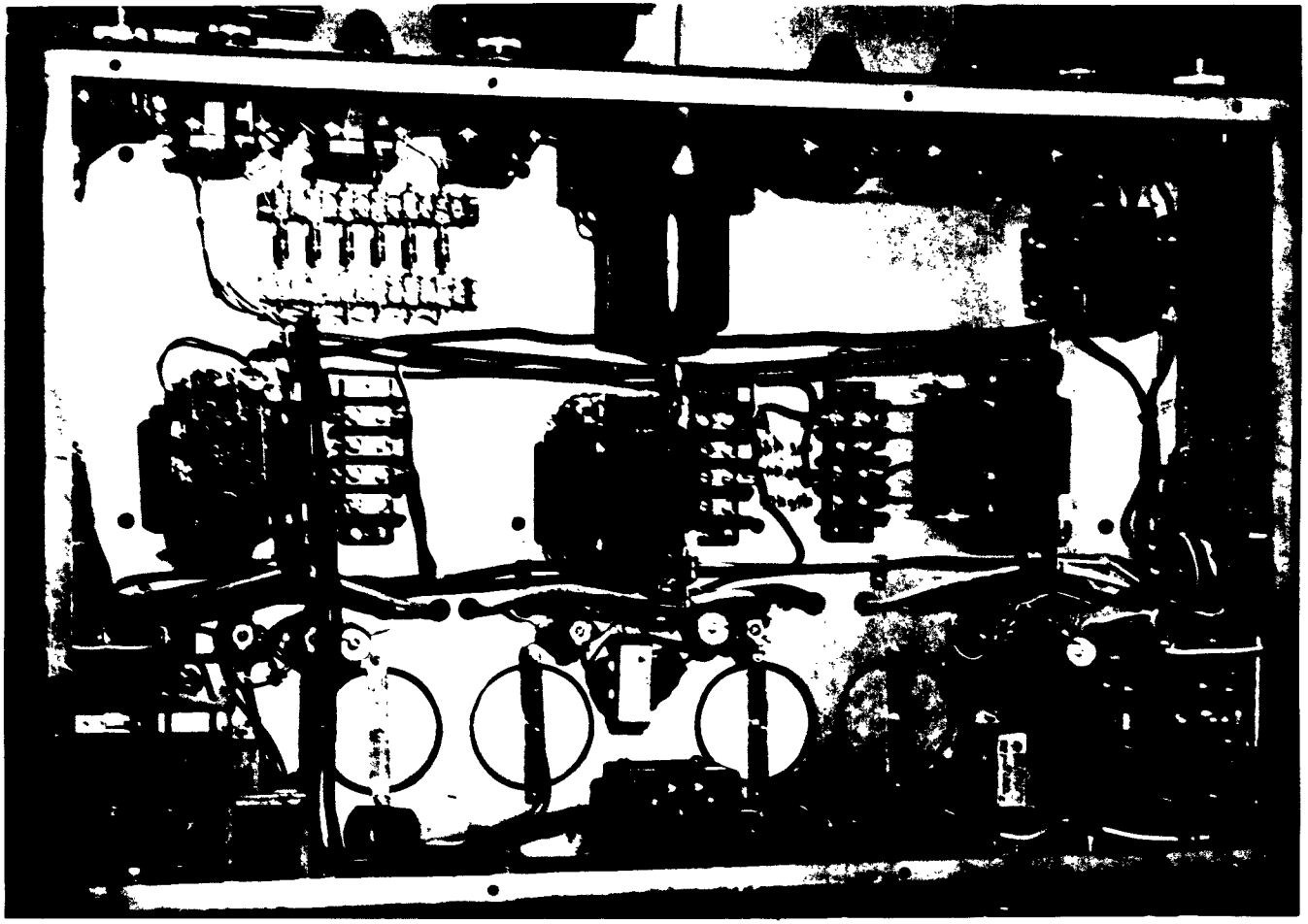

Figure 53. A lift power supply from below

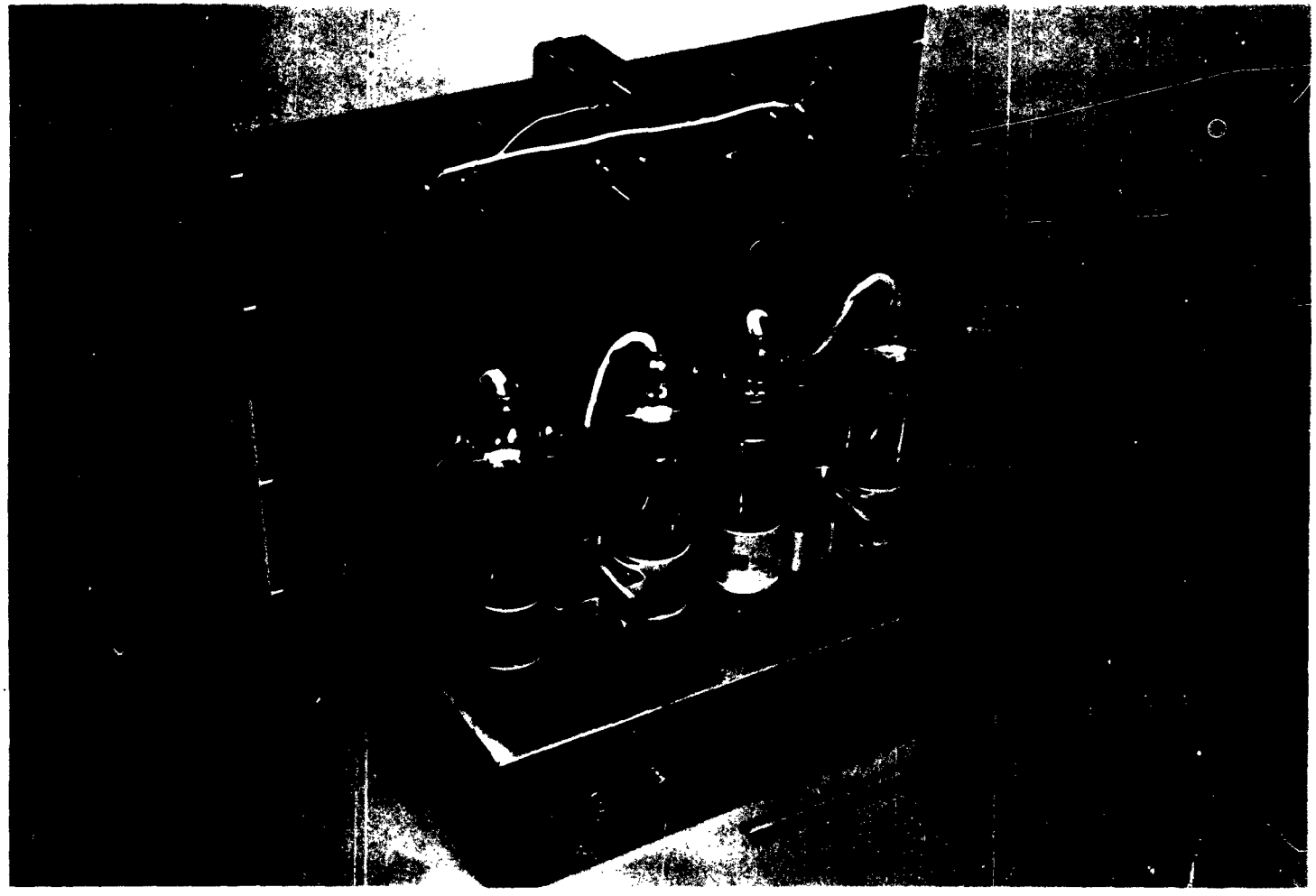

Figure 54. Back view of lift power supply

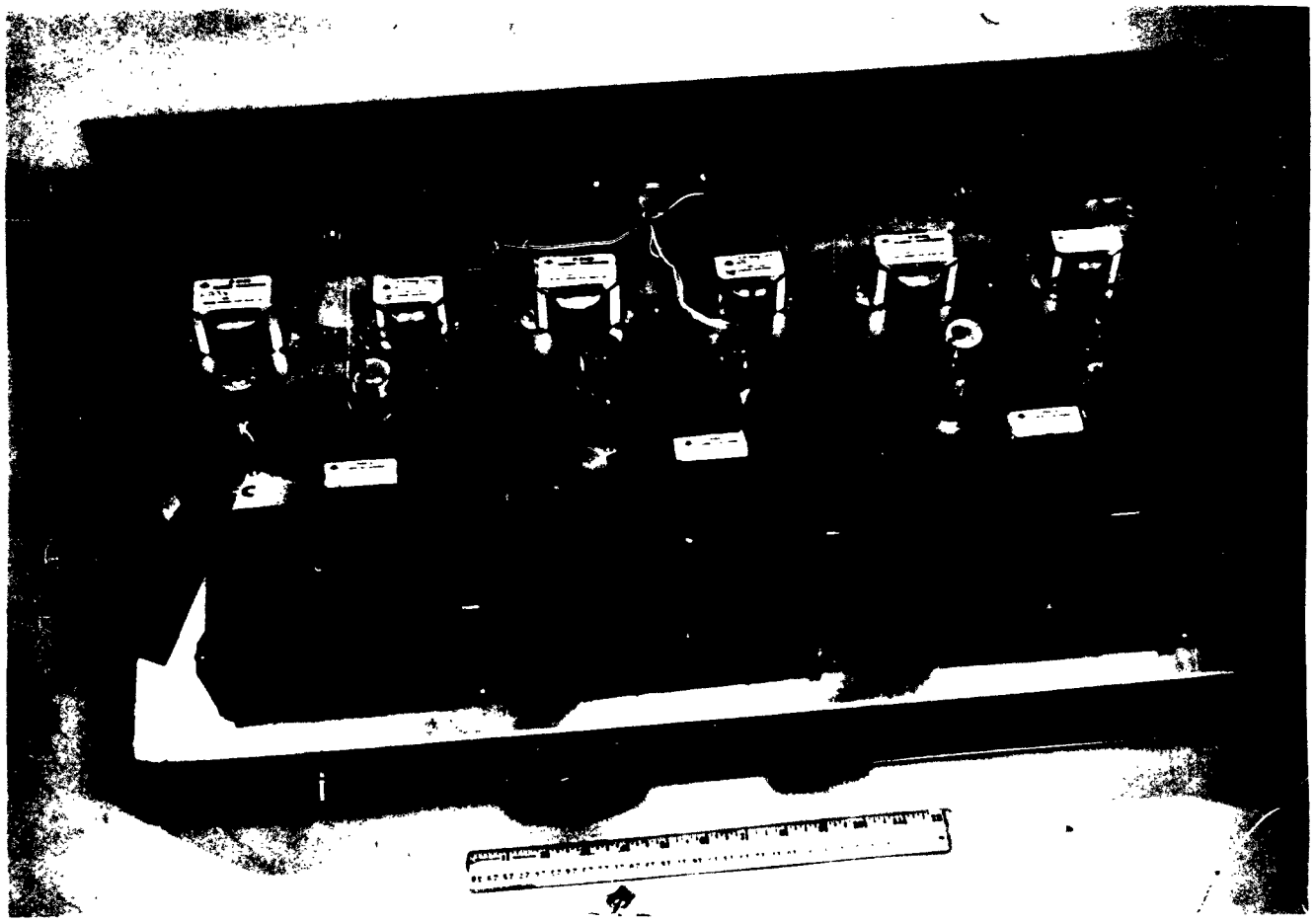

Figure 55. Top view of power control chassis

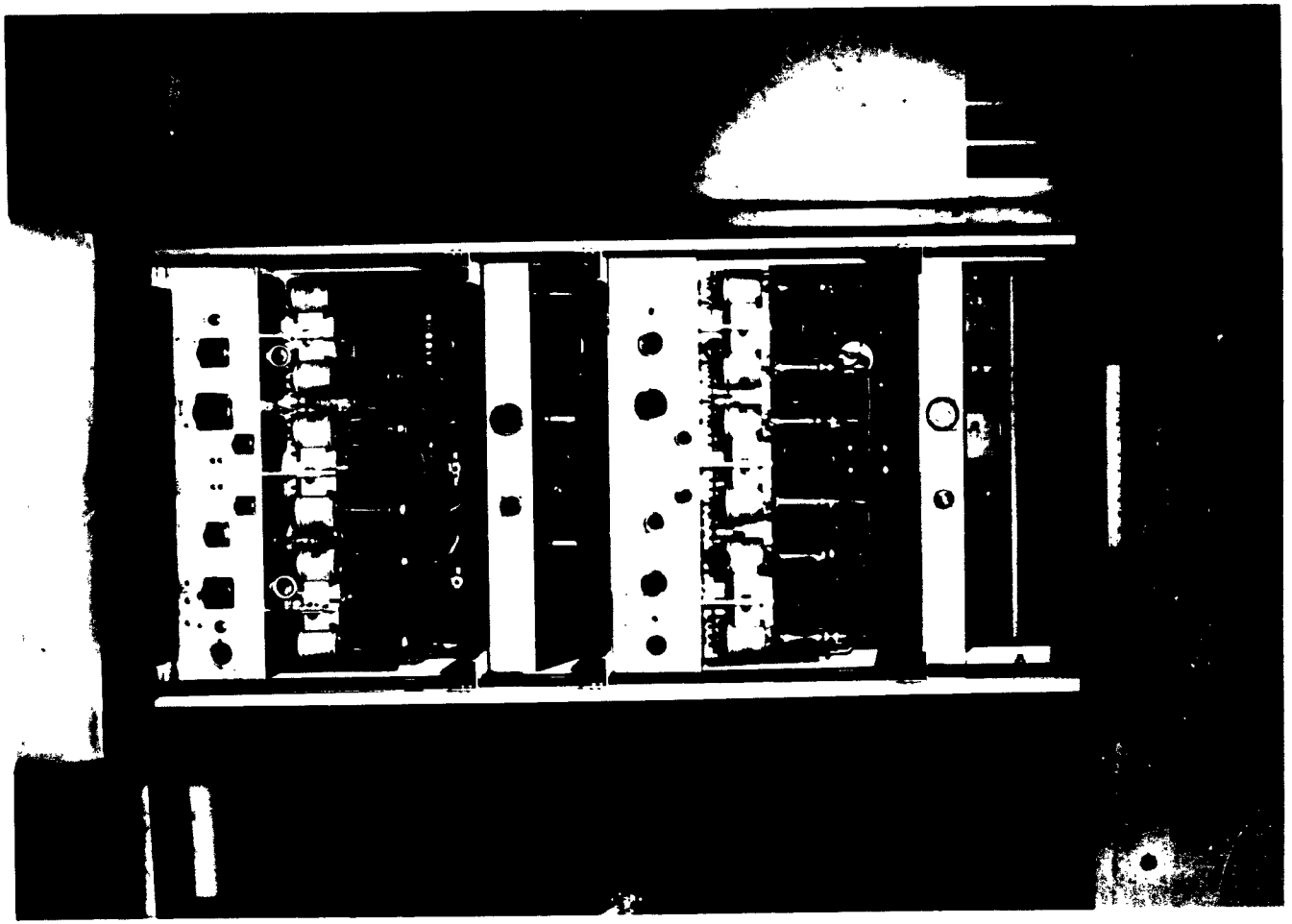

Figure 56. Back view of lift power cabinet (Note the two sets of control and amplifier chassis)

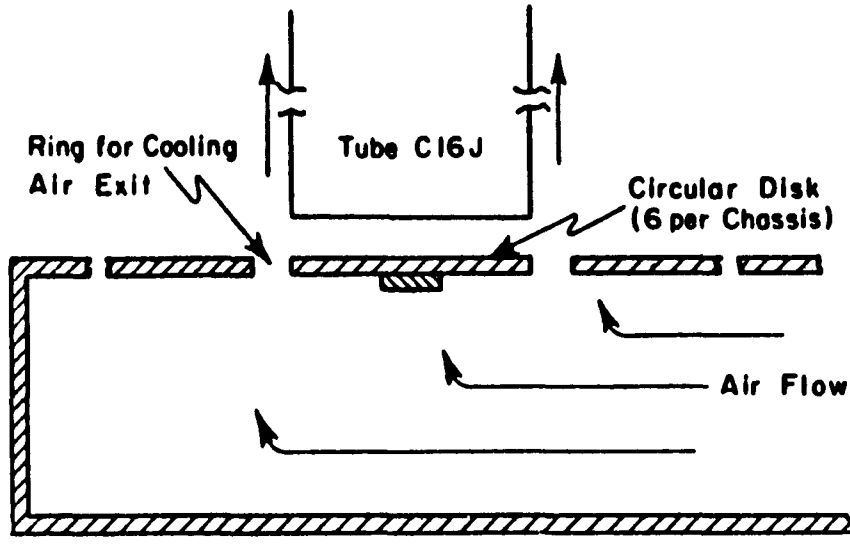

Figure 57. Cooling arrangements for C16J thyratrons

b. Lift, Lateral and Drag Cabinets

Each lift and lateral relay rack contains two power supplies and two control chassis. Each relay rack has three exhaust fans in the top to remove the hot air. The efficiency of the cooling within the cabinets was improved by the installation of baffles (Fig. 58). Baffles were also placed on the sides of the chassis to force the air to flow over these units. This cooling system has successfully maintained the lift and lateral relay rack temperatures within the temperature ratings of all the components.

The drag cabinet contains a power supply, control chassis and fifty two-hundred-watt resistors. The cooling requirements of this cabinet were more severe than that of the lift and lateral cabinets because the fifty resistors are capable of dissipating ten thousand watts at rated power. The cooling system used is the same as the lift and lateral cabinets except that the relay rack exhaust fan has a larger capacity. The flow produced, 500 cubic feet per minute, is equivalent to a complete change of air in the relay rack about every 10 seconds (Fig. 59). Thermocouples were placed on the front, middle, and rear resistor plates, and the fan motor in the drag cabinet. The fan motor was started and its temperature rose to 140°F; the power supplies were then turned on and the temperatures were monitored for 200 minutes at various power levels. At operating power the fan motor temperature rose to 180°F, a value which was within its rating. The front, middle, and back resistor panel temperatures reached equilibrium at 110°F, 132°F, and 120°F respectively, values which were also well within the ratings of the units. The power supplies were then run above rated coil current for a period of 15 minutes to produce an extreme load on the cooling system; this condition is not likely to occur in actual tunnel use. During this overload condition the fan motor temperature rose to 188°F and the front, middle and back resistor panel temperatures reached values of 127°F, 178°F, and 149°F respectively. Since the operating temperature of the fan motor was higher than intended, a vent was cut over the motor housing and a pipe inserted to allow cool air from the room to enter the motor housing (Fig. 60).

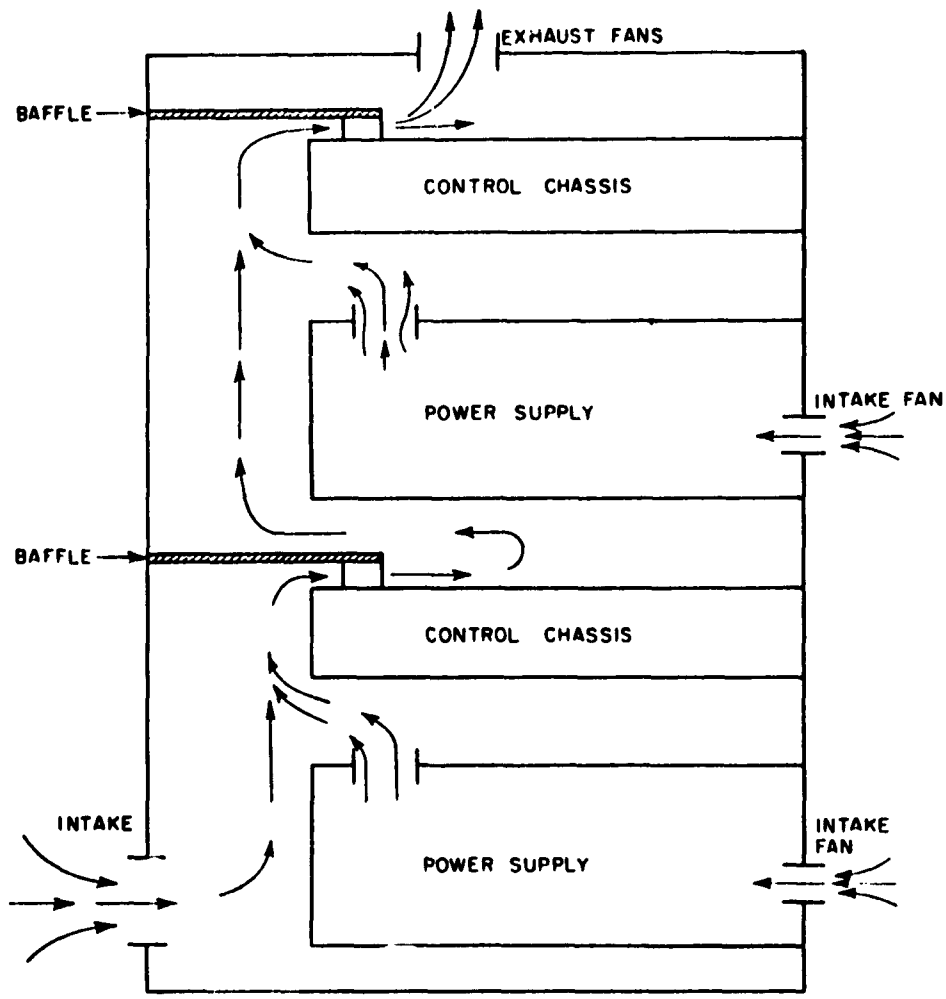

Figure 58. Side view of air flow in lift and lateral cabinets.

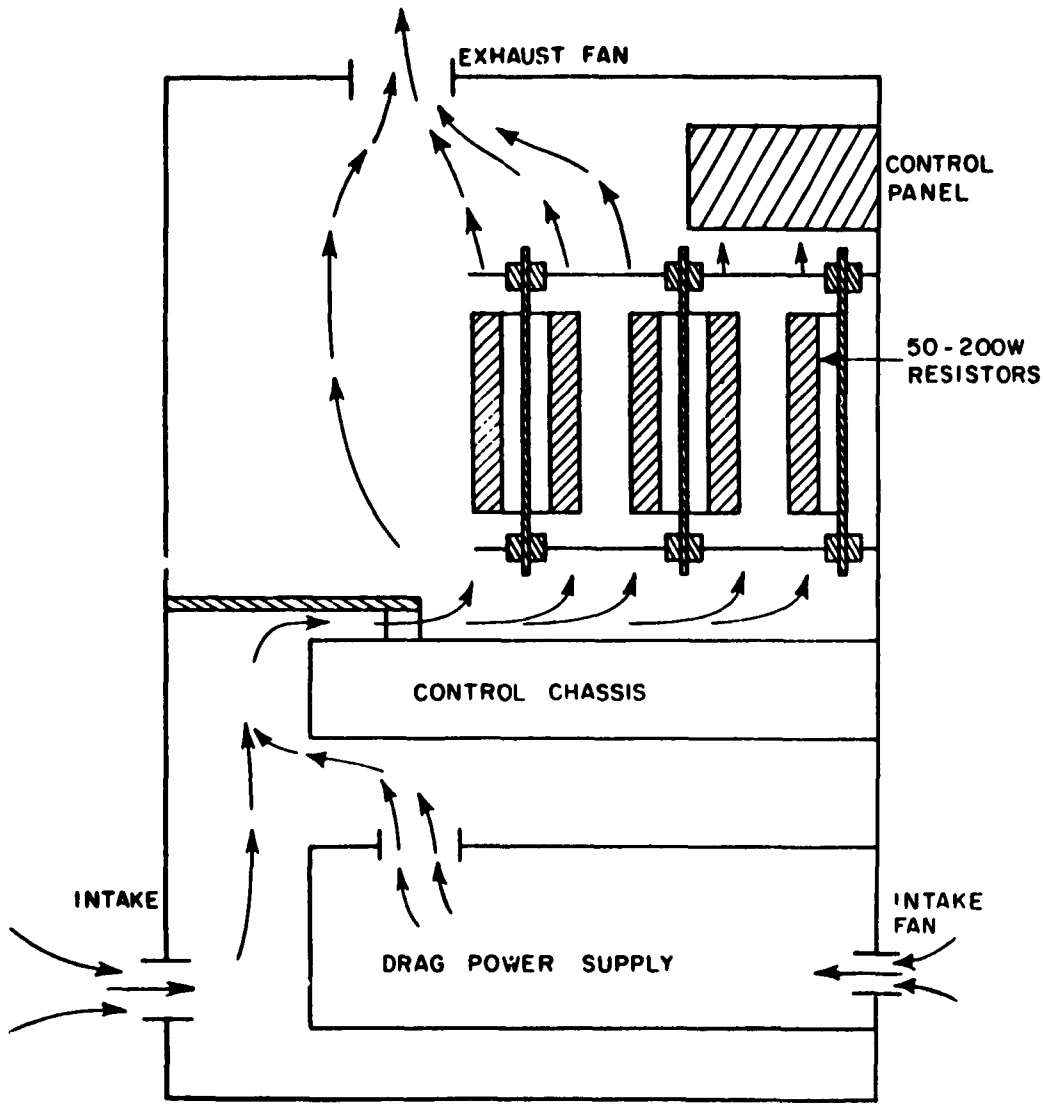

Figure 59. Side view of air flow in drag cabinet.

Structural and Cooling Considerations for the Magnets

1. Structural Considerations of the Magnets

a. Magnet Support Frame

The basic magnet support frame consists of two 1/4 inch thick steel sheets, 24 inches by 24 inches, attached to each other at the corners by four pieces of 32 inch long stainless steel angle stock. The angle stock was bolted to the plates at the contact points and corner braces were added to provide the necessary rigidity (Fig. 61). Slots were cut in the top plate to provide mounting points for the lift and lateral magnets. The drag coil was attached to both the top and bottom plates through additional slots. The bottom plate also supports the optical frame.

b. Lift System

The lift magnet assembly includes the two lift coils, the core (two legs and connecting yoke), and the necessary mounting brackets (Fig. 62).

The core was designed to be fabricated of thin laminations to minimize the possibility of significant hysteresis losses which could result from high frequency oscillations caused by the suspension control system. The presence of these losses would have an adverse effect upon the time constant of the control system, as well as cause heating of the electromagnet core. The laminations were clamped together at the yoke between two heavy rectangular textolite rods. The rods were attached to each other by heavy steel bolts which were positioned at each end of the yoke in such a way that they engaged the two V notches shown on Fig. 24. Insulation was provided by fitting a fiberous glass sheath material over the bolts before they were installed. Glass tape was used to bind the core leg laminations together.

The lift coils, #1 and #2, are placed on the legs of the magnet core. The coils are securely held in place by a stainless steel band. The silicon rubber placed between the steel band and the core and coils serves to protect the coils and eliminate an eddy current path which might develop through the pole faces and the steel band. This retaining band is anchored to bolts which pass through the ends of

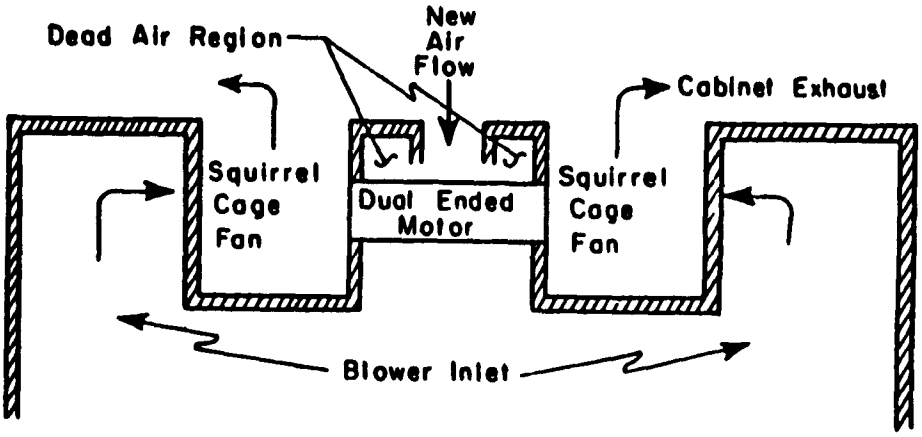

Figure 60. Front view of blower used to cool drag cabinet

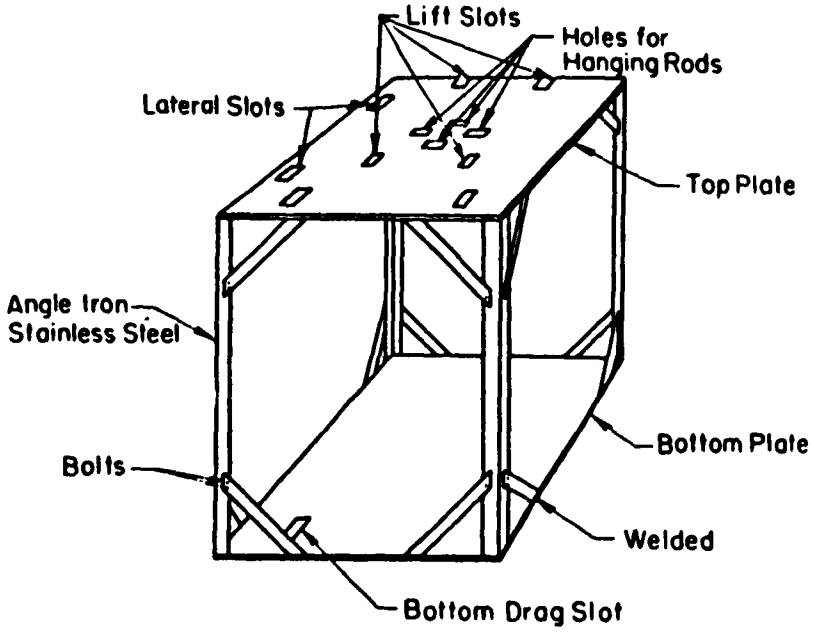

Figure 61. Magnet support frame

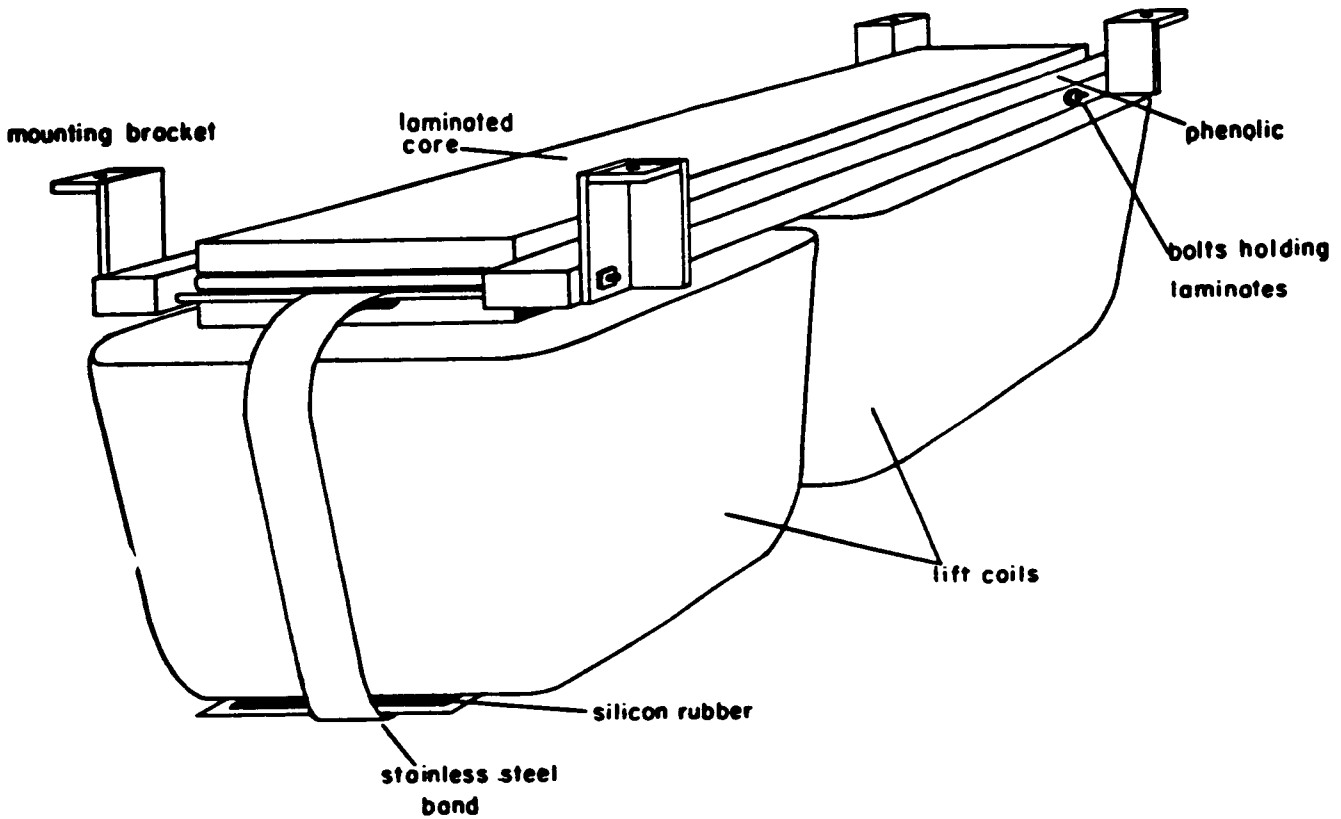

Figure 62. Lift system structure

the pair of phenolic compression pieces. These bolts also hold the four stainless steel angle stock mounting brackets that are used to attach the lift magnet assembly to the top of the mounting frame. The mounting brackets are fastened to the mounting frame by a bolt and slot arrangement which allows fore and aft adjustment of the assembly with respect to the wind stream. Provision was also made for a vertical adjustment, which was permanently accomplished during the initial installation.

c. Lateral System

The lateral magnet core is a laminated Hyperco horseshoe with straight legs (Fig. 25). The laminations are held in compression in the same manner as the lift core (Fig. 63). The lateral coils, #1, #2, #3, and #4, are secured to the poles with the same technique that is used on the lift coil assembly.

The lateral system is also suspended from the top plate of the frame with provisions for movement parallel with the air stream. The lateral magnet is fastened to two of the basic structure angle stock supports with a brace to prevent movement perpendicular to the air stream.

d. Drag System

The drag unit is an air core solenoid whose axis is parallel to the air stream of the wind tunnel. The winding is wrapped with a high temperature fiber glass tape for protection (Fig. 64). Next a layer of silicon rubber is placed between the solenoid and a stainless steel strap that is fastened around and held to the coil by tension. A shorted turn was avoided by inserting a phenolic block between the joining ends of the strap with insulated bolts. Corner brackets were mounted on each side of the strap and used to attach the coil to the top and bottom plates of the mounting frame (Fig. 64). These brackets are adjustable in the wind stream direction to allow the drag unit to be properly located.

e. Structure of the Coils

The coils were wound on a mandrel using 3/32 inch outside diameter copper tubing. The tubing has a triple coating of Formvar varnish which serves as layer to layer insulation. The coils are wound so that each layer is a separate piece of tubing. An epoxy resin was

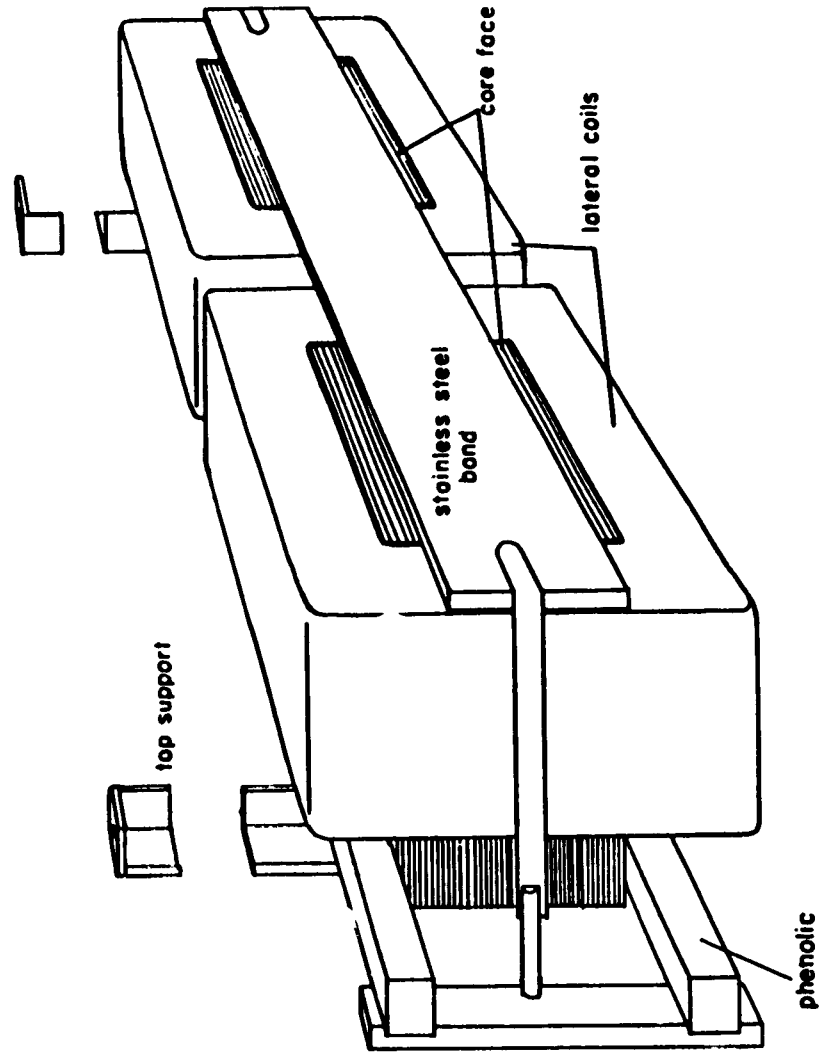

Figure 63. Lateral magnet structure

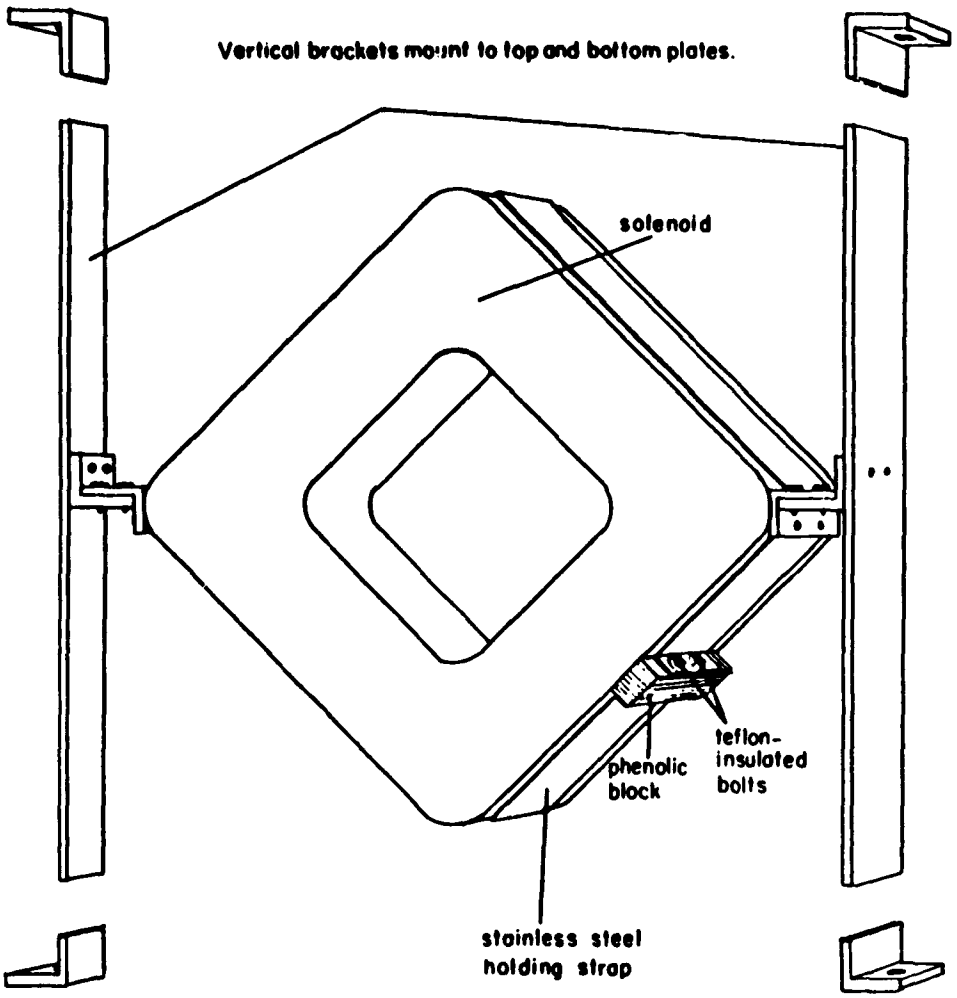

Figure 64. Drag coil structure

applied during the winding so that the layers would adhere to each other. Consequently, when the coils were completely wound and removed from the mandrel, they maintained their integrity without the aid of a casing structure. All of the coils were wound in the same manner. The two lift coils were wound so that they have 17 layers per coil. The lateral coils have 9 layers per coil and the drag coil has 24 layers.

2. Cooling Considerations for the Magnets

Cooling water is forced through the 0.040 inch inside diameter copper tubing which is used for the coil windings. The cooling for all coils is essentially the same; the difference appears only in the variation in the number of turns per coil. The inlet water is delivered from the laboratory water supply at a pressure of 40 psi. (Fig. 65). The water passes through a filter and then enters the inlet manifold and is distributed to each coil through 1/4 inch copper tubing (Fig. 66). Electrical isolation between the 1/4 inch manifold and the coil is maintained by a xylene union. After the xylene union the 1/4 inch copper tubing is connected with a 1/4 inch manifold and is led to the various layers of the coil. A second xylene union isolates the 1/4 inch manifold and the coil and this isolates the windings from each other as well. The system that carries the heated water away is an exact duplicate of the water supply system.

Prior to connecting the coils to the manifold system each layer of each coil was checked for flow rate (Table III). The table shows that the inner layers, with their shorter lengths, have better flow rates than the outer layers.

Thermocouples have been placed on the outlet manifolds of the coils, and the temperature has not risen above 100°F during wind tunnel operation of the system.

Figure 67 shows the lift magnet before completion of the cooling plumbing and final installation of the coils.

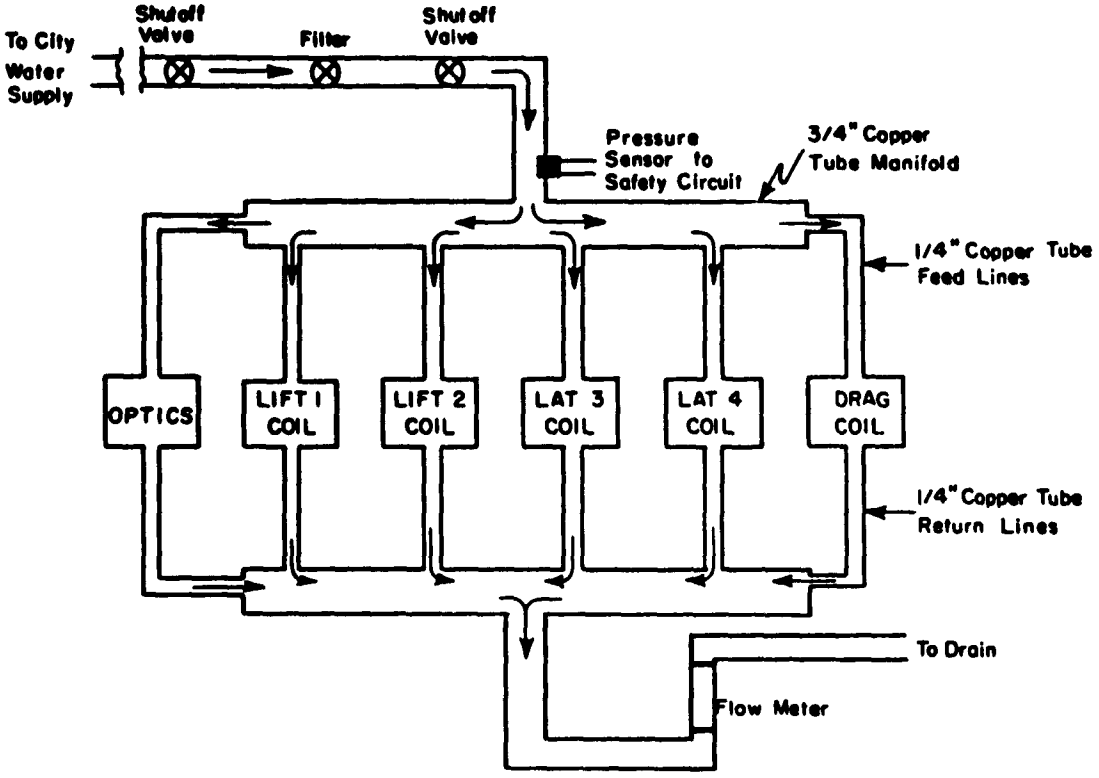

Figure 65. Schematic of cooling system

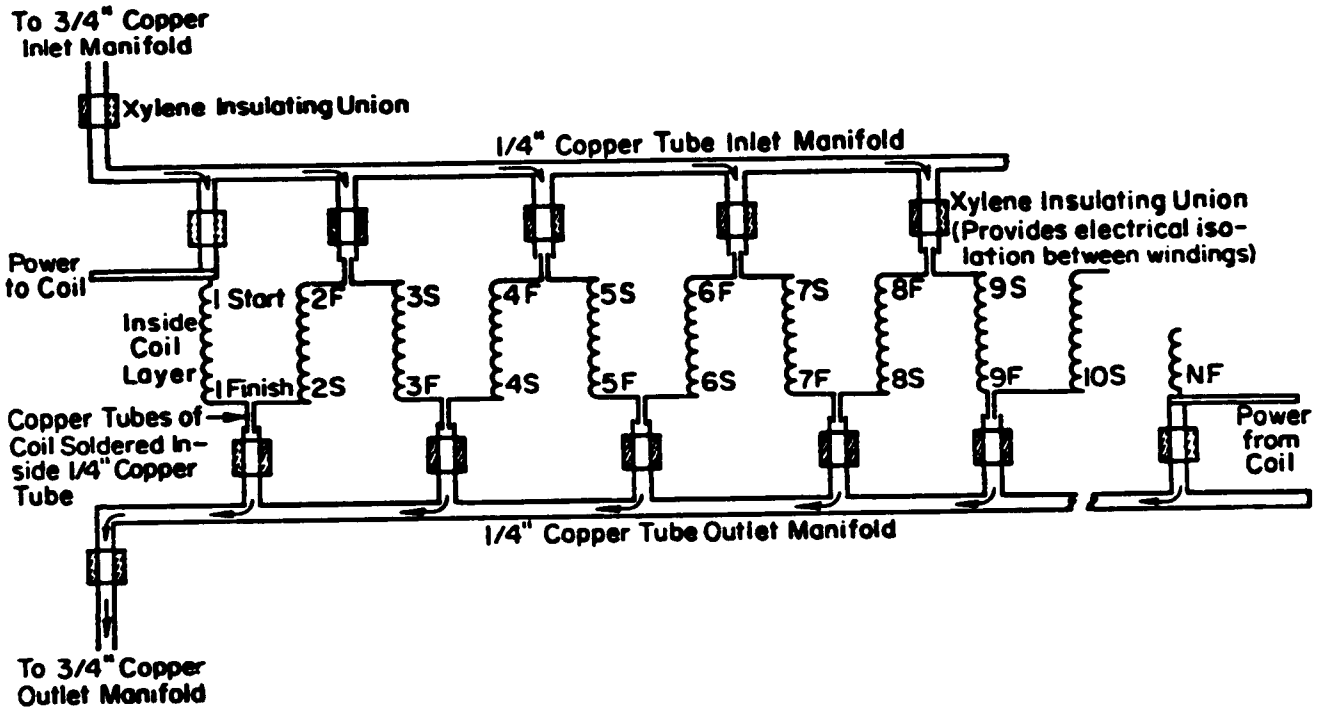

Figure 66. Schematic of typical coil- parallel water supply and series electrical circuit

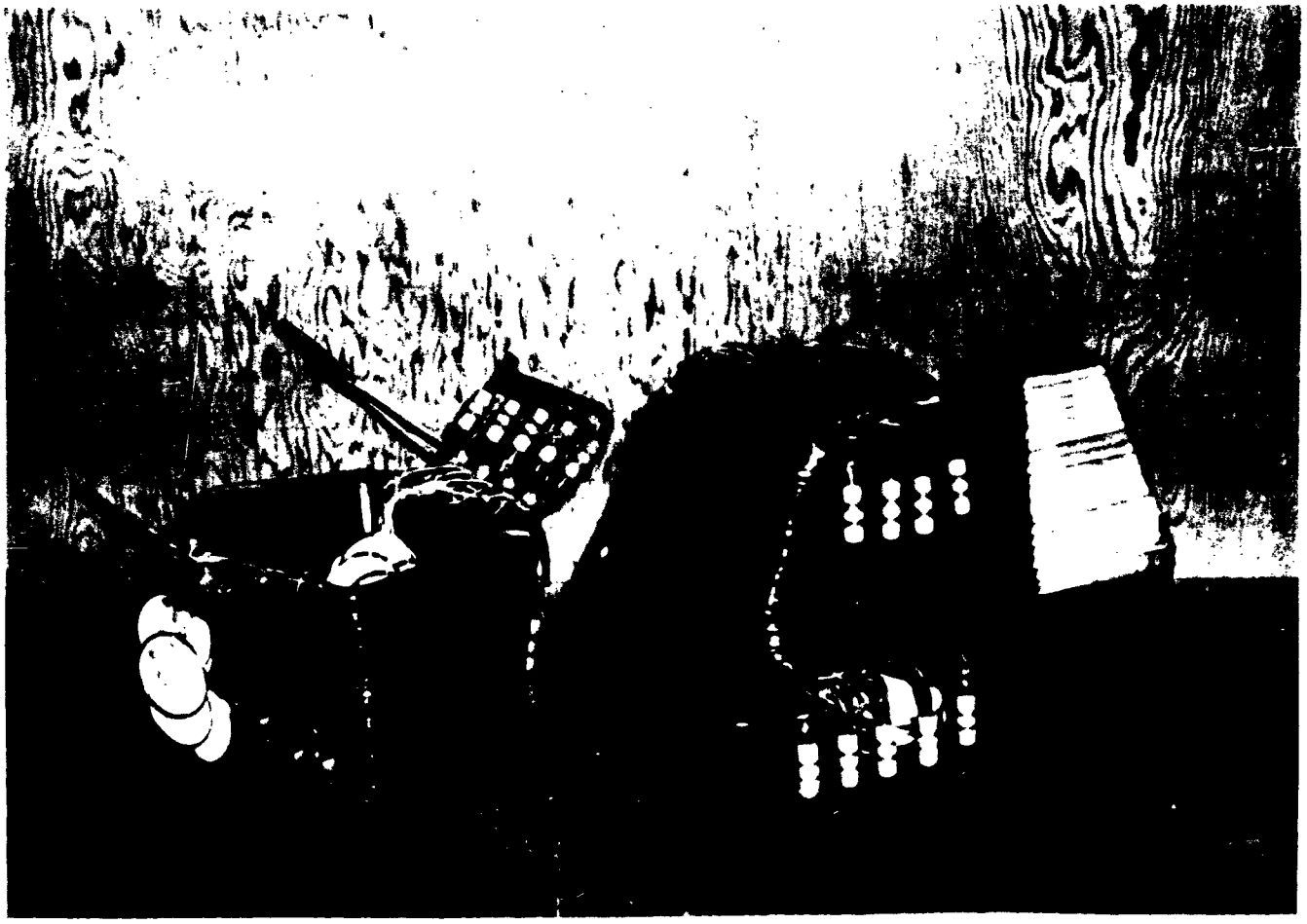

Figure 67. Lift magnet during assembly

TABLE III

WATER FLOW RATES/TURN

(AT CITY WATER PRESSURE, 40 psi nominal)

Layer Number	oz/min Lateral-1	oz/min Lateral-2	oz/min Lift-1	oz/min Lift-2	oz/min Drag
1	.938	.95	.938	.874	.750
2	.875	.95	.813	.775	.500
3	.938	.95	.775	.775	.625
4	.804	.874	.750	.780	.500
5	.800	.775	.750	.725	.625
6	.804	.775	.750	.725	.750
7	.775	.813	.724	.725	.750
8	.750	.750	.724	.725	.750
9	.750	.750	.724	.688	.688
10	.725	.725	.688	.688	.666
11	.725	.725	.688	.688	.666
12	.700	.688	.700	.650	.752
13	.688	.688	.688	.650	.583
14	.688	.688	.625	.688	.666
15	.688	.688	.650	.625	.666
16	.680	.700	.625	.600	.666
17	.688	.688	.625	.600	.666
18					.666
19					.666
20					.666
21					.666
22					.666
23					.666
24					.666

Optical System

1. Structural Considerations

The basic optical frame consists of two rectangles made from flat stainless steel stock that are joined together with channel pieces and box stock (Fig. 68). The optical frame has been made very rigid, and care was taken to insure that its resonant mechanical frequency will not interfere with the optical sensing system.

The optical frame is independent of the rest of the system and can be taken out of the magnet system and run separately for checkout and initial line up and rough calibration.

The light boxes are mounted on the optical cross frame members by two bolts and locating blocks to insure the proper orientation (Fig. 69). The mirror mounts are similar to the light source mounts and are also mounted on the cross member with locating screws and bolts (see also Fig. 36).

All of the optical components can be moved on the mounting channel so that they can be properly positioned.

2. Cooling

The photo cells in the optical system are temperature sensitive. Unfortunately the requirement for a folded system caused the photo cell and the light source to be located as close together as possible (Fig. 70). Each light source dissipates 1.2 watts. This small amount of heat can result in gross changes in temperature over a period of time. This difference shows up as a zero shift in the photo cell bridge circuit. This zero shift was reduced by fitting the light source boxes with two turns of square copper tubing which was soldered to the light box assembly (Fig. 70). These turns on the five light box assemblies are connected in series and are fed from the main water supply of the magnet assembly to maintain the photocells at a constant temperature.

F. RELIABILITY

The reliability of the magnetic balance electronic equipment (or any other electronic equipment for that matter) is difficult to calculate.

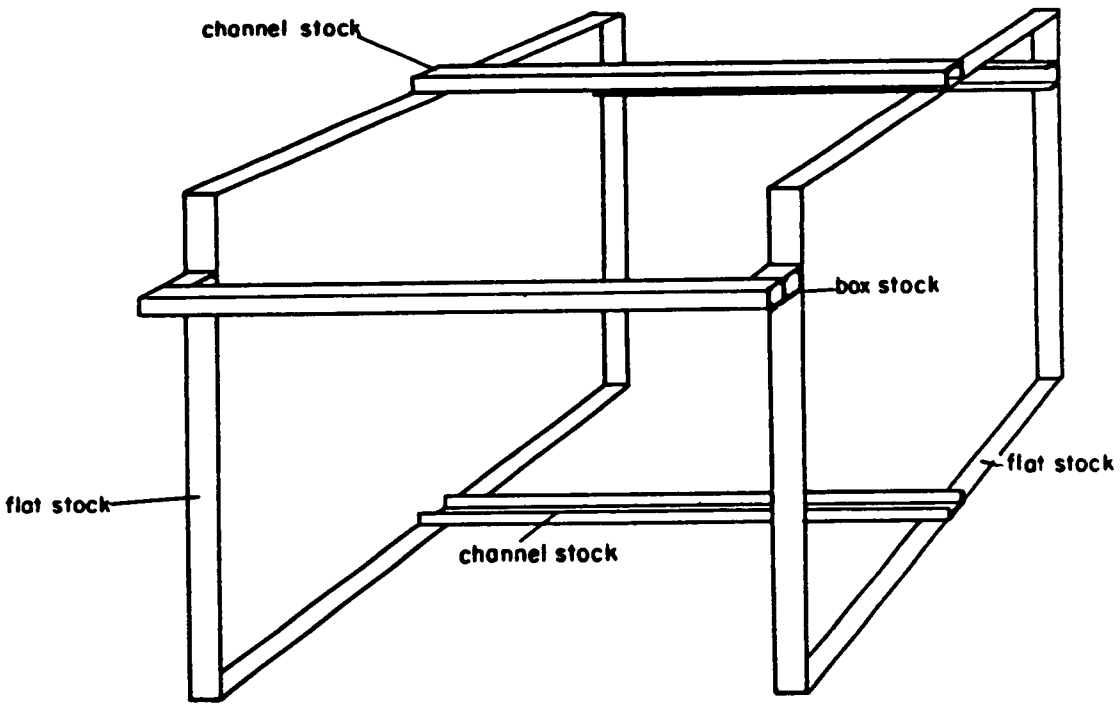

Figure 68. Basic optical frame.

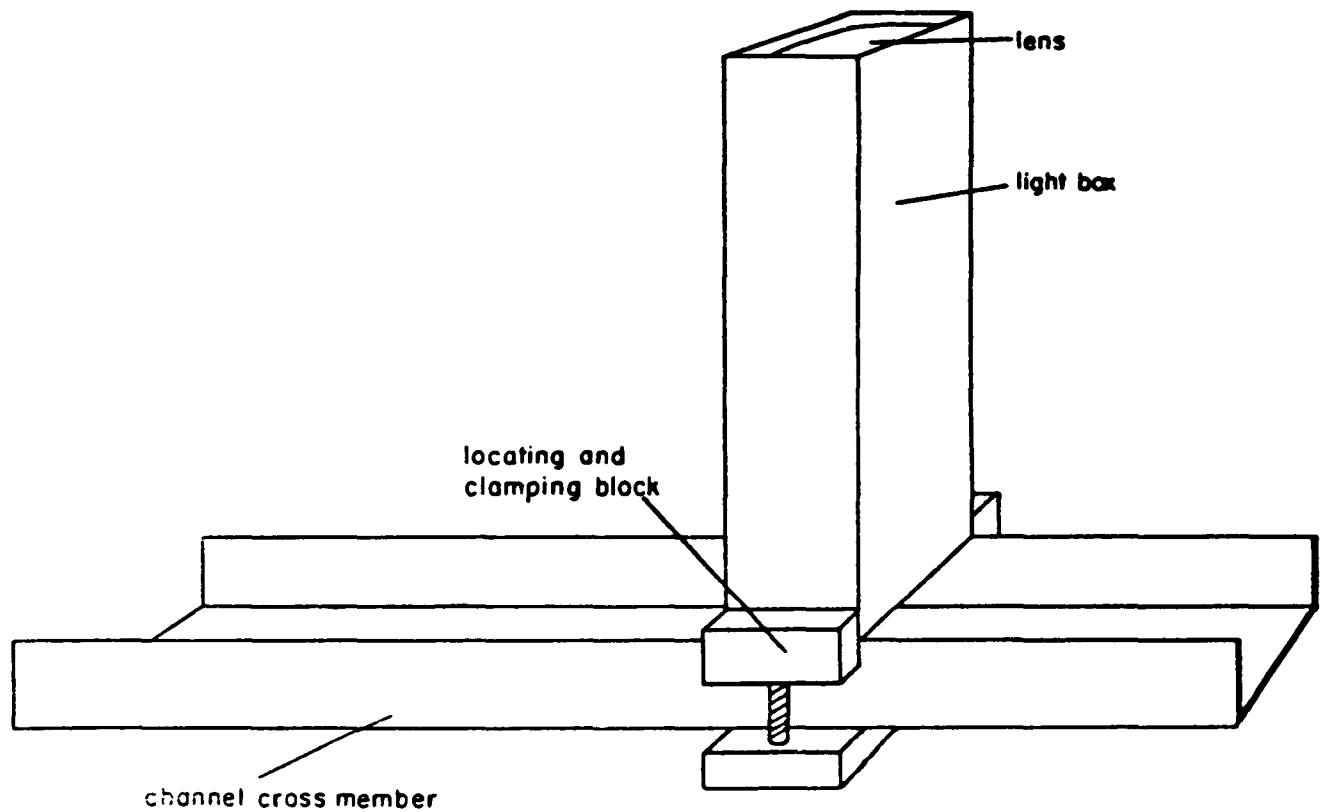

Figure 69. Lateral optical structure

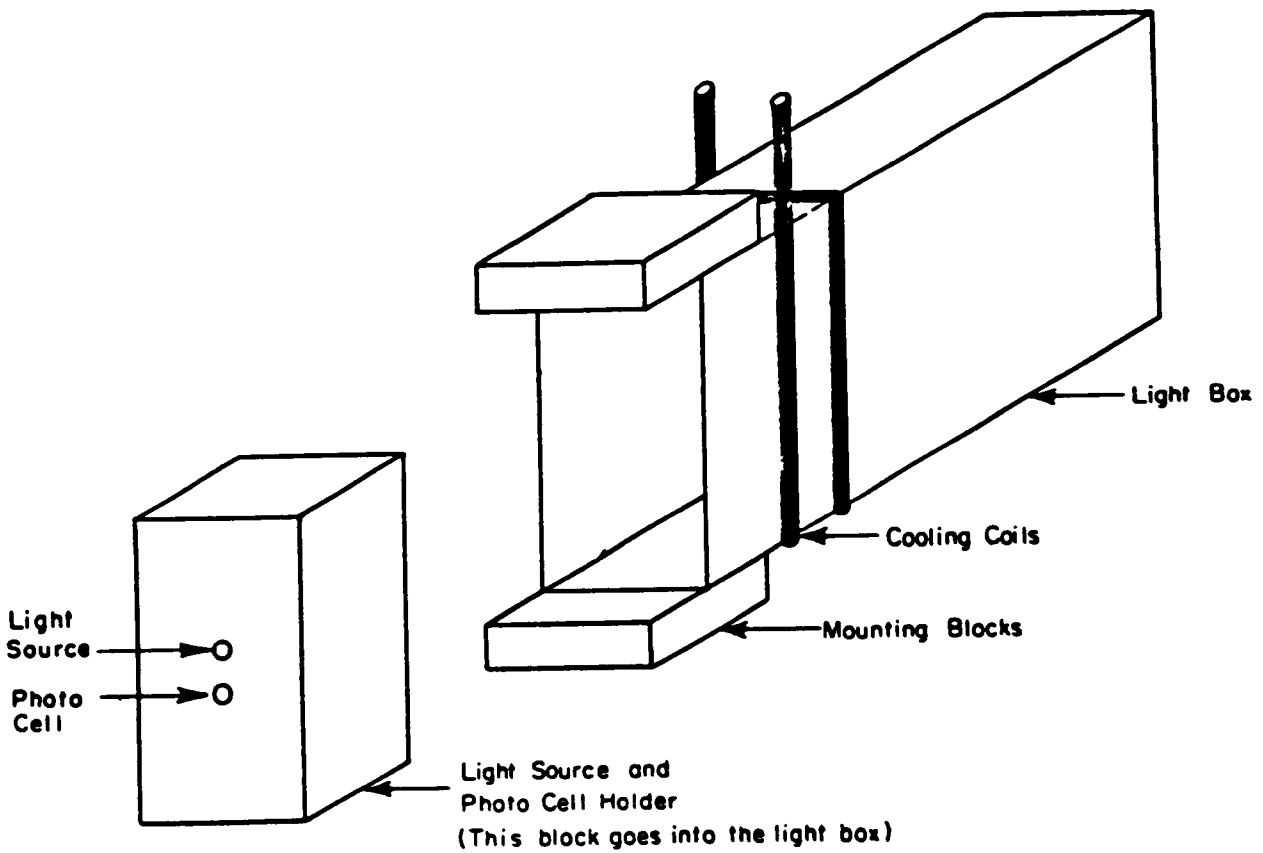

Figure 70. Light box and light source holder

However, several references are available which give a quick estimate of the mean time between component failure if the number of active elements are known (Refs. 19 and 20). The number of active elements (electron tubes, transistors, relays, rectifier diodes) in the present balance system is approximately 210. Using Ref. 21 and considering the electronics as ground-based equipment the mean time between component failures is between 100 and 400 hours.

To this date, most of the equipment has been operated at least 250 hours with no component failures.

CHAPTER III
OPERATIONAL RESULTS

A. STATIC BENCH TESTS

Cooling Tests

Before installation of the system in the wind tunnel the cooling system was tested on the bench. Current levels equal to those needed to suspend a typical model were fed through the magnet coils and the outlet water temperature from each coil was monitored. The power to be dissipated in all the coils under these conditions is between two and three kilowatts. A water flow rate of approximately three quarts per minute can be obtained through all the coils combined using city water pressure and temperature. At the power level mentioned above, this flow rate maintains the outlet water temperature well below 100°F.

Force Tests

The model shown in Fig. 71 was used for initial calibration of the balance. To keep the interactions mentioned in Chapter II, Section D, to a minimum, the volume of the electrical steel core was made just large enough to keep the drag solenoid current (for high p_0 operation) under the maximum of 30 amperes imposed by the cooling system. (This current maximum could be increased by increasing the cooling system flow rate through the use of a pump.)

To determine the current-force relations between the magnets and model the apparatus shown in Fig. 72 was used. No lateral calibrations were made. The calibrations for drag and lift are shown in Figs. 73 – 74. It can be seen from the curves that interactions exist due to changes in the strength of model polarization.

For a fixed model position the calibration (per pole) obeys the law

$$\vec{F} = \vec{M} \cdot \nabla \vec{B}$$

where $\vec{M}$ is the magnetization, and for an unsaturated core

$$M_i = \sum_k \alpha_k I_k$$

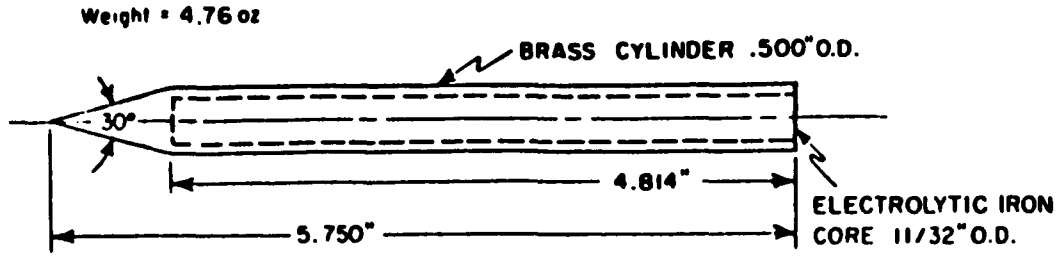

Figure 71. Model used for initial calibration and for preliminary testing

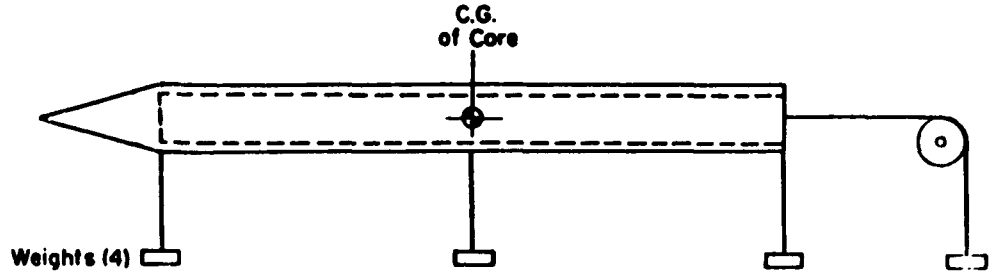

Figure 72. Calibration setup

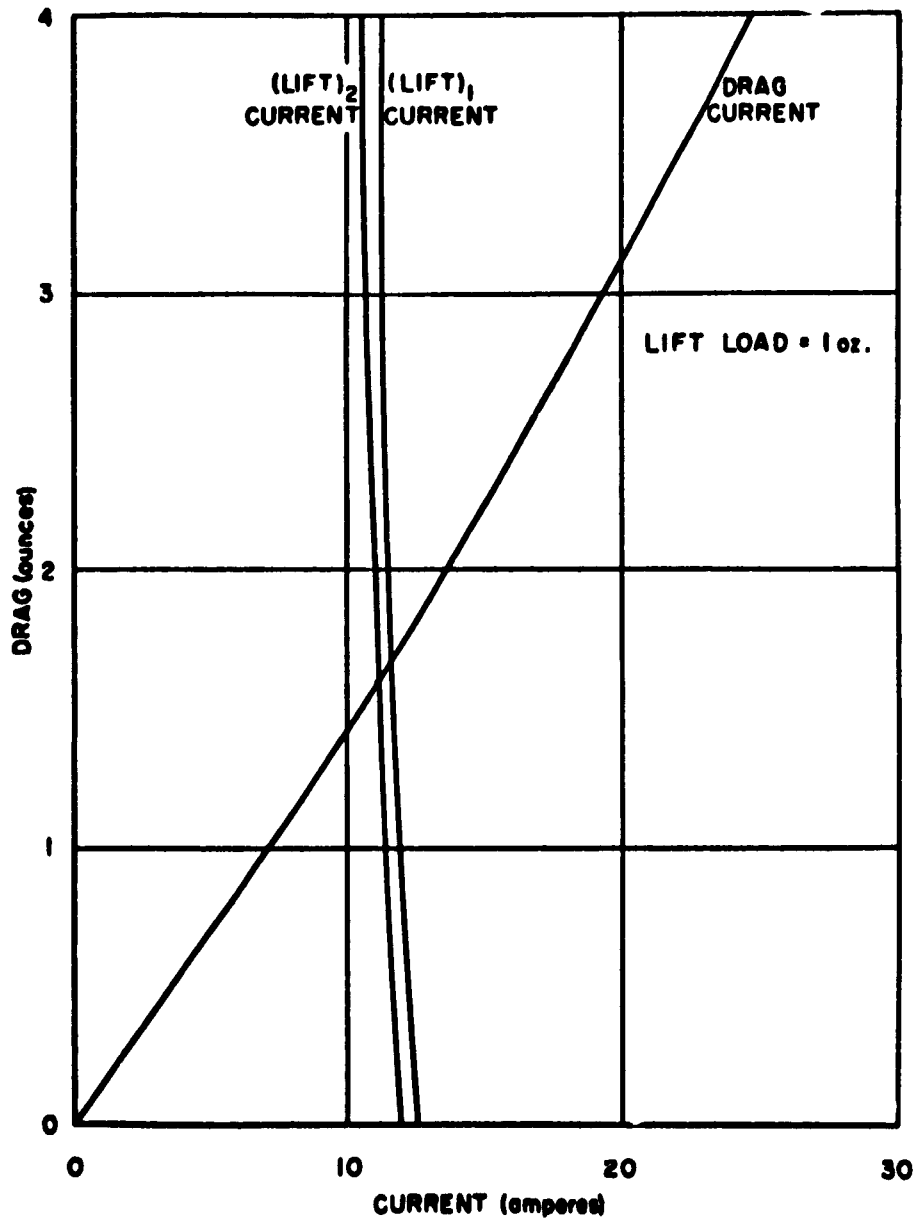

Figure 73a. Drag calibration curves-magnetic core 11/32" diameter , 5" length

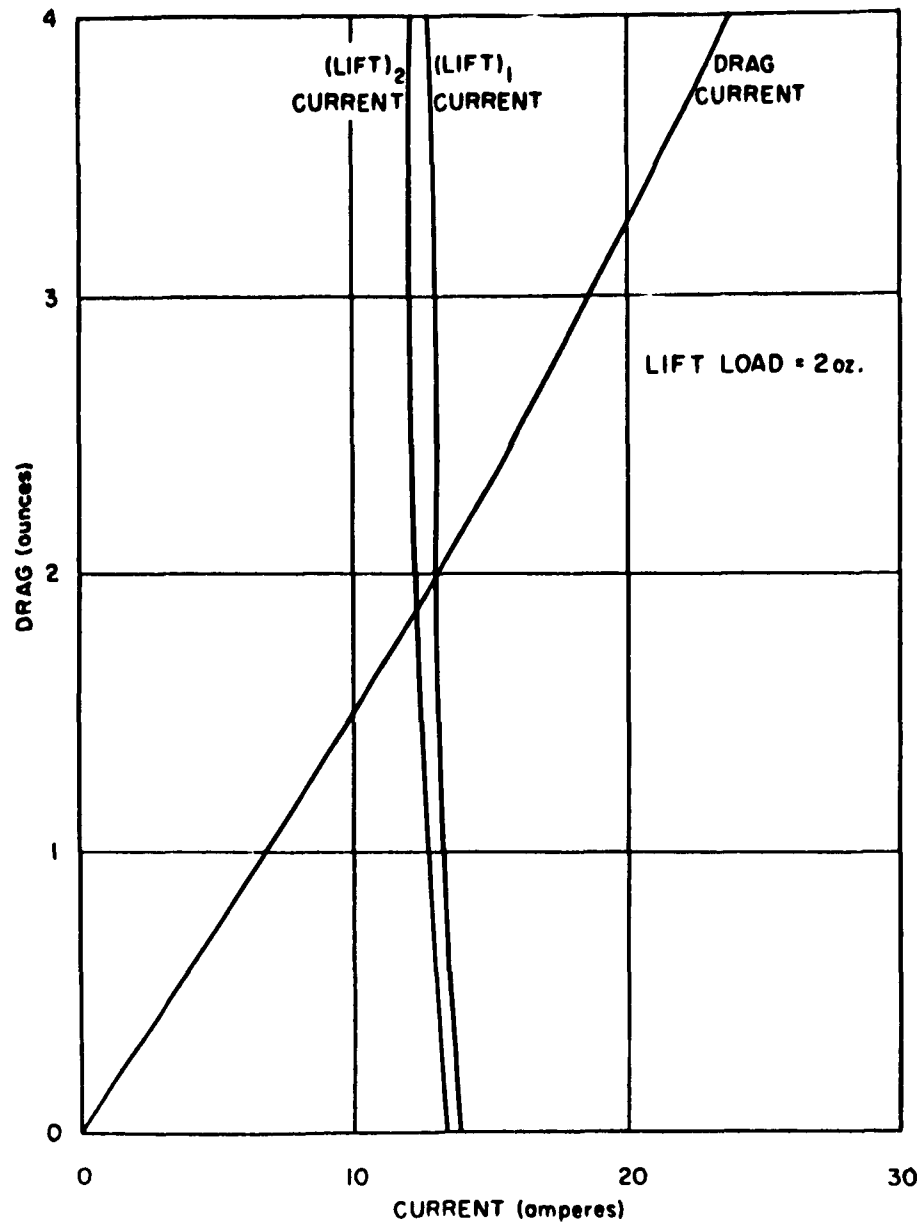

Figure 73b. Drag calibration curves-magnetic core 11/32" diameter , 5" length

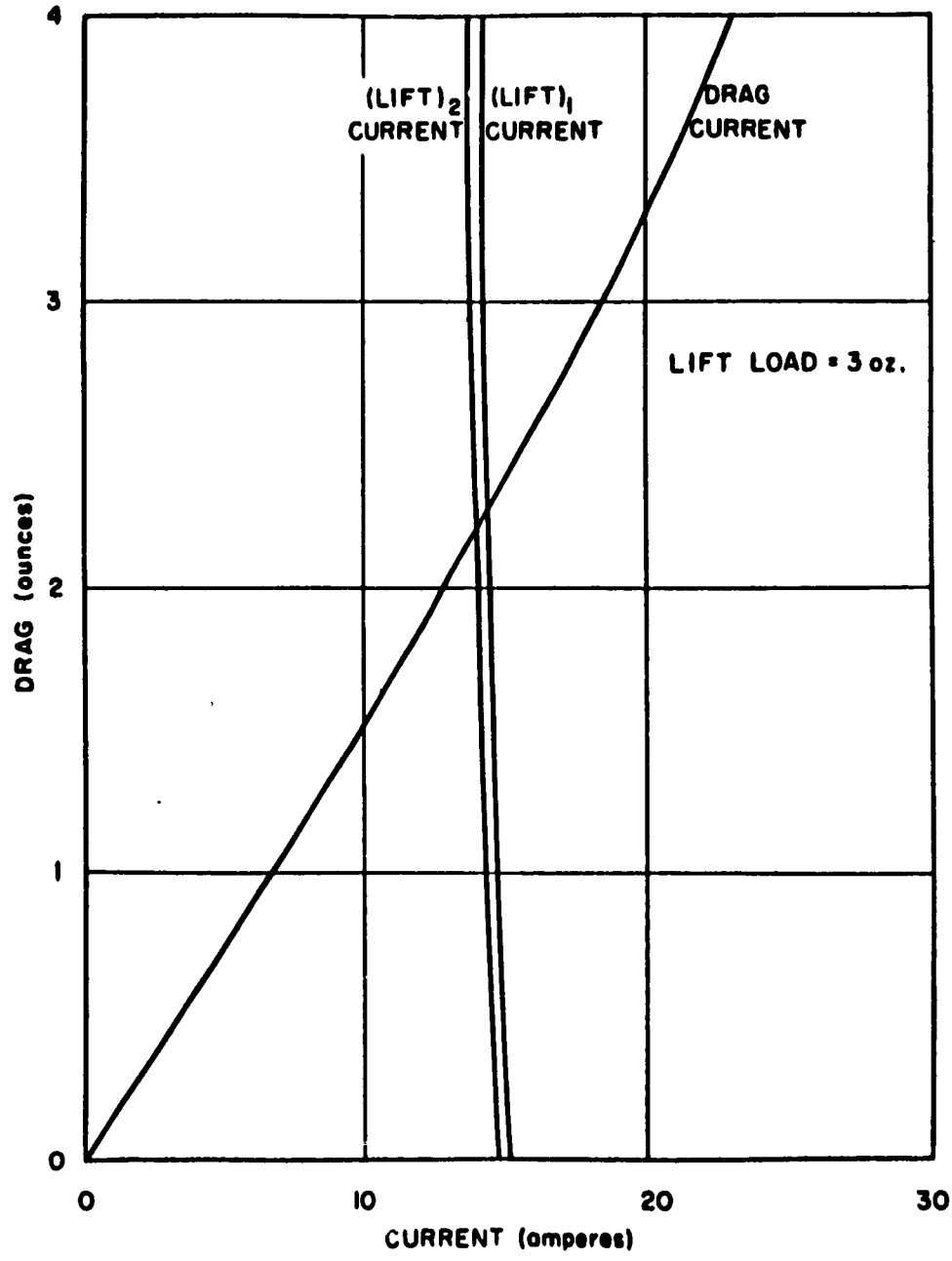

Figure 73c. Drag calibration curves-magnetic core 11/32" diameter, 5" length

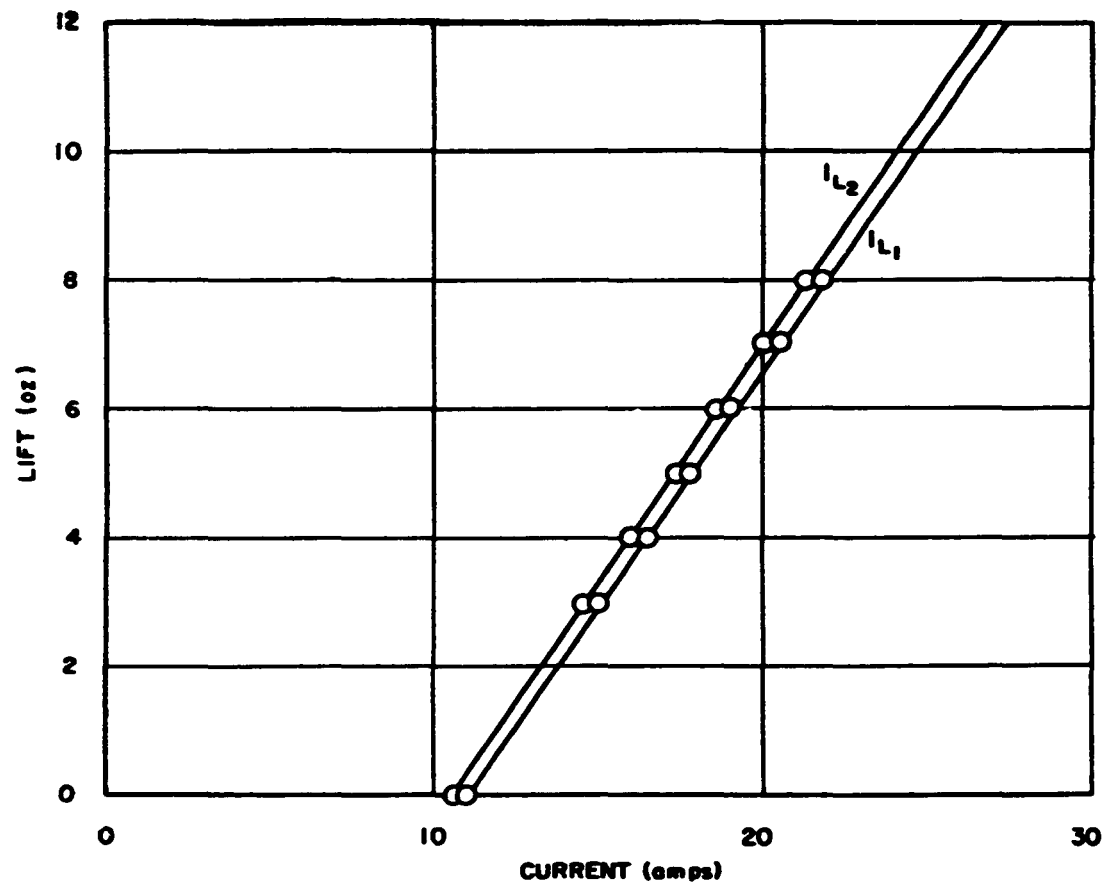

Figure 74. Lift calibration curves-magnetic core 11/32" diameter, 5" length

and

$$B_i = \sum_k \beta_k I_k$$

if α_k, β_k, are constants and I_k is the current in the coil. However, the magnitudes of the interactions are of the order of those that exist in an ordinary strain-gage balance and can be handled with existing data reduction techniques. A preliminary analysis of the drag calibration data showed that the interactions are predictable with simple formulas.

System Proof

Before installing the balance in the wind tunnel, the model was subjected to transient forces. Since the drag starting load was the main concern, weights were dropped from different heights in the longitudinal degree of freedom to simulate the starting transient. On the basis of the tunnel starting characteristics shown in Fig. 1 it was estimated that a three ounce weight dropped from a height of one inch would adequately simulate the starting load. The model response to this transient input was satisfactory. Model displacement remained well within the limits of the optical system.

B. WIND TUNNEL INSTALLATION

System Checkout

This balance was designed for a Mach 4.8 open jet wind tunnel capable of continuous operation at p_0's of 12 psia to 100 psia and at T_0's of 400°F to 1000°F (Ref. 21). The test section is surrounded by a boiler shaped ferrous shell. Figure 75 shows the shell with the front door open and the nozzle and diffuser installed.

The entire magnet and optical assembly was mounted on a frame for purposes of bench testing and for easy tunnel installation. The frame is equipped with grooved wheels and is rolled in and out of the tunnel on tracks. These tracks are mounted on a dolly for transportation of the balance. A picture of the balance on the dolly is shown in Fig. 76. When in the tunnel, the frame hangs by four rods from a hatch cover in the tunnel ceiling. It is braced to the test section shell at four points to prevent swaying. Figure 77 shows the system

Figure 75. Calibration rig

Figure 76. Magnetic balance on dolly (downstream view)

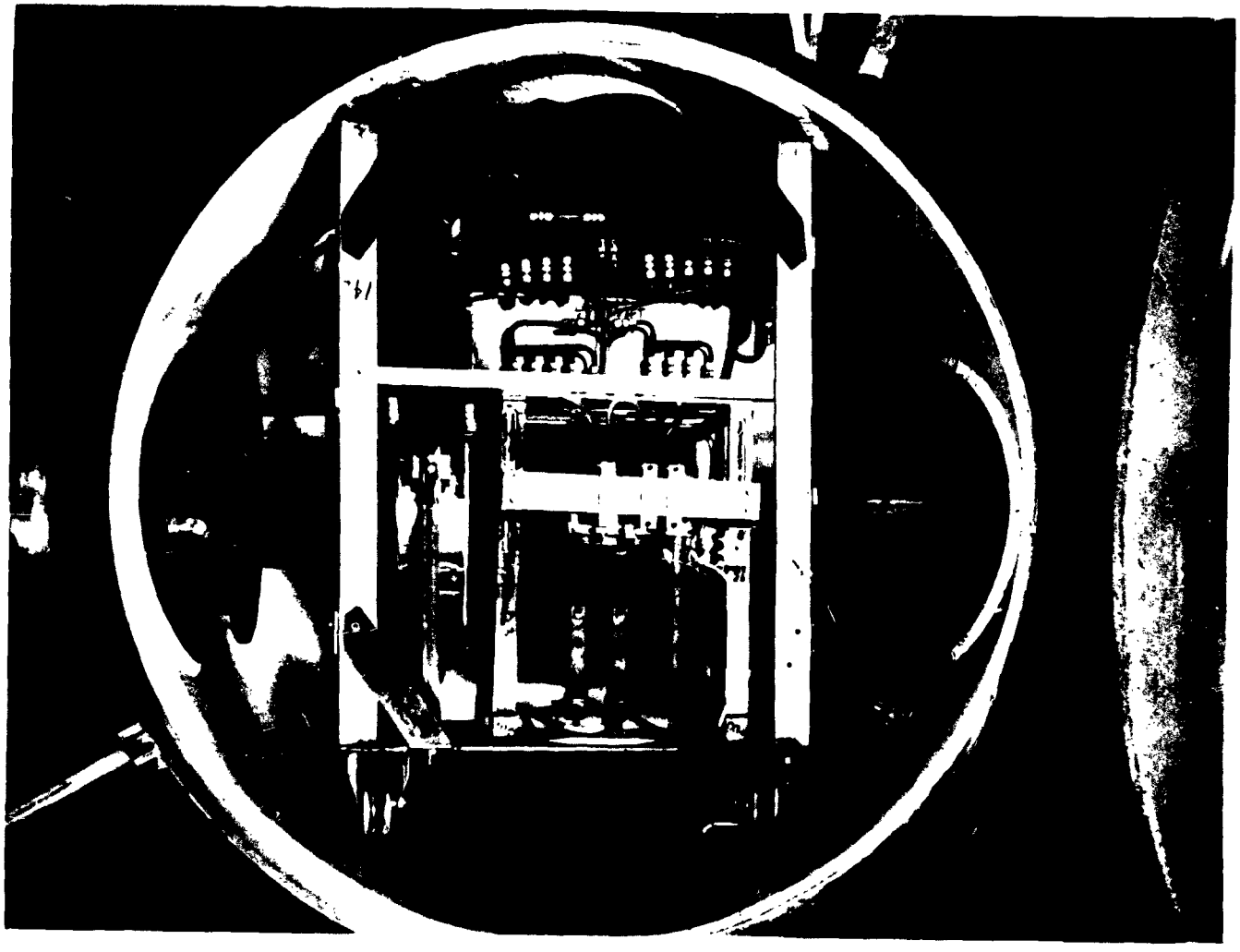

Figure 77. System installed in tunnel

installed in the tunnel. A complete tunnel installation takes approximately six man-hours.

Since the balance system is mounted inside the tunnel test section it must operate in a vacuum environment at an ambient temperature of approximately 125°F. To check the system out after installation all equipment was energized to operating levels but no model was suspended. The wind tunnel was pumped down and the balance was checked for cooling system leaks and corona around the magnet coils. No difficulties were encountered.

The coils and optical components were then equipped with thermocouples. With the coil currents at normal operating level and with no model suspended the tunnel was run at stagnation temperature of 600°F. Since the wind stream does not touch any part of the balance and radiation heating is small, all of the water-cooled components remained below 100°F during continuous operation. The balance frame approaches ambient temperature of 125°F and, therefore, a small amount of expansion was present but this is not a serious problem.

The final step in the checkout previous to starting the tunnel with a model installed was to pump the tunnel down while a model was being suspended. During this operation the magnets released the model. It was then realized that the condensed moisture in the test section air due to the decreasing pressure was blocking the light in the optical system. This decrease in light intensity on the photocells was enough to shift the model position past the limits of the optical masks and therefore the command signals to the power supplies stopped. This problem was solved by insuring that the tunnel air was dry before pumping down.

Figure 78 shows a cone cylinder model with a pointed base being suspended in the tunnel.

System Checkout – Air On

After the usual starting procedure was carried out and the tunnel was preheated to 800°F, a model was suspended in the balance and the tunnel started at a p_0 of 15 psia. This model represented about the largest size that would be encountered with this system and it demonstrated the system's capability of holding a model during the starting shock.

Figure 78. Model being suspended in tunnel

The results of the test are shown in Figs. 79 and 80. The points represent the data and the line is the predicted value. Figure 79 shows the measured zero-lift drag as a function of Reynolds number. The lines represent estimates of this drag for a laminar boundary layer. Each curve is for a constant base pressure. The Reynolds number corresponds to a range where the base pressure is not known to within five percent. The calculations were not carried out in more detail since the data was read from a 0-50 ampere meter, marked in increments of one ampere.* The drags in question correspond to the lower third of the scale range. These meters are adequate for obtaining preliminary data, but are not adequate for general instrumentation. The induced drag is shown in Fig. 80 and is remarkably smooth. Also shown in Fig. 80 is the variation in lift coefficient with angle of attack. Most of the scatter is due to the primitive method of measuring angle of attack. It is estimated that the error in angle of attack (other than zero) is about ±0.7 degrees. The line is the theoretical value and falls well within the estimated error. The moment center of the balance is near the center of volume, thus the moment data at these low angles tends to reflect the lift data. The estimated error in the center of pressure is ±1.0 diameter.[22]

Additional experiments under way have indicated that a single vertical fin made of magnetic material (Permendur) will provide roll stiffness up to one ounce-inch. This torque is large enough to provide adequate roll position control. Further, damping in roll can be developed by making the remaining fins and wings from copper and using eddy current damping.

It is planned to install a more accurate current measuring scheme as well as an angle measuring system for pitch and yaw in the immediate future. The further developments include a roll position control and the application of the system to several dynamic problems. In the opinion of the authors this type of balance offers great promise in the measurement

*Preliminary results using a standard shunt and a potentiometer have indicated that reading to ±0.04 amperes presents no difficulty.

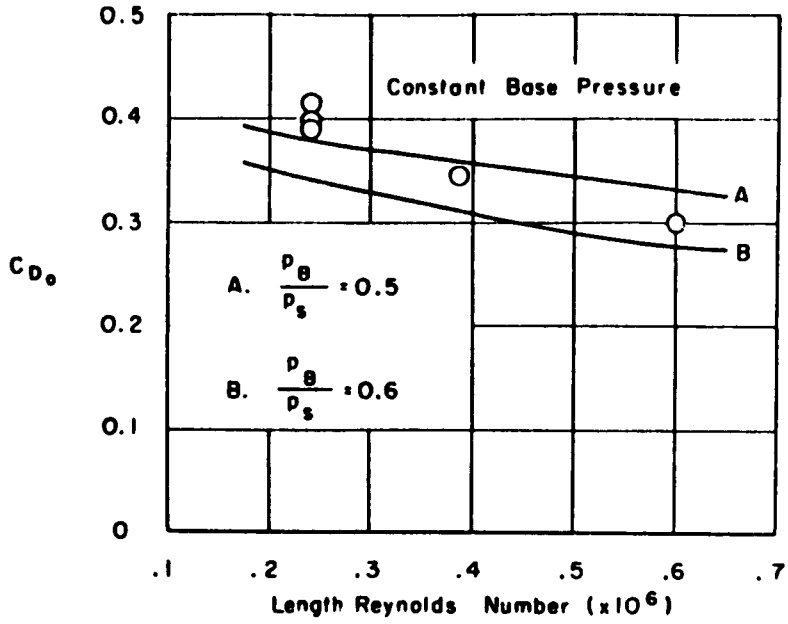

Figure 79. Zero-lift drag at M = 4.8

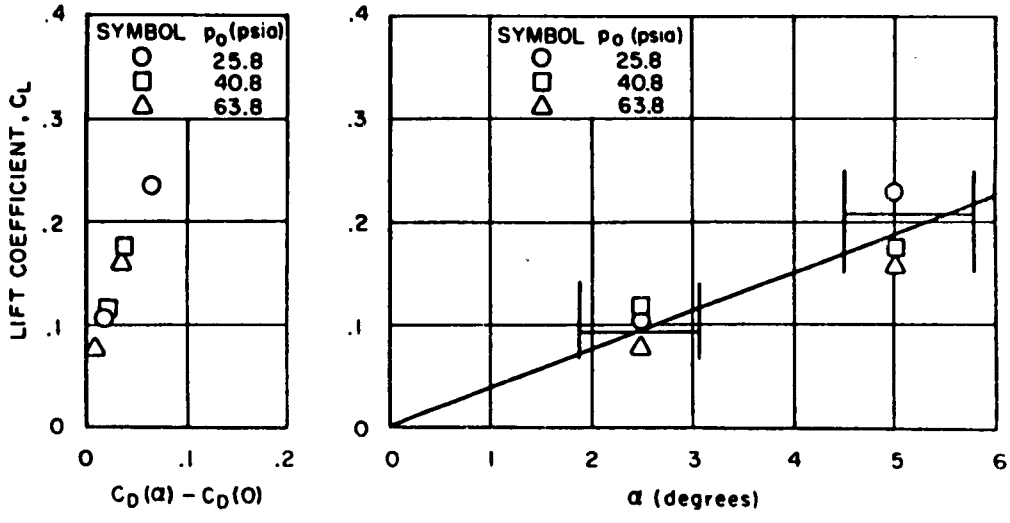

Figure 80. Lift and induced drag coefficients at M = 4.8

of dynamic stability derivatives, but this promise has yet to be achieved. It also offers promise in measuring other unsteady processes for the future.

At the present this kind of system provides the means for obtaining data with improved accuracy, (a) on bodies with pointed bases and (b) on wakes near the body without sting interferences.

REFERENCES

1. Tournier, M. and Laurenceau, P., Suspension Magnetique d'une Maquette en Soufflerie, La Recherche Aeronautique, No. 59, Juillet – Aout 1957, p. 21 – 27.

2. Holmes, F. T., "Axial Magnetic Suspensions" The Review of Scientific Instruments, Vol. 8, 1937 (also Phys Rev, Vol. 51, p. 689, 1937).

3. Beams, J. W., "Magnetic Suspension Ultracentrifuge Circuits," Electronics, March 1954.

4. Gilinsen, P. J., Garcia, G. E., and Aronson, J. H., 8-Pole Microsyn Magnetic Suspension, Massachusetts Institute of Technology, Instrumentations Laboratory Engineering Notes E-588, October 5, 1956.

5. Kuhlthau, A. R., "The Investigation of Low Density Drag Phenomena Utilizing Laboratory Techniques," Paper 29, Proceedings of the Fourth U. S. Navy Symposium on Aeroballistics, Nav. Ord. Report 5904, May 1, 1958.

6. Chrisinger, J. E., An Investigation of the Engineering Aspects of a Wind Tunnel Magnetic Suspension System, Aeronautical Engineering Degree Thesis, Department of Aeronautics, Massachusetts Institute of Technology, June 1959.

7. Tilton, Lee, and Schwartz, Stuart, Static Tests on the Magnetic Suspension System, Massachusetts Institute of Technology, Naval Supersonic Laboratory AR Memo 399 of July 20, 1959.

8. Cowling, R. G., Magnetohydrodynamics, Interscience Publishers, Inc., New York, 1956.

9. Bozarth, Richard M., Ferromagnetism, Chapter 14 and Appendix 4, D. Van Nostrand Co., Inc., New York.

10. Pender, H. and Del Mar, W. A., Electrical Engineers Handbook, 3rd ed., John Wiley and Sons, New York, p. 4 – 38 et seq.

11. Rotors, H. C., Electromagnetic Devices, John Wiley and Sons, New York, 1941, p. 322.

12. Sears, F. W. and Zemansky, M. W., University Physics – Electricity, Magnetism and Optics, Addison-Wesley Press, Inc., Cambridge, Mass., 1949.

REFERENCES (Concluded)

13. Goodbar, I. and Uluant, C. A., Investigation of the Magnetic Field Near a Round Cylindrical Coil Having a Short Axis, Massachusetts Institute of Technology, Course VI M.S. Thesis, 1945.

14. _____, Magnetic Circuits and Transformers, A volume of the Principles of Electrical Engineering Series, by the staff of the Electrical Engineering Department, Massachusetts Institute of Technology, John Wiley and Sons, New York.

15. _____, " Design and Application of Permanent Magnets" Indiana Steel Products Company Permanent Magnet Manual Series 5, Valparasso, Indiana.

16. Marks, Lionel S., Mechanical Engineers Handbook, 4th Ed., p. 2056

17. Tilton, Edward Lee, III, and Baron, Larry, Design Construction and Testing of an Automatic Control System for a Wind Tunnel Magnetic Suspension System, Thesis for B. S. Degree, Department of Aeronautics, Massachusetts Institute of Technology, May, 1960.

18. _____, "Applications Manual for Philbrick Octal Plug-In Computing Amplifiers" GAP/R K2 Series G.A., Philbrick Researches Inc., 6th printing, 1959.

19. _____, A Research Plan for Developing Methods of Maintainability Measurement and Prediction, Government Services, RCA Service Company, A division of Radio Corporation of America, Cherry Hill, Camden 8, New Jersey, Rome Air Development Center RADC-TN-60-5, January 1960.

20. Packard, Karl S., "Quick Reliability Prediction for Electronic Equipment," Space/Aeronautics, Vol. 37, No. 2, February 1962.

21. Goldberg, Alfred, Description and Calibration of a Hypersonic Wind Tunnel, Massachusetts Institute of Technology, Naval Supersonic Laboratory TR-293, April 1959.

22. LaGraff, John E., Some Calibrations and Measurements on Models Magnetically Suspended in a Hypersonic Tunnel, Thesis for B.S. Degree, Department of Aeronautics and Astronautics, Massachusetts Institute of Technology, May 1962.

BIBLIOGRAPHY*

Magnetic Suspension of Wind Tunnel Models

1. A Proposal to Complete a Magnetic Model Suspension System for Use in Wind Tunnels, Massachusetts Institute of Technology, Naval Supersonic Laboratory, PR 59-26, August 1959.

2. Chrisinger, John Edvil, An Investigation of the Engineering Aspects of a Wind Tunnel Magnetic Suspension System, Massachusetts Institute of Technology Thesis, TR 406, 1959.

3. Desmet, E., Suspension Magnetique ONERA-Essai d'Application a l'Etude des Oscillations de Lacet d'un Corps Fusele, ONERA N. T. 10/1579 AP.

4. Desmet, E. and Rosset, Characteristiques et Notice d'Emploi de la Suspension Magnetique Destinee aux Souffleries S. 19 et S.8, ONERA N.T. 9/1579 AP.

5. Laurenceau, P., Description et Reglage de l'Amplificateur-Correcteur Utilise sur les Suspensions Magnetiques, ONERA N.T. 13/1579, AP, 1959.

6. Laurenceau, P., Etude, Realisation et Mise au Point d'une Suspension de Maquette Aerodynamique par Action Magnetique Pour une Petite Soufflerie, ONERA N.T. 2/1579 AP.

7. Laurenceau, P., La Suspension Magnetique des Maquettes, ONERA Discussion Technique OP, June 1956.

8. Laurenceau, P. and Desmet, E., Adaptation de la Suspension Magnetique des Maquettes aux Souffleries S. 19 and S. 8 L Ch, ONERA N.T. 7/1579 AP, 1957.

9. Matheson, L. R., Some Considerations for Design and Utilization of Magnetic Suspension, Aerodynamics Fundamental Memo No. 84, The General Electric Company.

10. Tilton, Lee and Schwartz, Stuart, Static Tests on the Magnetic Suspension System, Massachusetts Institute of Technology, AR Memo 399, July 20, 1959.

11. Tournier, M., Dieulesaint, E., and Laurenceau, P., Etude, Realization et Mise au Point d'une Suspension de Maquette Aerodynamique par Aerodynamique par Action Magnetique Pour une Petite Soufflerie, ONERA N.T. 1/1579.

* Compiled by A. H. Cortner, Von Karman Facility, ARO Inc., Tullahoma, Tennessee

12. Tournier, M., Laurenceau, P., and Dubois, G., La Suspension Magnetique ONERA, ONERA.

13. Tournier, M., and Laurenceau, P., Perfectionnements a la Suspension Magnetique des Maquettes, ONERA N.T. 5/1579 AP, 1956.

14. Tournier, M., and Laurenceau, P., "Suspension Magnetique d'une Maquette en Soufflerie," La Recherche Aeronautique, No. 59, July - August 1957.

Magnetic Suspension - Other than Wind Tunnel Models

1. "A Technique for Eliminating Crucibles in Heating and Melting of Metals," Journal of the Electrochemical Society, Vol. 99, No. 5, May 1952.

2. Beams, J. W., "Magnetic Suspension Ultracentrifuge Circuits," Electronics, March 1954.

3. Breazeale, J. B., McIlwraith, C. G., and Dacus, E. N., "Factors Limiting a Magnetic Suspension System," Journal of Applied Physics, Vol. 29, No. 3, March 1958.

4. Breazeale, J. B., Dissertation, University of Virginia, 1955.

5. Carpenter, D. R., Jr., A New Equilibrium Ultracentrifuge for Determination of Molecular Weights, Dissertation, University of Virginia, 1956.

6. Davisson, C. J. and Beams, J. W., "A New Variation of the Rotation-by-Magnetization Method of Measuring Cyromagnetic Ratios," Reviews of Modern Physics, Vol. 25, No. 1, January 1953.

7. Fosque, H. S. and Miller, G. H., An Electromagnetic Support Arrangement with Three Dimensional Control, Part II - Experimental, University of Virginia Report UVA/ORL-04-58 TR 3, 1958.

8. Holmes, F. T., "Axial Magnetic Suspensions," The Review of Scientific Instruments, Vol. 8, November 1937.

9. Jenkins, A. W., Jr., and Parker, H. M., An Electromagnetic Support Arrangement with Three Dimensional Control, Part I - Theoretical, University of Virginia Report UVA/ORL-04-58 TR 1, 1958.

10. Journal of Applied Physics, Vol. 23, No. 5, May 1962 (see also Erratum of December 1952).

11. Journal of Applied Physics, Vol. 17, 1946, p. 886.

12. McIlwraith, C. G., Breazeale, J. B., and Dacus, E. N., "Improved Magnetic Suspension System," The Review of Scientific Instruments, Vol. 29, No. 11, November 1958.

13. Melting Without a Crucible, Westinghouse Electric Corporation Research Memorandum 60-94472-2-5.

14. Nelson, W., Trachtenbarg, A., and Grundy, A., Jr., An Apparatus for the Study of High Speed Air Flow Over a Freely Suspended Rotating Cylinder, Columbia University, WADC Technical Report 57-338, ASTIA No. AD 142127, 1957.

Related to Magnetic Suspension

1. Adair, T. W., Squire, C. F., and Utley, H. B., "High Field Solenoid Magnet with Liquid Nitrogen Cooling," The Review of Scientific Instruments, Vol. 31, No. 4, April 1960, Pages 416 – 418.

2. Agusta, B., "Dynamic Test of Choke Inductance," Electronics, January 23, 1959, p. 54.

3. Anderson, H. L., Dunning, J. R., and Mitchell, D. P., "Regulator Systems for Electromagnets," The Review of Scientific Instruments, Vol. 8, December 1937, pp. 497 – 501.

4. Autler, S. H., "Superconducting Electromagnets," The Review of Scientific Instruments, Vol. 31, No. 4, April 1960, pp. 369 – 373.

5. Borg, K. C., and Milford, F. J., "High Precision Large Current Regulator," The Review of Scientific Instruments, Vol. 31, No. 3, March 1960, pp. 321 – 2.

6. Burnett, J. H., "Applying Thyratrons to Control – Part I," Control Engineering, January 1957, pp. 88 – 96.

7. Burnett, J. H., "Applying Thyratrons to Control – Part II," Control Engineering, February 1957, pp. 73 – 77.

8. Giauque, W. F. and Lyon, D. N., "Design of a 100-Kilogauss 4-Inch Core Solenoid for Continuous Operation," The Review of Scientific Instruments, Vol. 31, No. 4, April 1960, pp. 374 – 390.

BIBLIOGRAPHY (Concluded)

9. Gutzwiller, F. W., Overcurrent Protection of Semiconductor Rectifiers, General Electric Company, ECG-328, June 1958.

10. "How You Can Save Time Estimating Leakage Factors for Magnetic Circuits," The Indiana Steel Products Company.

11. Jurgen, R. K., "Hall-Effect Devices," Electronics, January 16, 1959, p. 63.

Aeronautical Research Laboratories, Wright-Patterson AFB, O. THE DESIGN AND INTIAL OPERATION OF A MAGNETIC MODEL SUSPENSION AND FORCE MEASUREMENT SYSTEM by Edward Lee Tilton, III, William J. Parkin, Eugene E. Covert, James B. Coffin, John E. Chrisinger, MIT, Cambridge, Mass. January 1963. 136 p. incl. illus. (project 7065; Task 7065-01) (Contract AF 33(616)-7023) (ARL 63-16)

Unclassified Report

The design, construction and proof tests of a magnetic model suspension system capable of use in a M = 4.8 wind tunnel is described. The results indicate that the model can be suspended magnetically during the wind tunnel starting conditions, that the model can be angulated and left and drag forces measured with the model at angle of attack.

(over)

UNCLASSIFIED

Aeronautical Research Laboratories, Wright-Patterson AFB, O. THE DESIGN AND INTIAL OPERATION OF A MAGNETIC MODEL SUSPENSION AND FORCE MEASUREMENT SYSTEM by Edward Lee Tilton, III, William J. Parkin, Eugene E. Covert, James B. Coffin, John E. Chrisinger, MIT, Cambridge, Mass. January 1963. 136 p. incl. illus. (project 7065; Task 7065-01) (Contract AF 33(616)-7023) (ARL 63-16)

Unclassified Report

The design, construction and proof tests of a magnetic model suspension system capable of use in a M = 4.8 wind tunnel is described. The results indicate that the model can be suspended magnetically during the wind tunnel starting conditions, that the model can be angulated and left and drag forces measured with the model at angle of attack.

(over)

UNCLASSIFIED